# Experimental Results on Hadron Production: Reviewing the AGS and the Fixed-Target Program at STAR

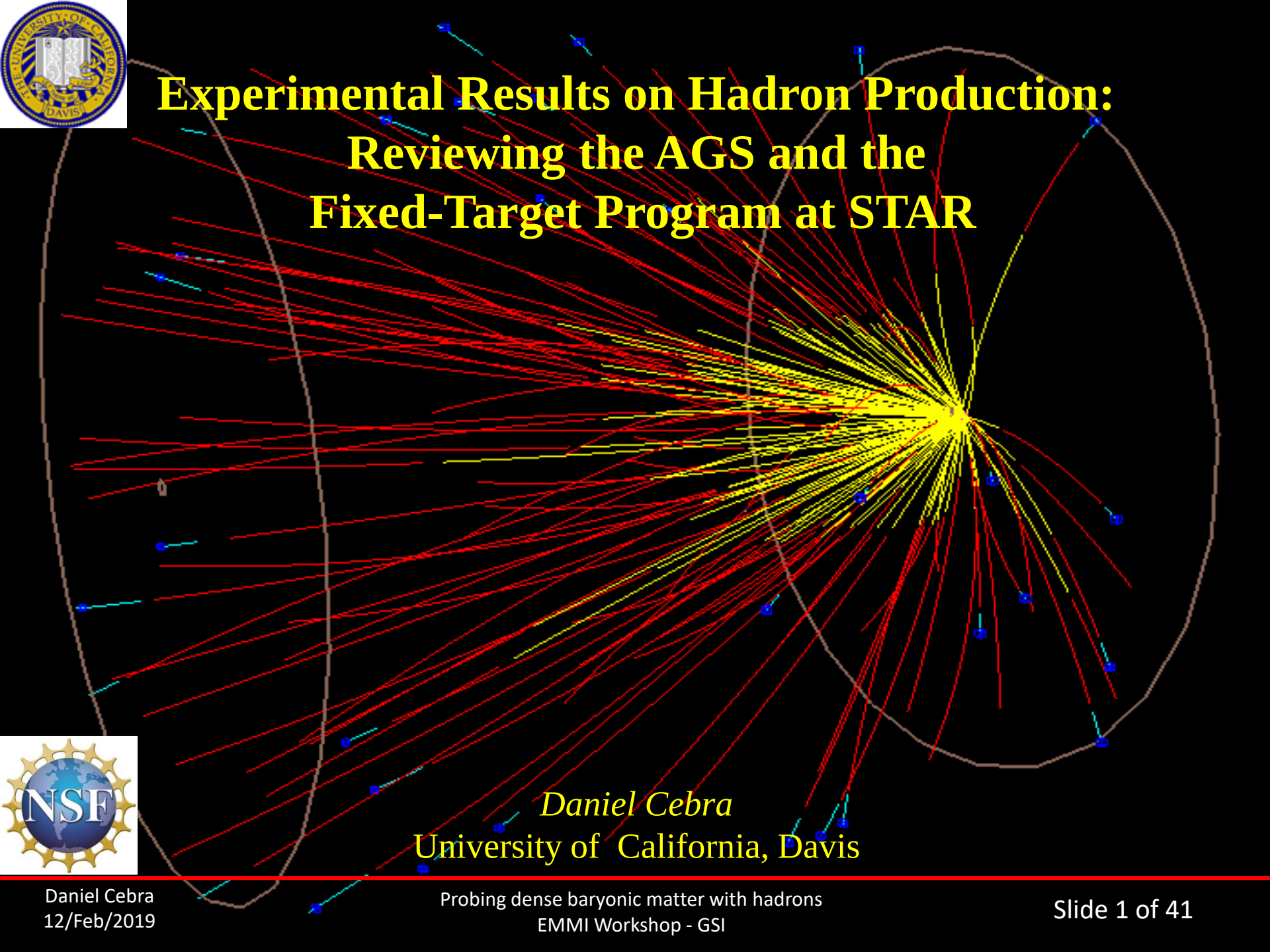

*Daniel Cebra*
University of California, Davis

# Outline

- The AGS heavy-ion program
  - History and overview of AGS heavy-ion program
  - Particle spectra and yields
  - Collective Behavior
  - HBT
- The fixed-target program at STAR
  - History and overview
  - Review of test run results
  - Preview of 2018 – first physics run at 3.0 GeV
  - Plans for runs in 2019, 2020, and 2021
- Perspective and Conclusions

# Alternating Gradient Synchrotron

- The first accelerator utilizing strong-focusing principle
- July 29, 1960: First beam, 33 GeV
- Three Nobel Prizes:
  - 1962: L. Lederman, M. Schwartz and J. Steinberger

    muon neutrino

    1988 Nobel Prize
  - 1964: J. Cronin and V. Fitch

    CP violation in Kaon decay

    1980 Nobel Prize
  - 1974: S. C.C. Ting

    discovery of J/ψ

    1976 Nobel Prize
- 1988-92: Silicon beams at 14.6 AGeV/c
- 1993-95: Gold beams, 2.8-11.7 AGeV/c
- 1999-present: Injector for RHIC

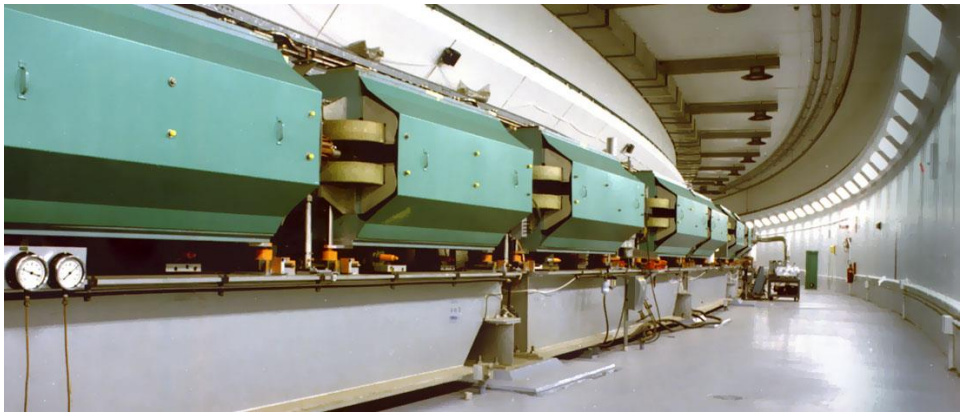

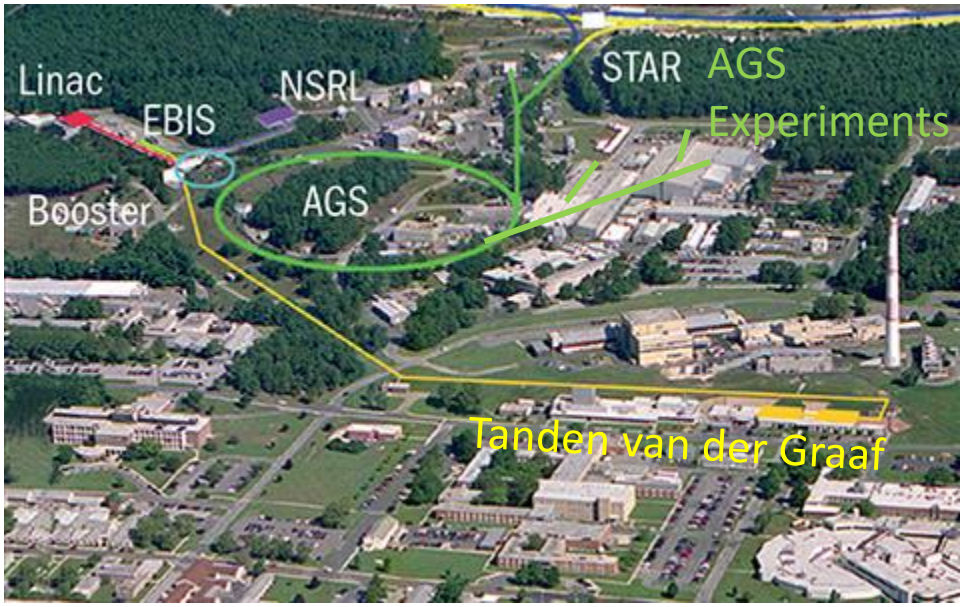

# E802/E859/E866/E917 Experiment

E802 – **Spokesperson:** Chellis Chasman, Shoji Nagamiya
E859 -- **Spokesperson:** Ledoux, Robert J.; Remsberg, Louis P.; Zajc, William A.
E866 -- **Spokesperson**: Chasman, Chellis; Hamagaki, Hideki; Steadman, Steve G.
E917 -- **Spokesperson:** Mignerey, Alice; Seto, R.K.

- Mid-rapidity spectrometer

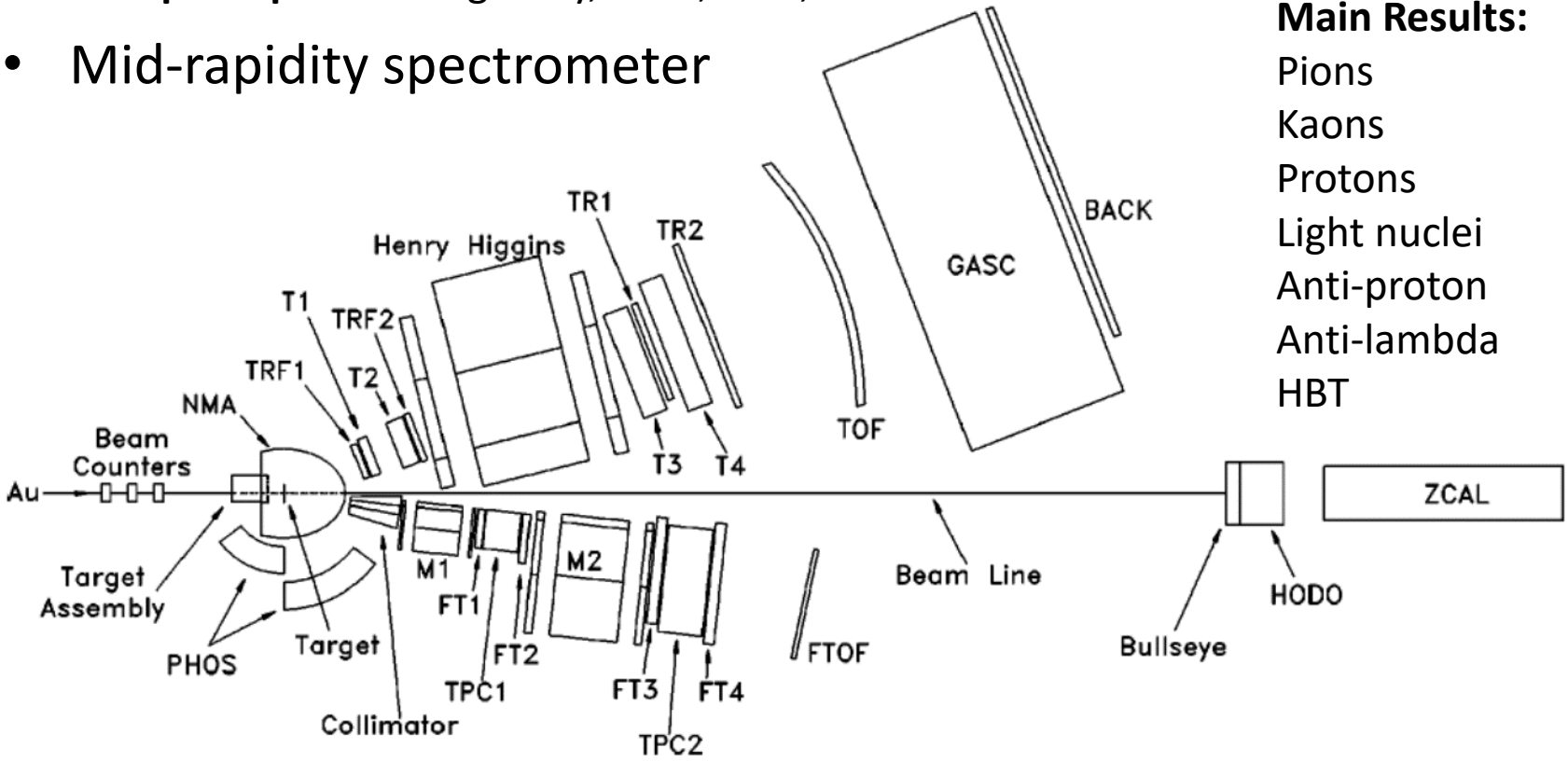


**Main Results:**
Pions
Kaons
Protons
Light nuclei
Anti-proton
Anti-lambda
HBT

# E810/E891 Experiment

E810 – **Spokesperson:** Lindenbaum, S.J.; Platner, E.D.
E891 – **Spokesperson:** Platner, E.D.

- Time Projection Chamber

**Main Results:**
$K^0s$ (Si+Au)
Lambda (Si+Au)

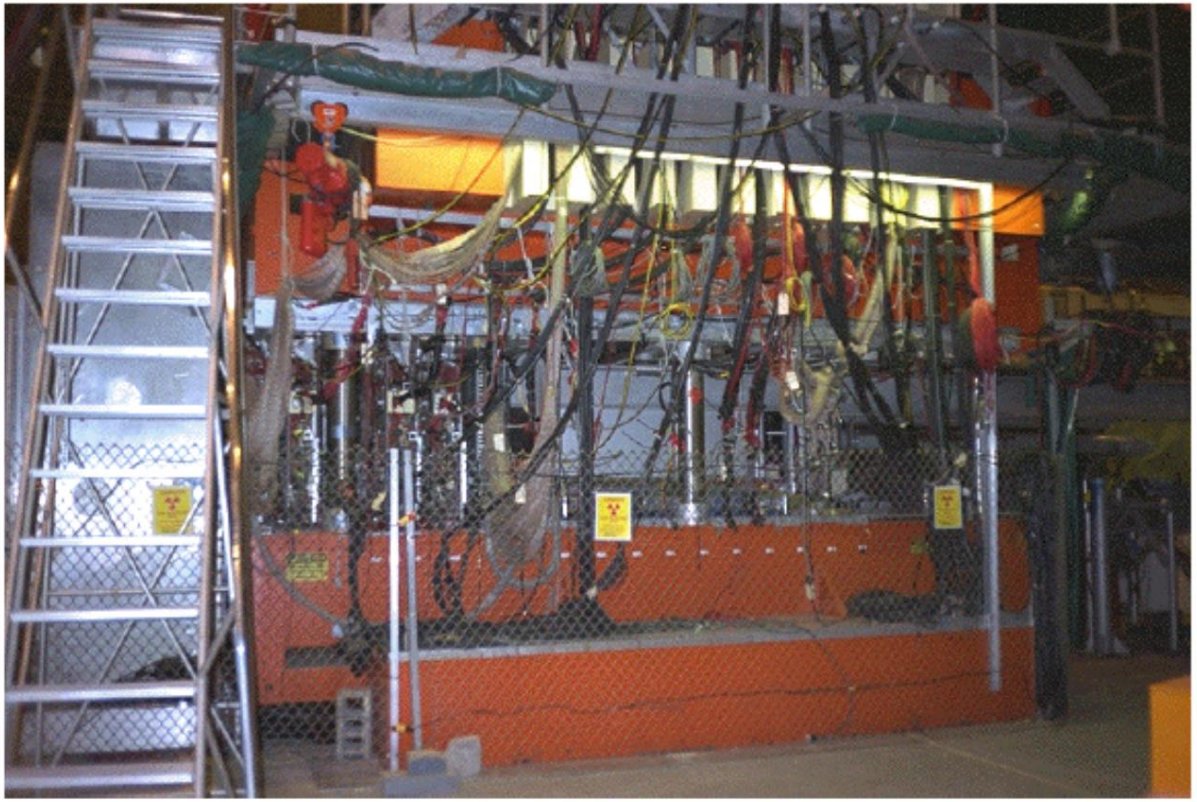

# E814/E877 Experimental Setup

E814 – **Spokesperson:** Braun-Munzinger, Peter
E877 – **Spokesperson:** Braun-Munzinger, Peter

- Forward spectrometer
- TOF & Calorimetry

**Main Results:**
Pions
Protons
Light nuclei
Lambda
Anti-lambda
Directed flow
Elliptic flow
HBT

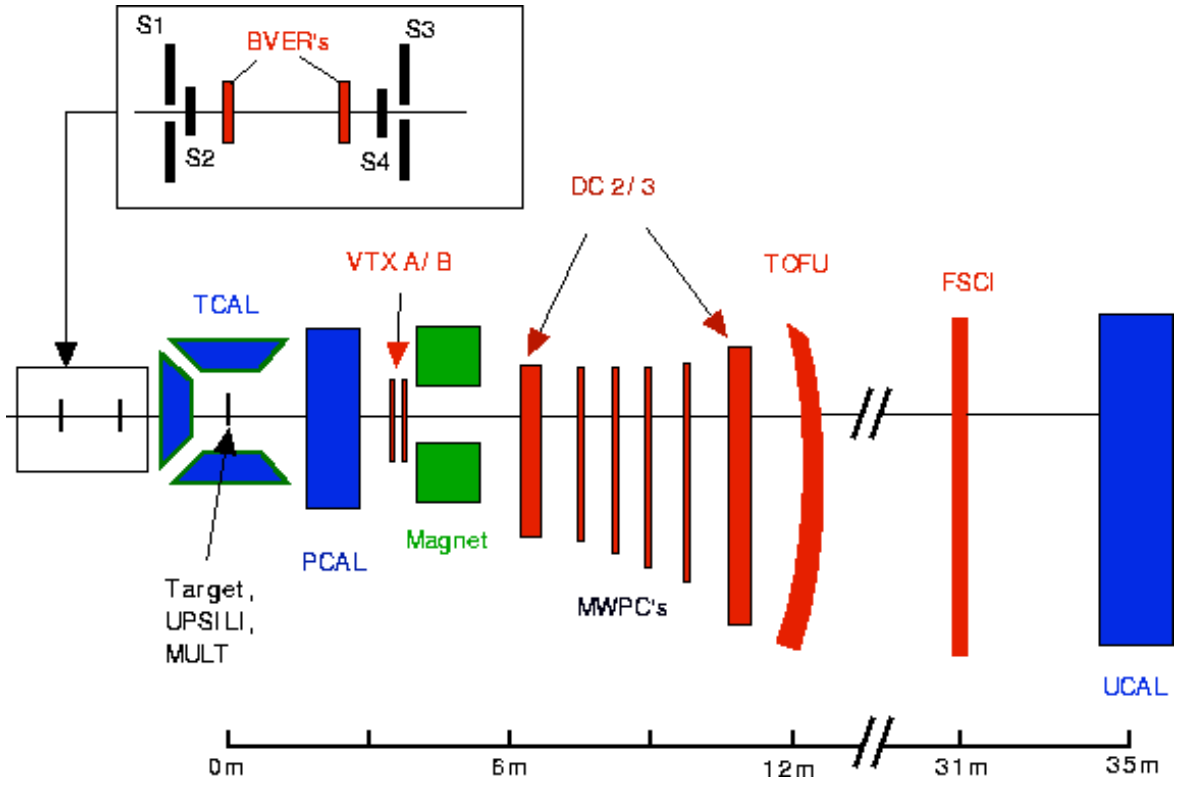

# E864 Experiment

E864 – **Spokesperson:** Majka, Richard D.; Sandweiss, Jack
E941 – **Spokesperson:** Huan Huang

- Forward spectrometer
- TOF & Calorimetry

**Main Results:**
Protons
Light nuclei
Anti-proton
Anti-deuteron

Found no strangelets

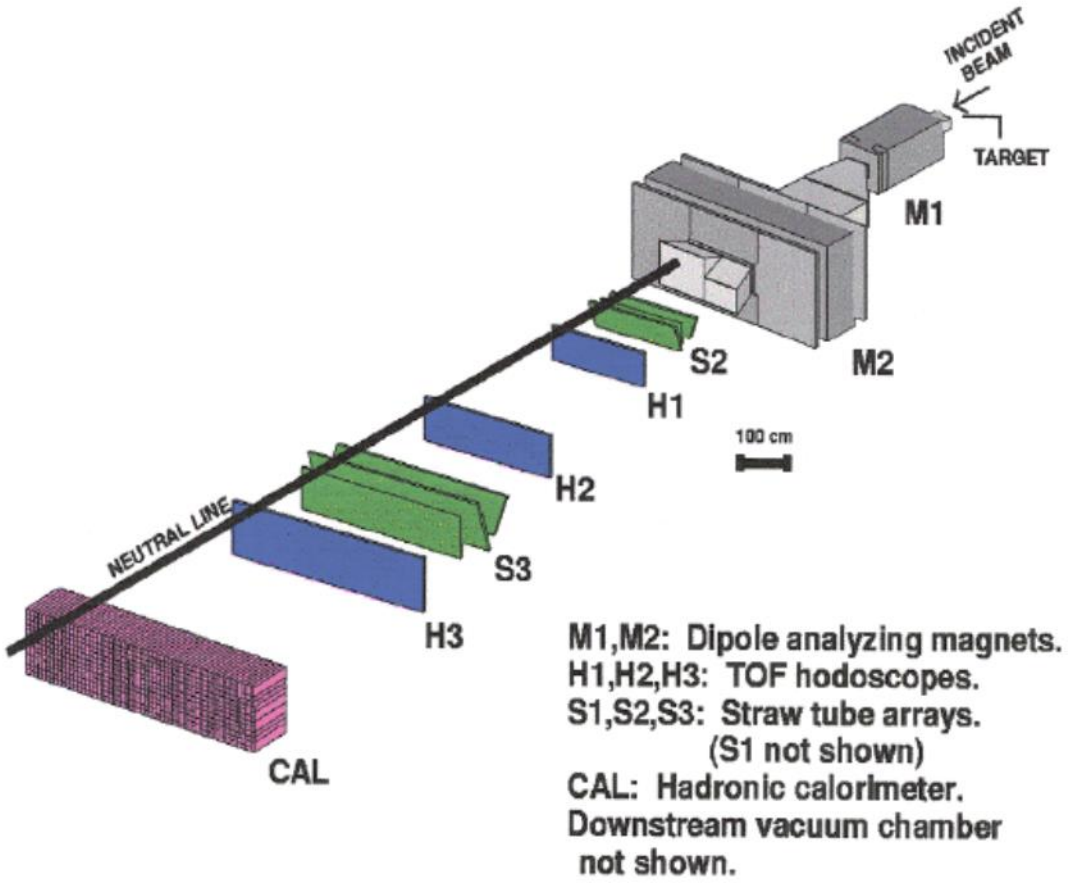

# E895/E910 Experiment

E895 – **Spokesperson**: Gulshan Rai
E910 -- **Spokesperson:** Cole, Brian A.

- Time Projection Chamber

**Main Results:**
Pions
Protons
Lambdas
Directed flow
Elliptic flow
HBT

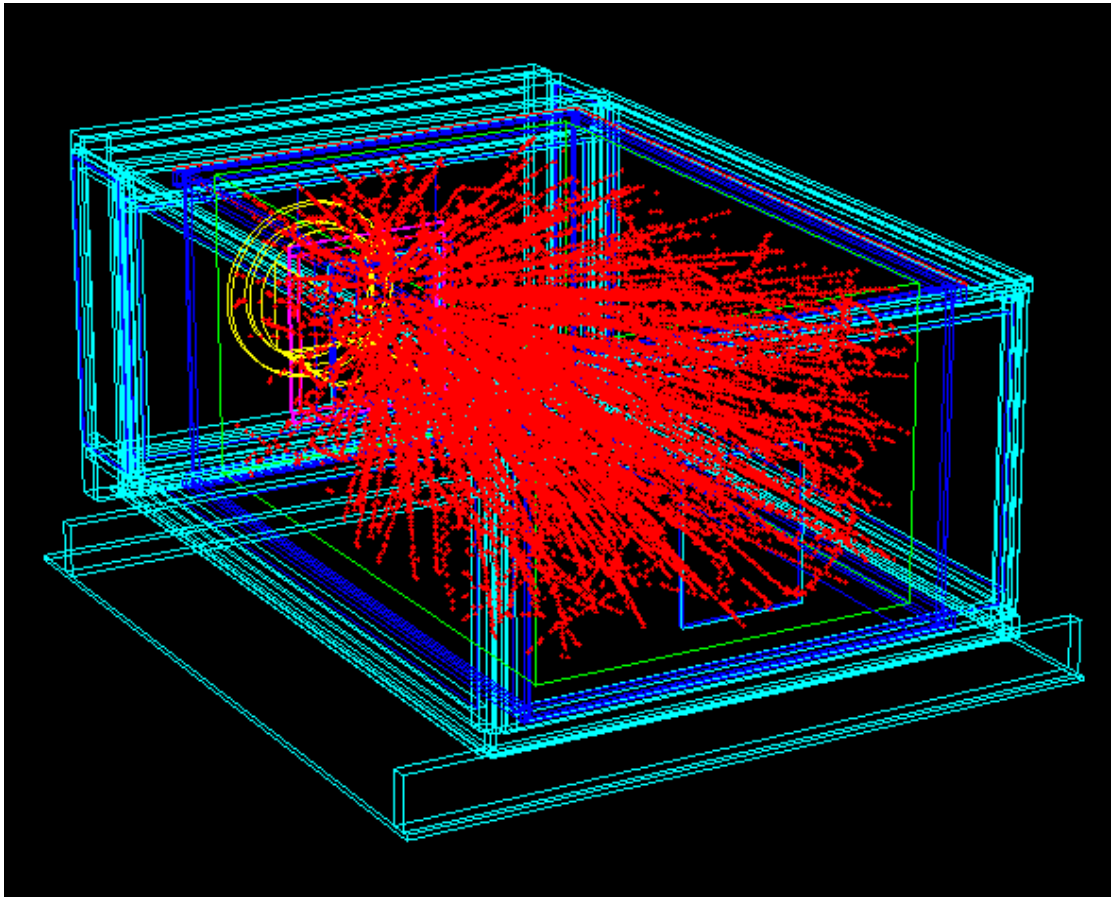

# AGS Results: pion, kaon, proton spectra

**Spectra – pions:**

- E895_PRC68(2003)054905 – $\pi^+$ and $\pi^-$ spectra and dN/dy at 2, 4, 6, 8 AGeV
- E802_PRC57(1998)R466 – $\pi^+$ and $\pi^-$ spectra and dN/dy at 10.5 AGeV
- E877_PRC62(2000)024901 -- $\pi^+$ and $\pi^-$ high rapidity spectra and dN/dy at 10.5 AGeV
- E917_PLB476(2000)1 – $\pi^+$ mid-rapidity spectra at 2, 4, 6, 8 AGeV

**Spectra – Kaons:**

- E866_PLB490(2000)53 – $K^+$ and $K^-$ mid-rapidity spectra at 2, 4, 6, 8, 10.5 AGeV
- E866_NPA630(1998)571c – $K^+$ and $K^-$ dN/dy at 10.5 AGeV

➔ Need Charged kaon dN/dy for AGS scan energies

**Spectra – Protons:**

- E895_PRL88(2002)102301 – proton spectra and dN/dy at 2, 4, 6, 8 AGeV
- E917_PRL86(2001)1970 – proton spectra and dN/dy at 6, 8, 10.5 AGev

} Some issues

- E802_PRC57(1998)R466 – proton spectra and dN/dy at 10.5 AGeV
- E802_PRC60(1999)064901 – proton spectra and dN/dy at 10.5 AGeV
- E877_PRC56(1997)3254 – forward rapidity proton spectra at 10.5 AGeV
- E877_PRC62(2000)024901 – forward rapidity proton spectra at 10.5 AGeV

# AGS Results: pion and kaon spectra

- pion ratio comes from initial n:p ratio as low $p_T$ pions are produced primarily through the $\Delta$ channel ➔ accounted for by $\mu_Q$ is statistical models related to stopping
- Pion ratios provide another way to 'image' the size of the source

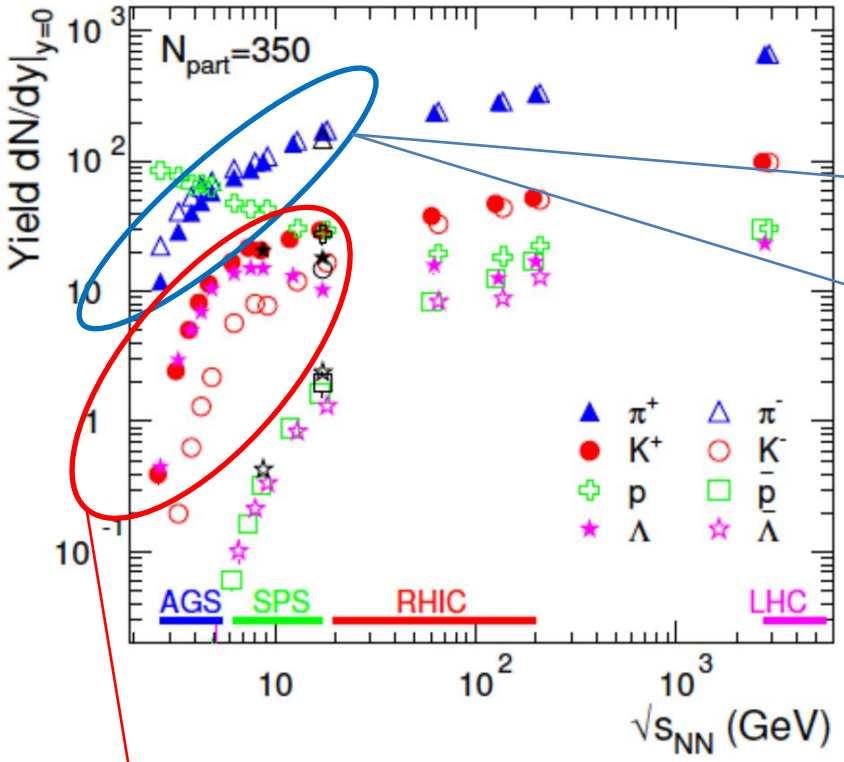


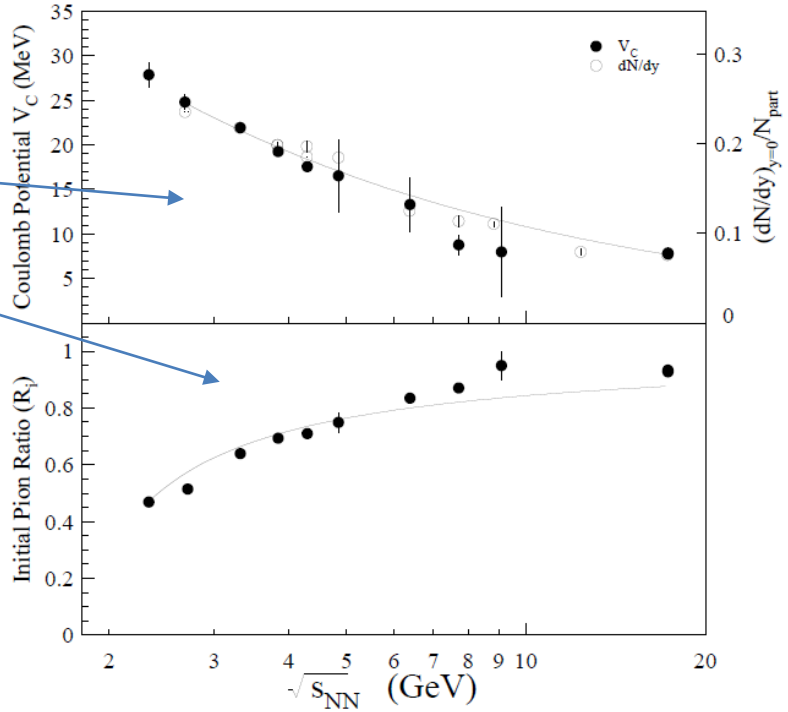


- Kaon ratios come from associated production, which feeds $K^+$ only

# AGS Results: proton spectra

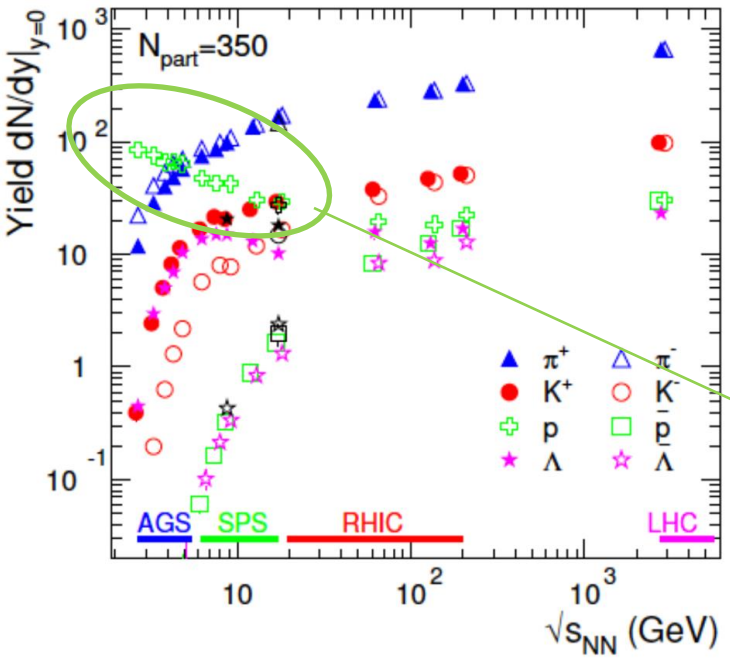


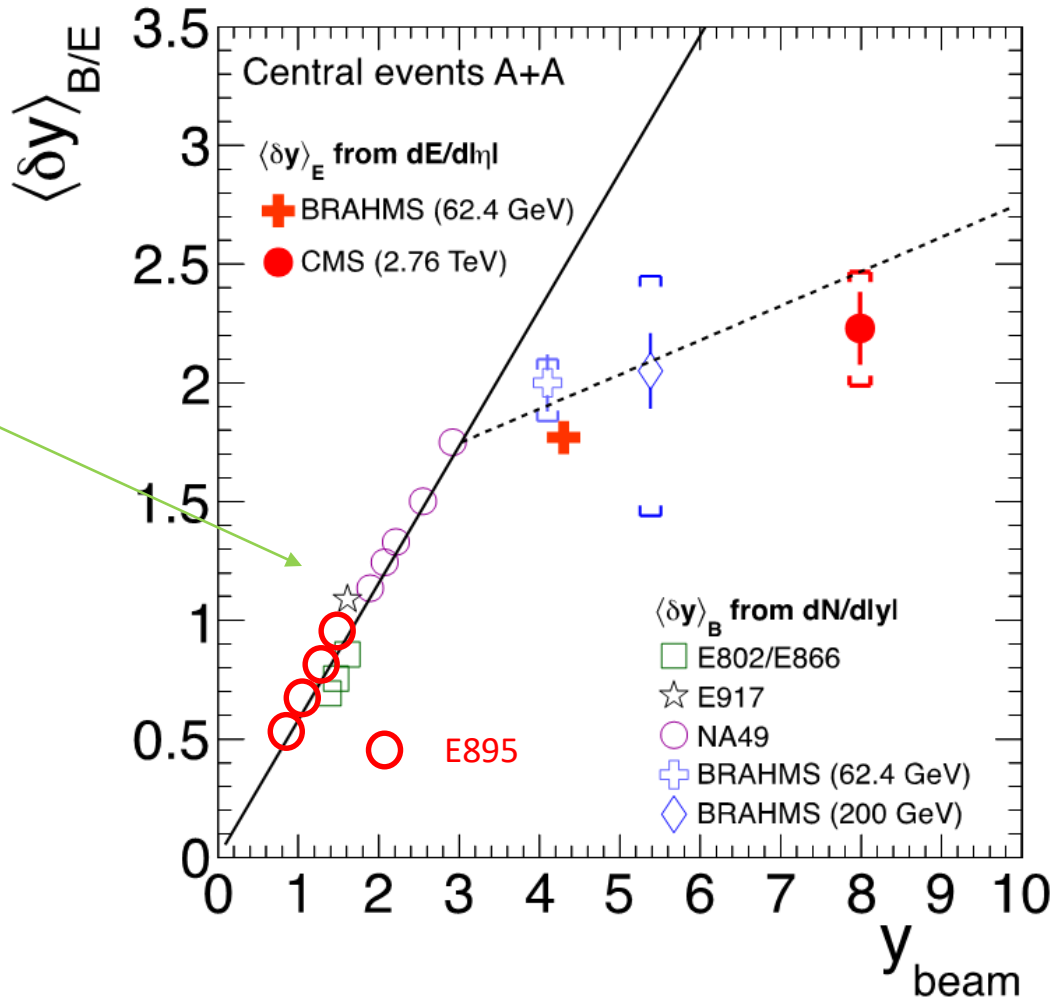


Evolution of stopping, a drop in stopping would indicate a development of transparency

# AGS Results: anti-protons and light nuclei

**Spectra – Other:**

- E864_PRC60(2000)064903 – neutron spectra and dN/dy at 10.5 AGeV
- E864_PRC61(2000)064908 – p, d, t, $^{3}$He, $^{4}$He spectra and yields at 10.5 AGeV
- E864_PRL85(2000)2685 – anti-deuteron yields at 10.5 AGeV
- E864_PRL79(1997)3351 – anti-proton yields at 10.5 AGeV
- E917_PRL(2001)242301 – anti-proton spectra at 10.5 AGeV
- E802_PRL81(1998)2650 – anti-proton spectra t 10.5 AGeV
- E814_PRC61(2000)044906 – deuteron spectra at 10.5 AGeV
- E802_PRC60(1990)064901 – deuteron spectra and dN/dy at 10.5 AGeV
- E814_PRC61(2000)044906 – t and $^{3}$He yields at 10.5 AGeV

Need to map these out across the AGS energy scan range

# AGS Results: Strangeness ($V^0$'s)

**$V^0$s – Kaons:**

- No spectra of yields

**$V^0$s – Lambdas:**

- E877_PRC63(2001)014902 – $\Lambda$ spectra and dN/dy at 10.5 AGeV
- E895_PRL91(2003)202301 – $\Lambda$ yields at 6 AGeV

**$V^0$s – Anti-Lambdas:**

- E917_PRL(2001)242301 – mid-rapidity yield at 10.5 AGeV

**$V^0$s – Phi:**

- E917_PRC69(2004)054901 – $\phi$ mid-rapidity spectra t 10.5 AGeV

**$V^0$s – Cascades:**

- E895_PRL91(2003)202301 – $\Xi^-$ yields at 6 AGeV

Need energy scan results to identify the turn on of multi-strange baryons

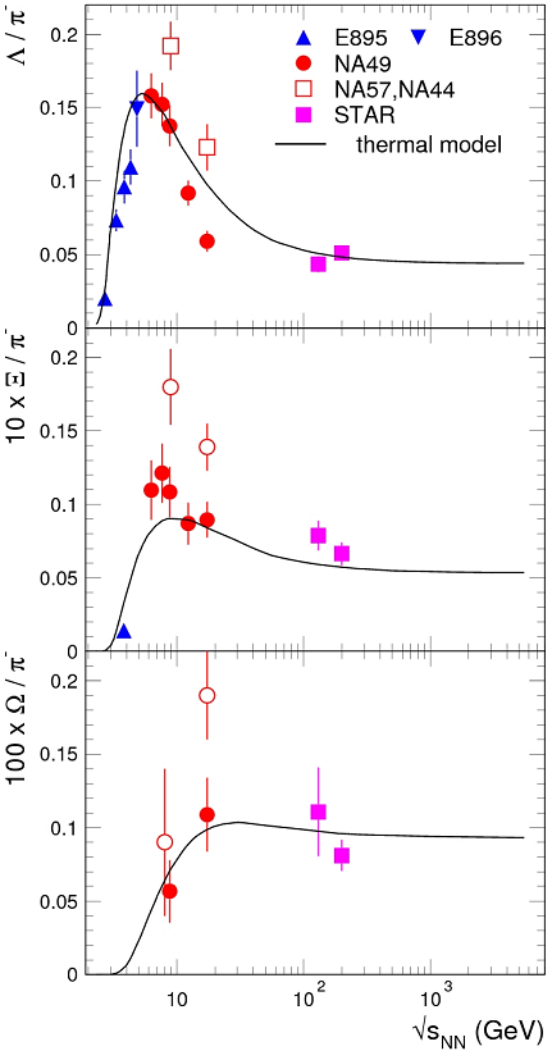

# AGS Results: Directed Flow

**Directed Flow – pions:**

- E877_PRC56(1997)3254 – $\pi^+$ and $\pi^-$ at 10.5 AGeV ← Need energy scan

Influenced by shadowing and Coulomb

**Directed Flow – Kaons:**

- E895_PRL85(2000)940 – $K^0_S$ at 6 AGeV ← Need charged kaons

Influenced by shadowing

**Directed Flow – Protons:**

- E895_PRL84(2000)5488 – at 2, 4, 6, 8 AGeV
- E877_PRC56(1997)3254 – at 10.5 AGeV

No anticipated minimum →

**Directed Flow – Anti-protons:**

- E877_PLB485(2000)319 – at 10.5 AGeV

← Need energy scan

**Directed Flow – Lambdas:**

- E895_PRL86(2001)2533 – at 2, 4, 6 AGeV
- E877_PRC63(2001)014902 – at 10.5 AGeV

Follow protons

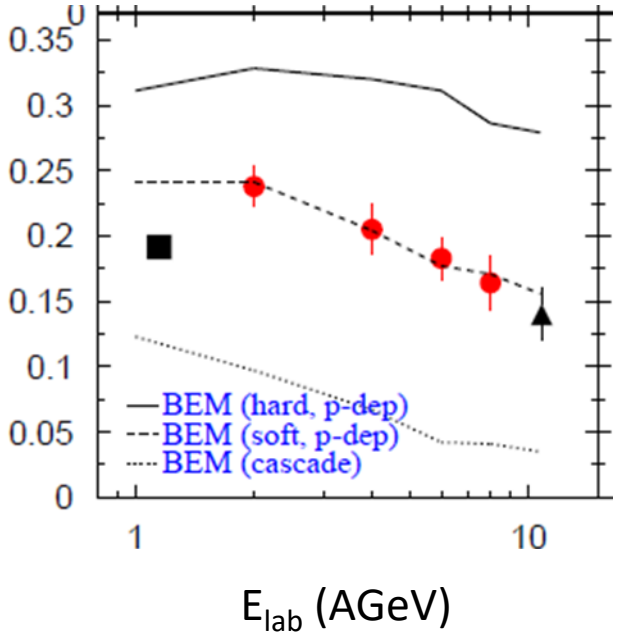

# AGS Results: Elliptic Flow

**Elliptic Flow – Protons:**

- E895_PRL83(1999)1295 – at 2, 4, 6, 8 AGeV
- E877_PRC56(1997)3254 – at 10.5 AGeV
- E895_PRC66(2002)021901 – at 2, 4, 6 AGeV with centrality cuts

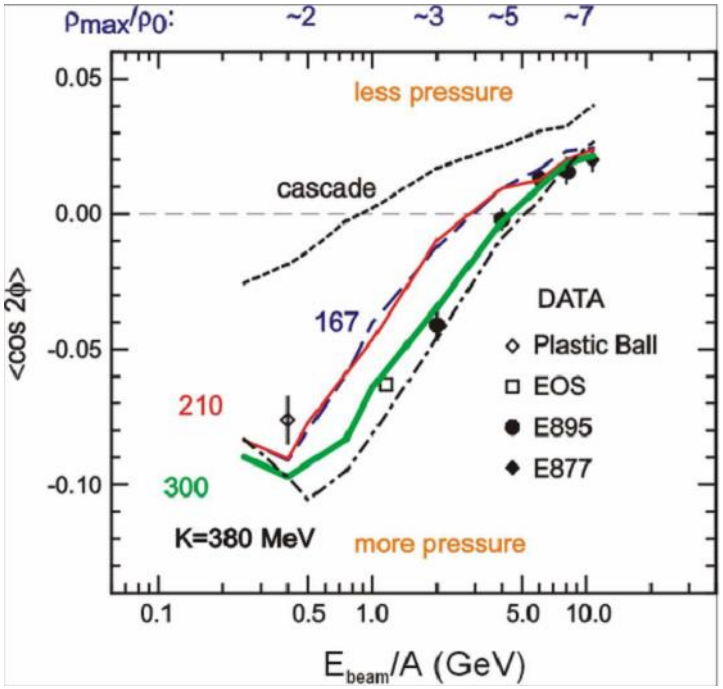


- Crossover from squeeze-out to in-plane at 4 AGeV
- Relevance to the change of stiffness of EoS?

Need other particle species

# AGS Results: HBT

**HBT – Pions:**

- E895_PRL84(2000)2798 – $R_{out}$, $R_{side}$, $R_{long}$ at 2, 4, 6, 8 AGeV
- E802_PRC66(2002)054096 – $R_{out}$, $R_{side}$, $R_{long}$ at 10.5 AGeV
- E877_PRL78(1997)2916 – $R_{out}$, $R_{side}$, $R_{long}$ at 10.5 AGeV

**HBT – protons:**

- E814_PRC60(1999)054905 – correlation functions for protons

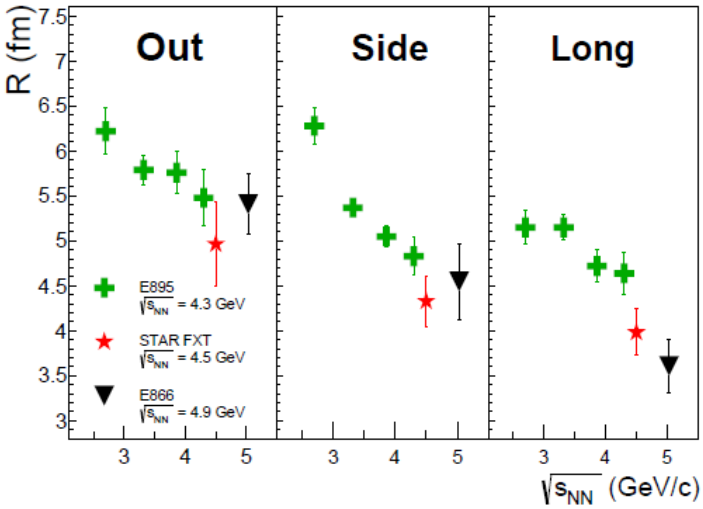


Across the AGS energy range, the source radii are falling

- Need to do negative pion positive pions separately
- Need to get the "tilt" angle
- Need more pp HBT

# Fixed-Target Program

The Fixed-Target Program will extend the reach of the RHIC BES to higher $\mu_B$.

Goals:

1) Search for evidence of the first entrance into the mixed phase
2) Control measurements for BES collider program searches for Onset of Deconfinement
3) Control measurements for Critical Point searches

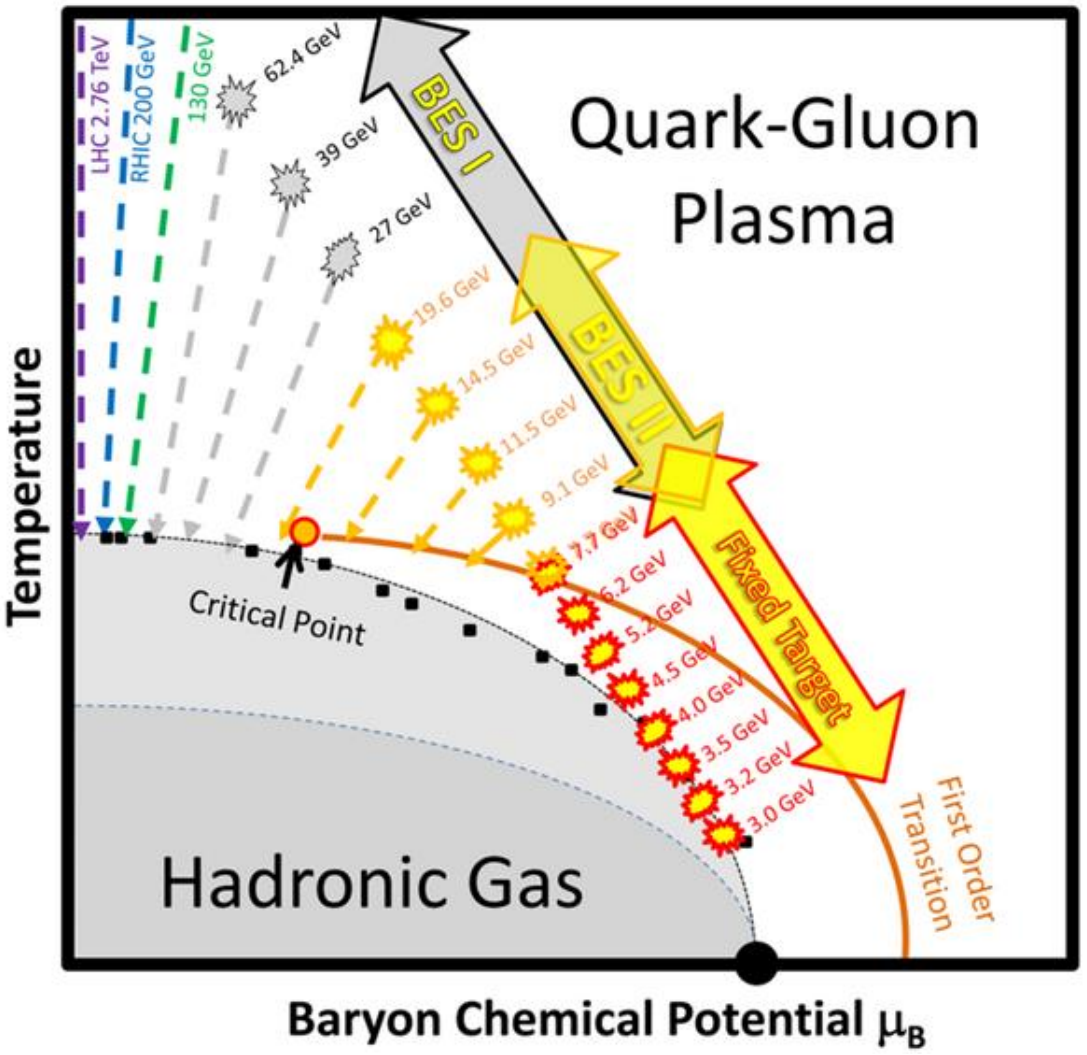

# History of Low Energy Running at RHIC

## RHIC Runs at or Below Nominal Injection Energy:

| | | |
|---|---|---|
| 1. | Au+Au 19.6 GeV 2001 | 100 k events |
| 2. | Cu+Cu 22.4 GeV 2005 | 250 k events |
| 3. | Au+Au 9.0 GeV 2007 | 0 events |
| 4. | Au+Au 9.2 GeV 2008 | 7 k events |
| 5. | Au+Au 7.7 GeV 2010 | 4 M events |
| 6. | Au+Au 11.5 GeV 2010 | 12 M events |
| 7. | Au+Au 5.5 GeV 2010 | 0 events |
| 8. | Au+Au 19.6 GeV 2011 | 36 M events |
| 9. | Au+Au 5.0 GeV 2011 | 1 event |
| 10. | Au+Au 14.5 GeV 2014 | 20 M events |

We learned that background was a serious concern

We conclude that RHIC can not achieve a useful collider event rate at 5.0 GeV

STAR and RHIC recognized the importance to run at energies down to and below 7.7 GeV

# Studies using Beam Halo Background

# 2010 - 2014

Goals:

- Understand the Beam Halo Background
- Determine the applicability of STAR for fixed-target
- First of FXT results ➔ Au+Al

# Beam Halo on Al Vacuum Pipe

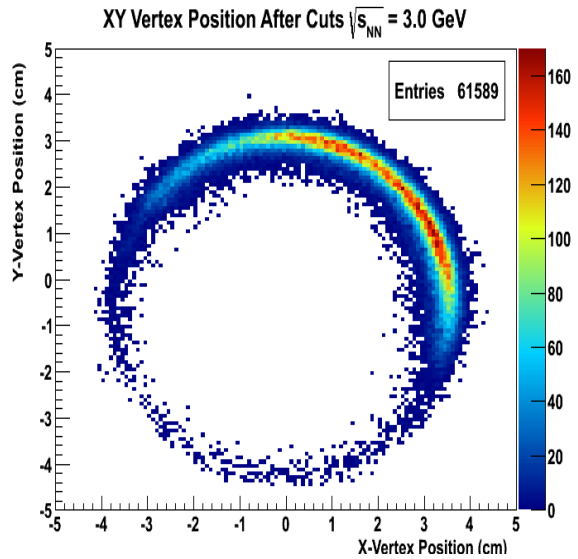


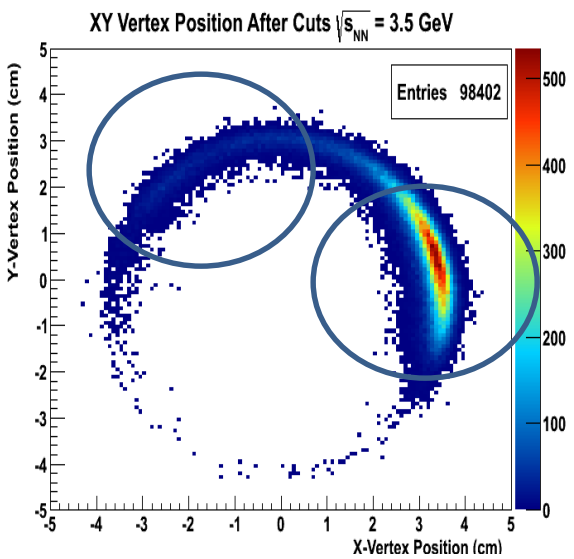


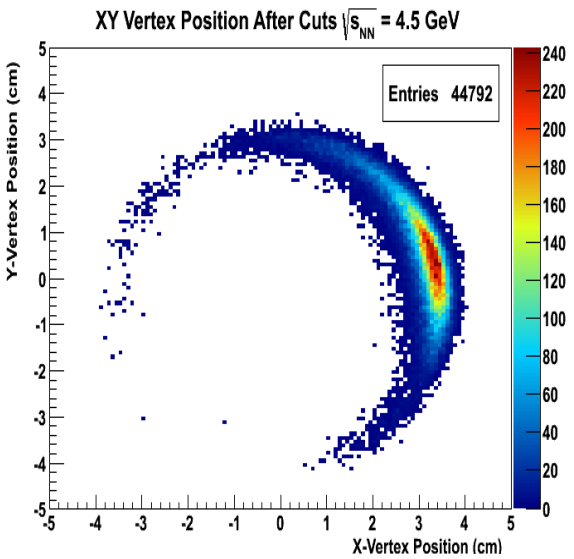


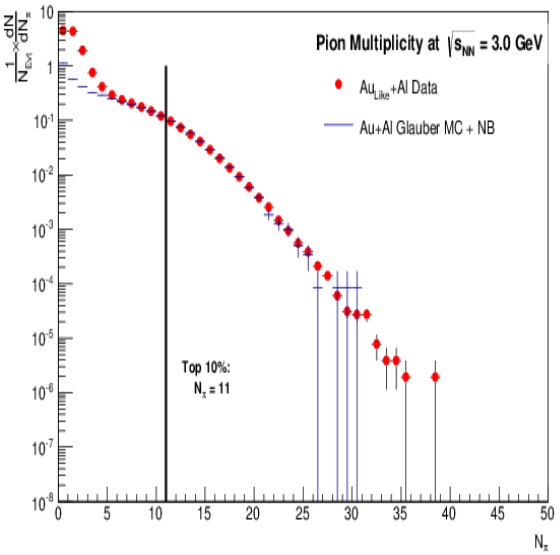


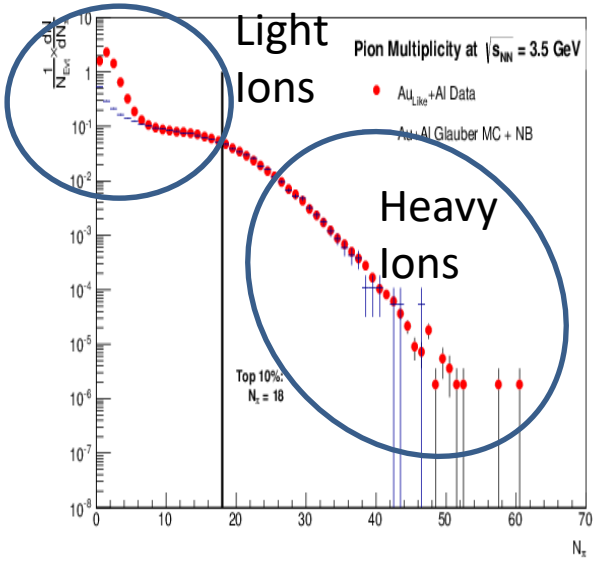


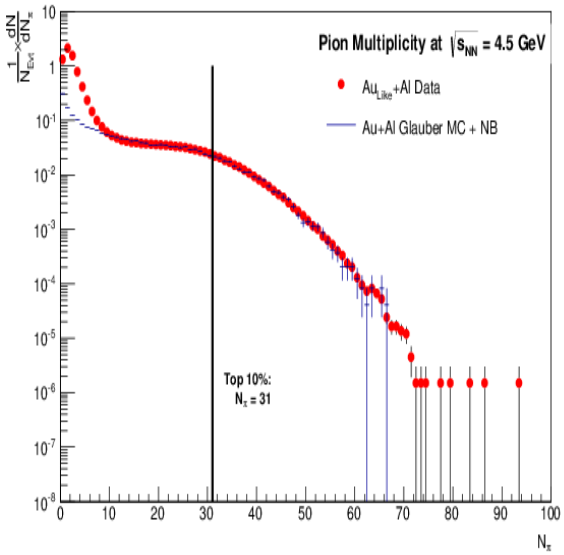

# Pion Ratio Analysis

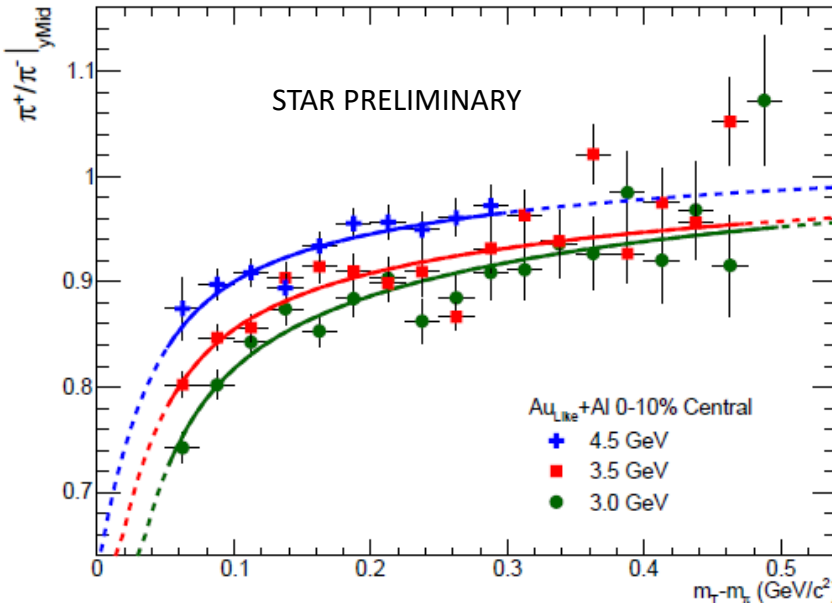


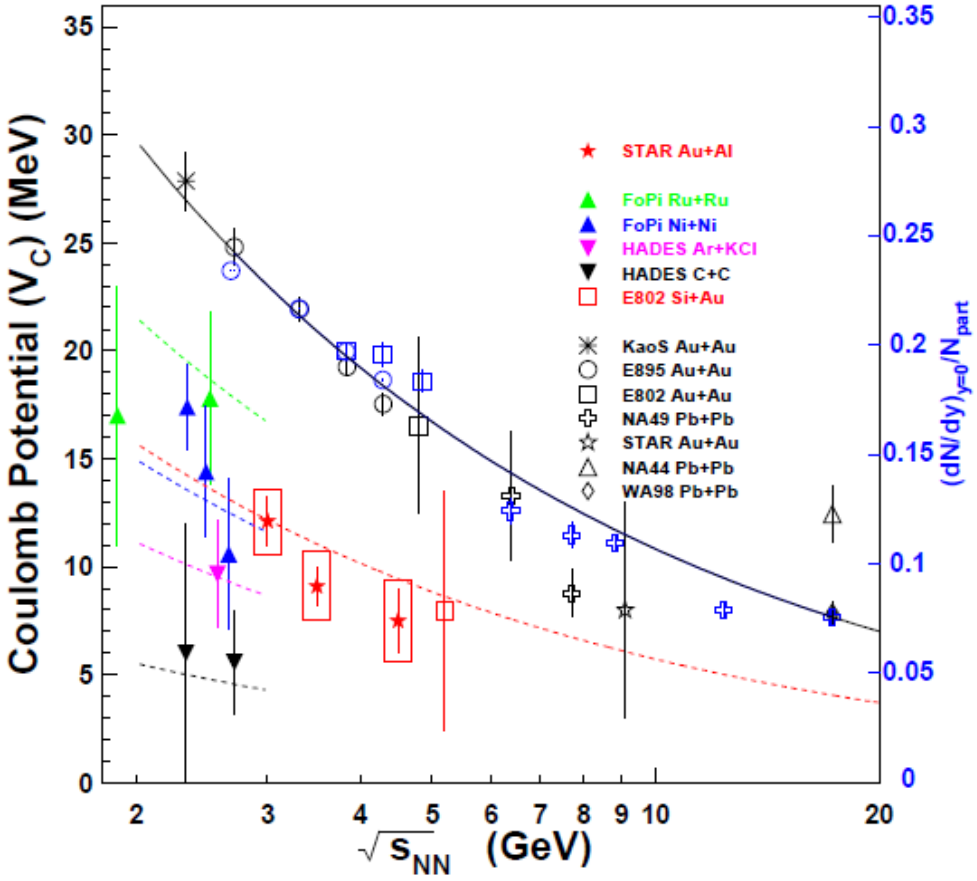


We conclude that there are gold nuclei in the beam halo

# Target Design 2014 and 2015

The success of the beam pipe studies motivated installing an internal gold target

**Target design:**

**Gold foil**
**1 mm Thick (4%)**
**~1 cm High**
**~4 cm Wide**
**~2 cm below beam axis**
**210 cm from IR**

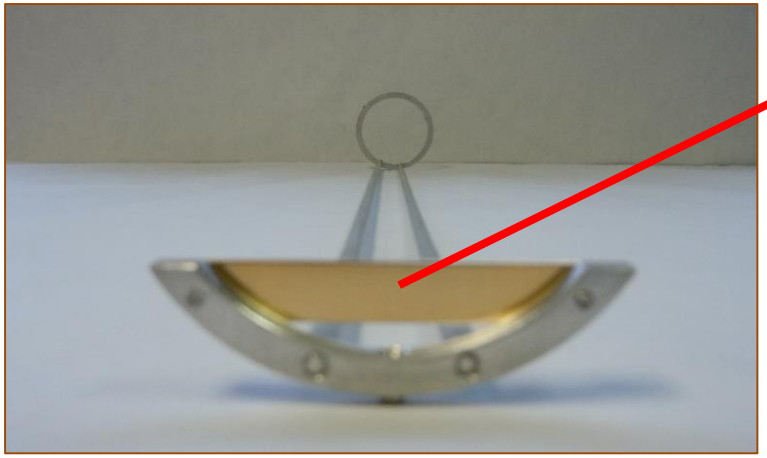

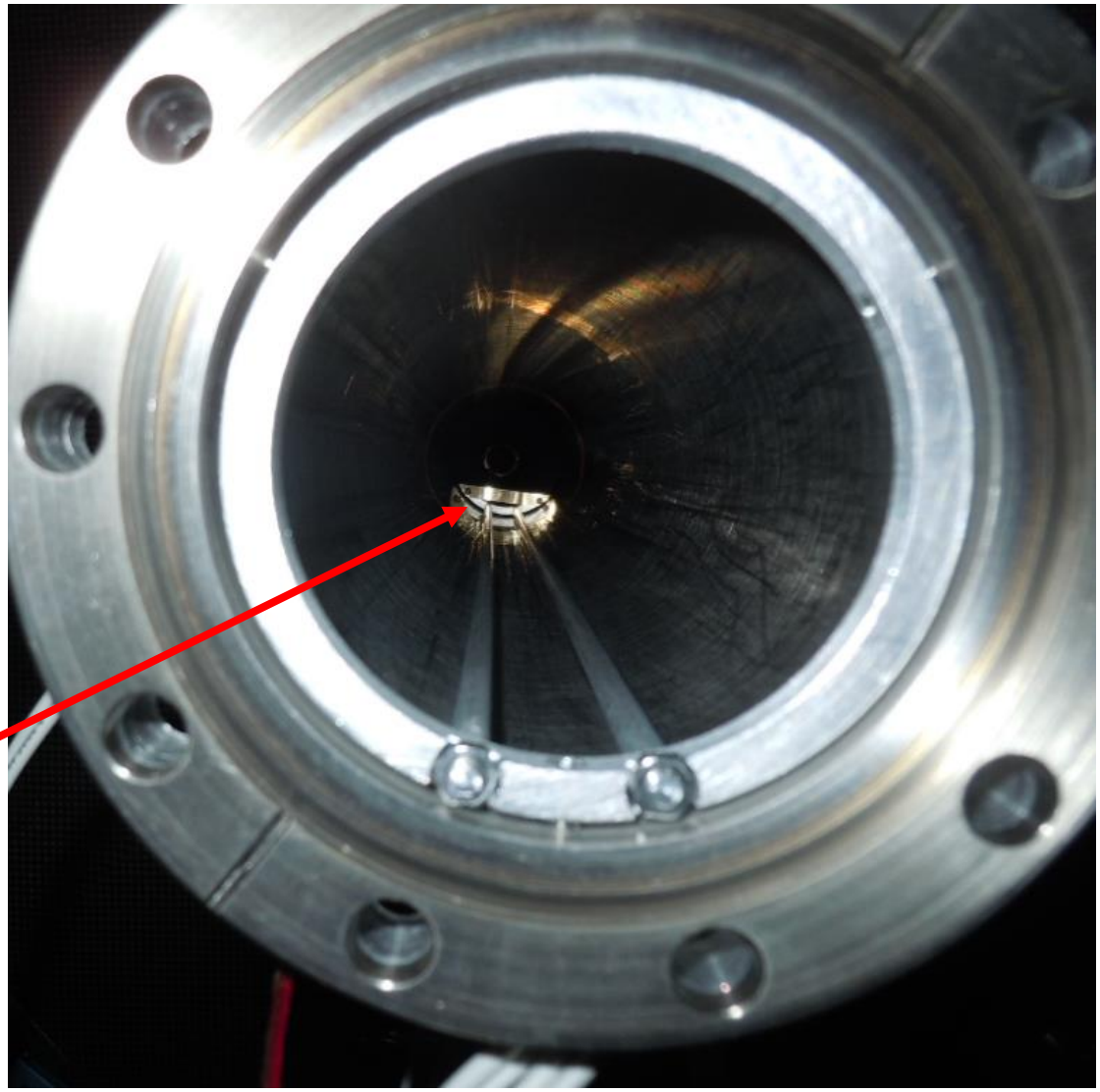

# 2014 ➔ 3.9 GeV Au halo + Au target

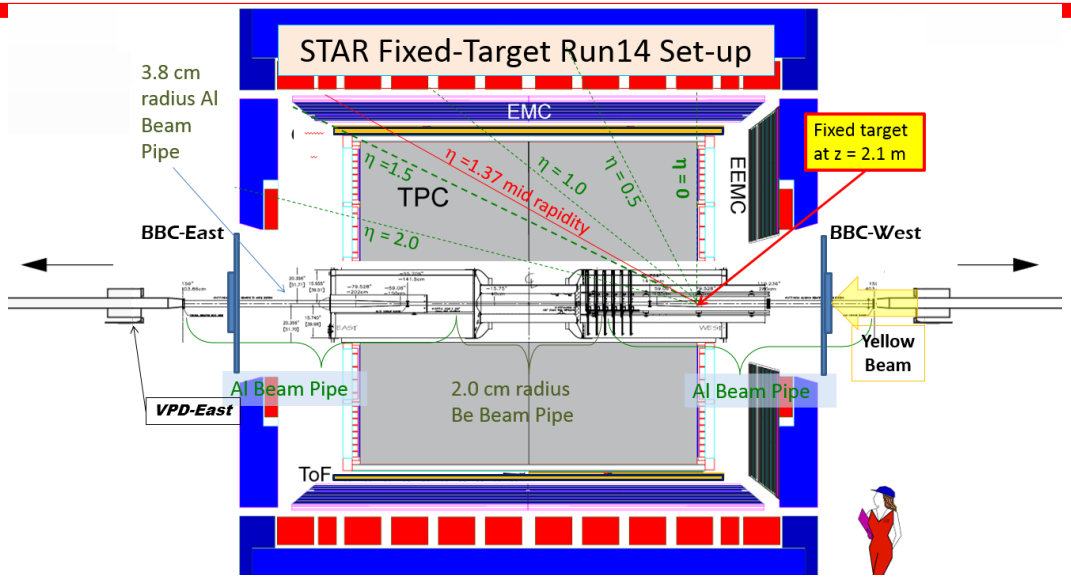


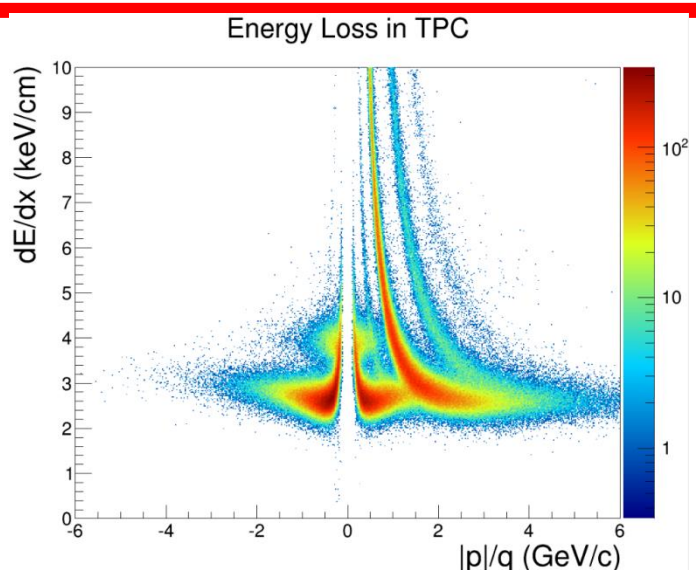


Lots of background, but the target events are evident

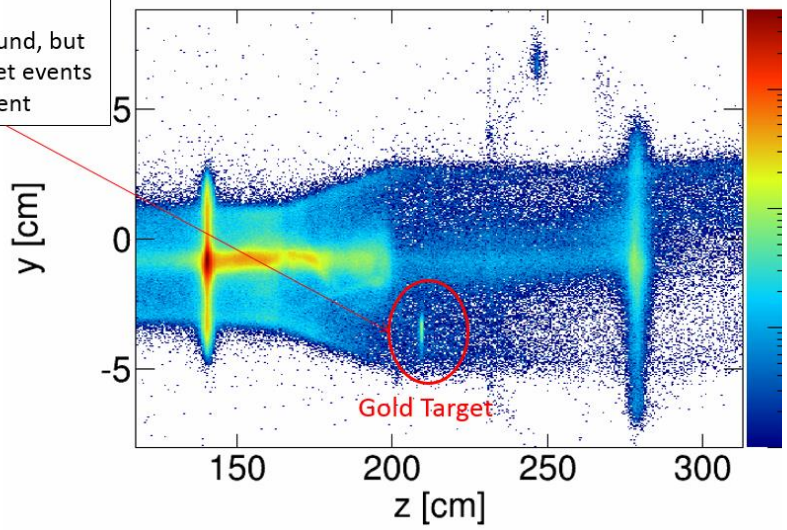


The most intense beam halo is deflected by the dipole magnets in the positive *x* direction. These are $Au_{Halo}$+$Al_{Beampipe}$ background

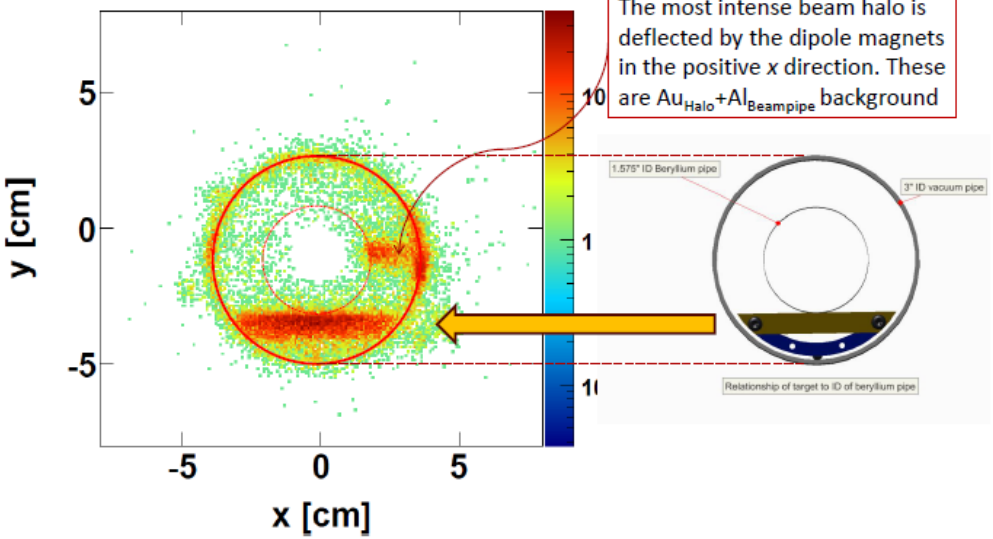

# Direct Beam Test Run 2015

**Goals:**

- Check the conclusion that there are gold ions in the halo
- Determine if the direct beam is a better conduct of operations
- Acquire enough data for significant feasibility studies
- Physics Analyses ➔ Reproduction of AGS results

# FXT Results: pion spectra

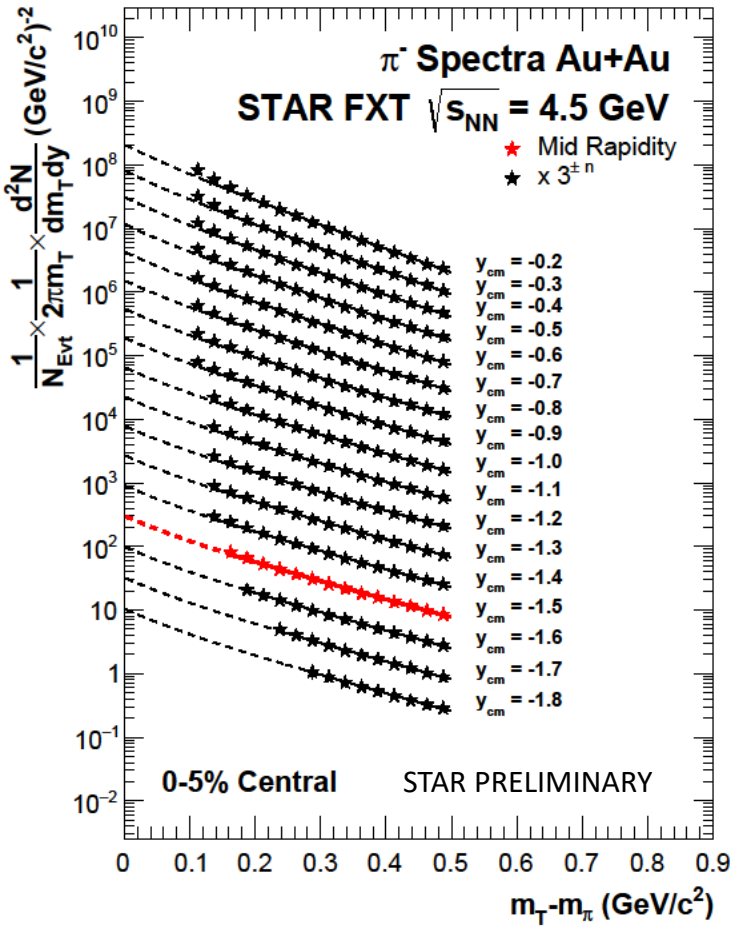


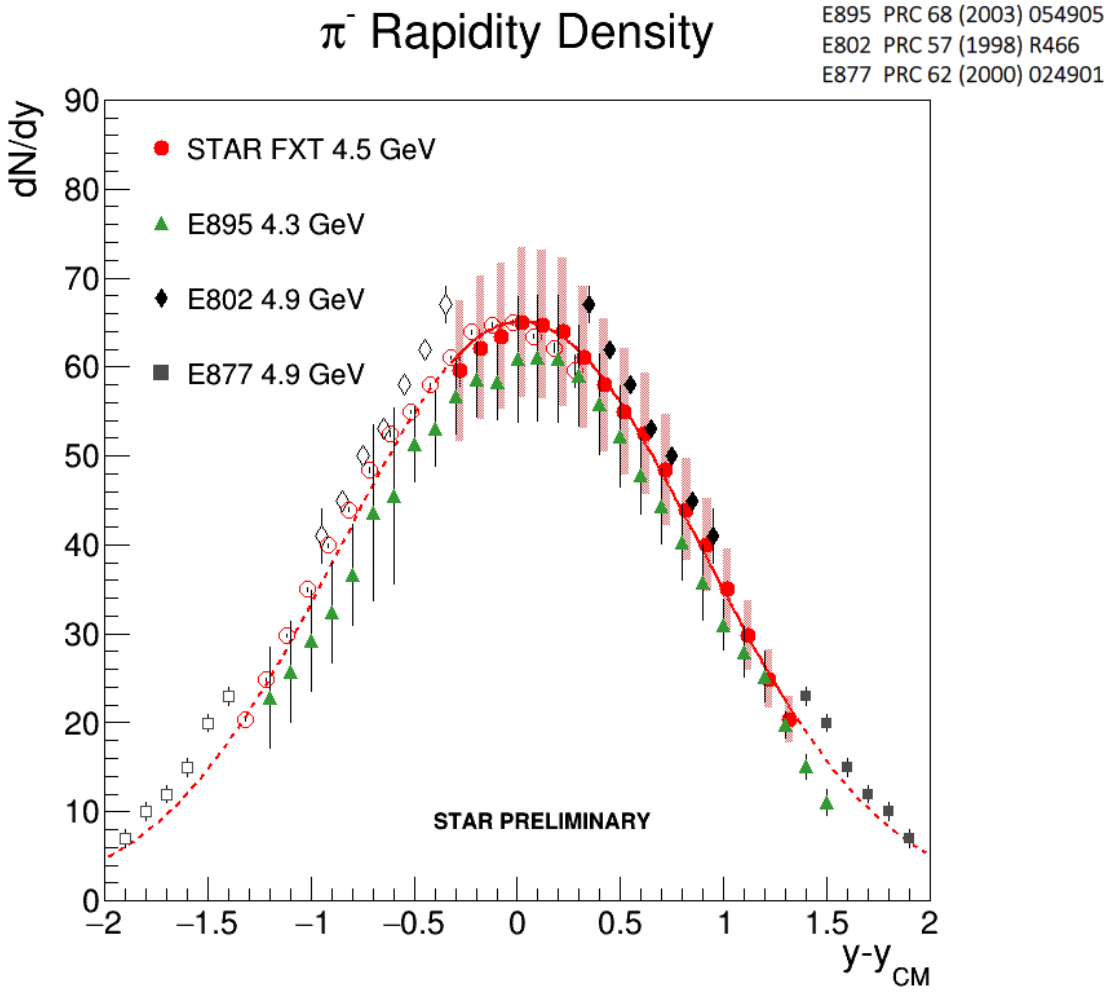


Consistent with AGS results

# FXT Results: proton spectra

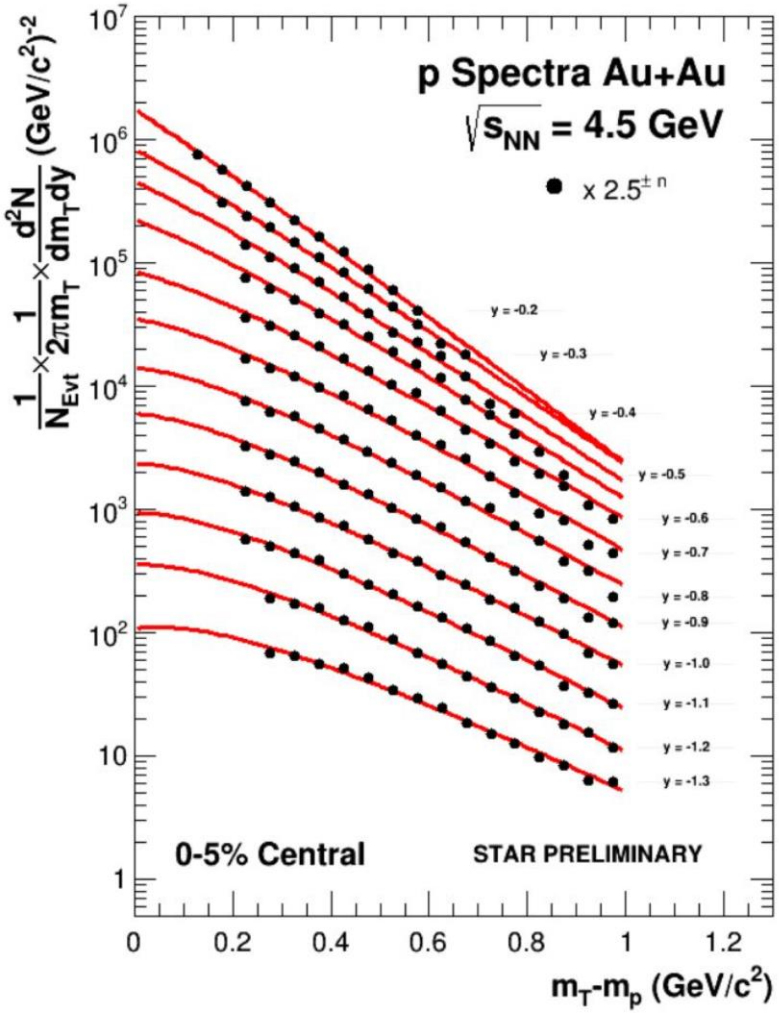


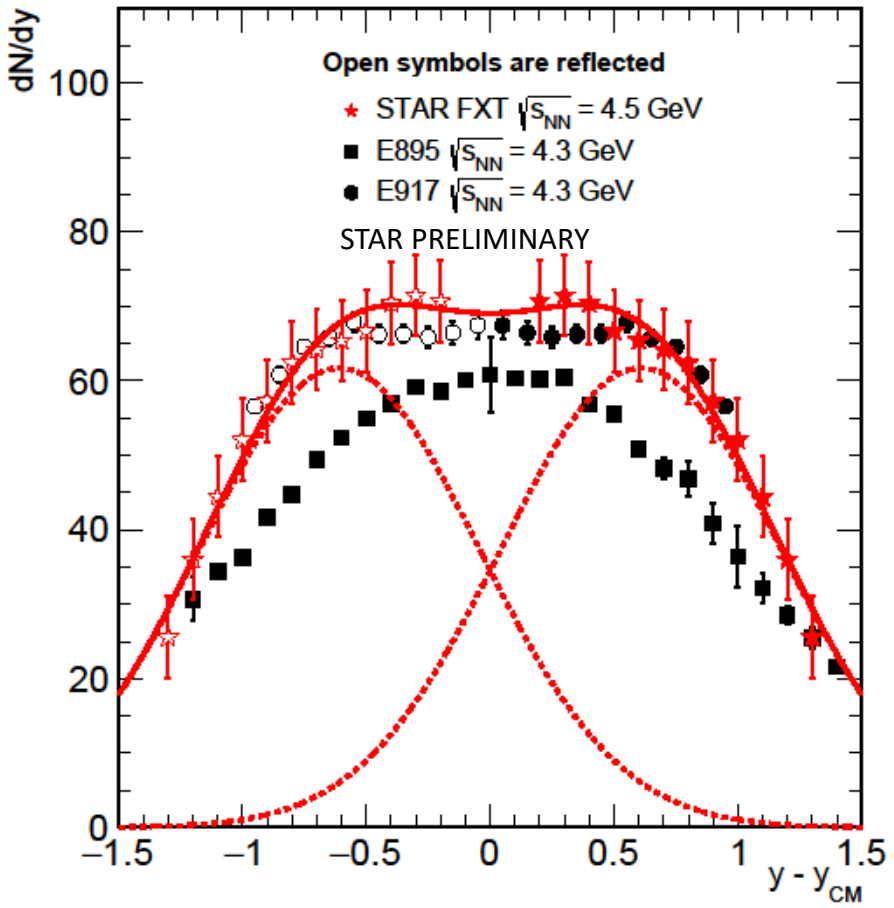


Consistent with AGS results (*)

# FXT Results: $V^0$ yields

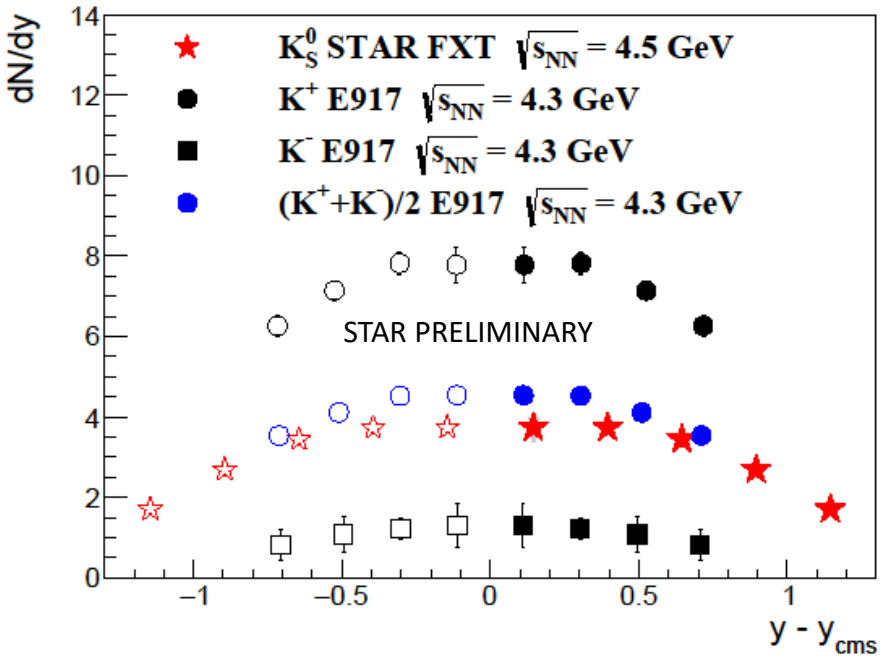


No AGS $K^0_S$ results at this energy
But similar to $K^+/K^-$ average

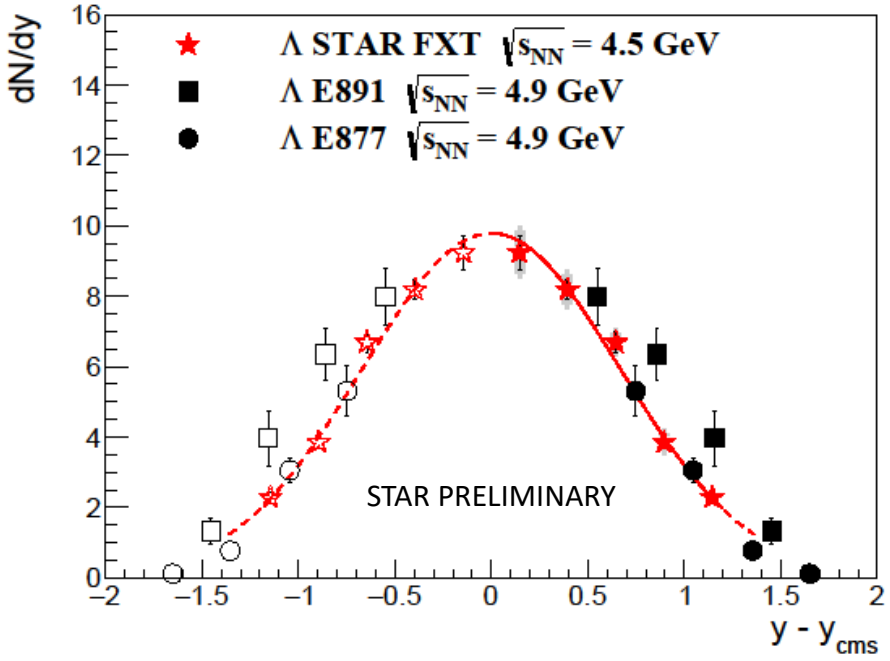


Consistent with AGS results

# FXT Results: spectra overview

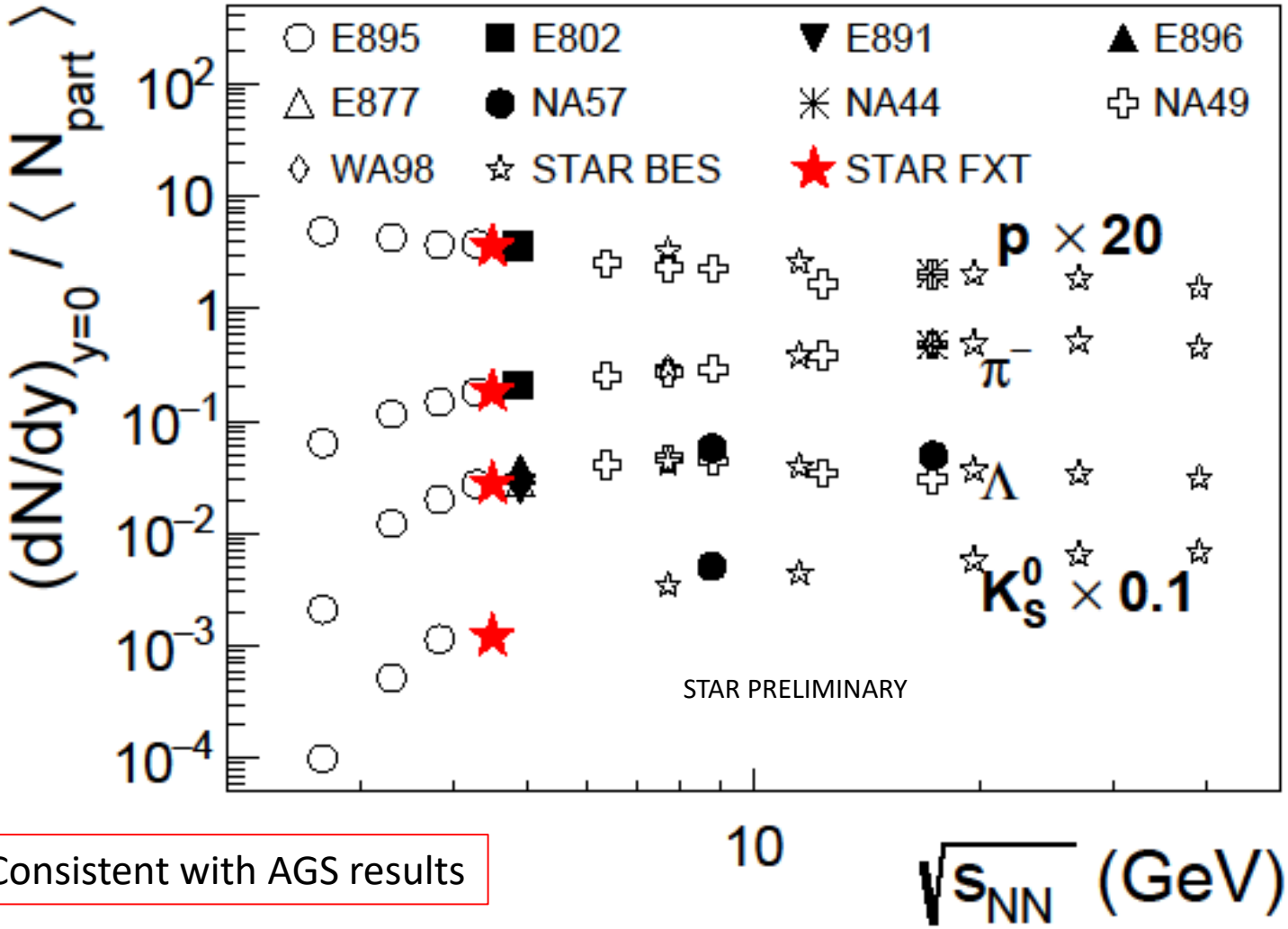


E896 PRL 88 (2002) 062301
NA44 PRC 66 (2002) 044907
NA49 JPG 30 (2004) S701
NA49 PRL 93 (2004) 022302
NA57 JPG:NPP 32 (2006) 2065
WA98 PRC 67 (2003) 014906
E895 RPC 68 (2003) 054905
E895 NPA 698 (2002) 495c
E917 PLB 476 (2000) 1
E802 NPA 610 (1996) 139c
E877 PRC 63 (2001) 014902
E891 PLB 382 (1996) 35

Consistent with AGS results

# FXT Results: baryon directed flow

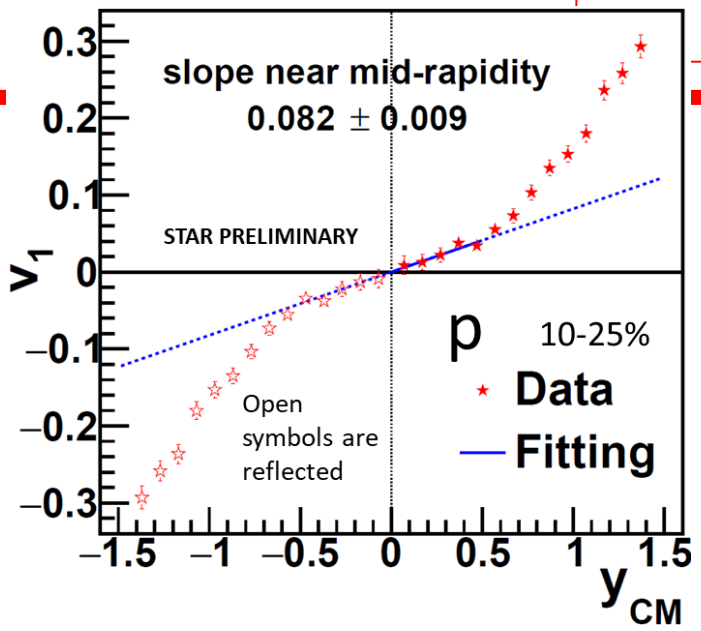


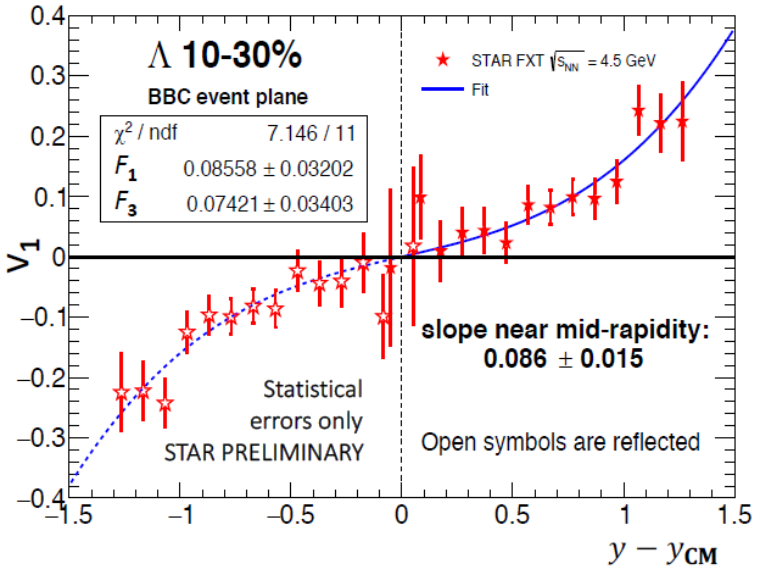


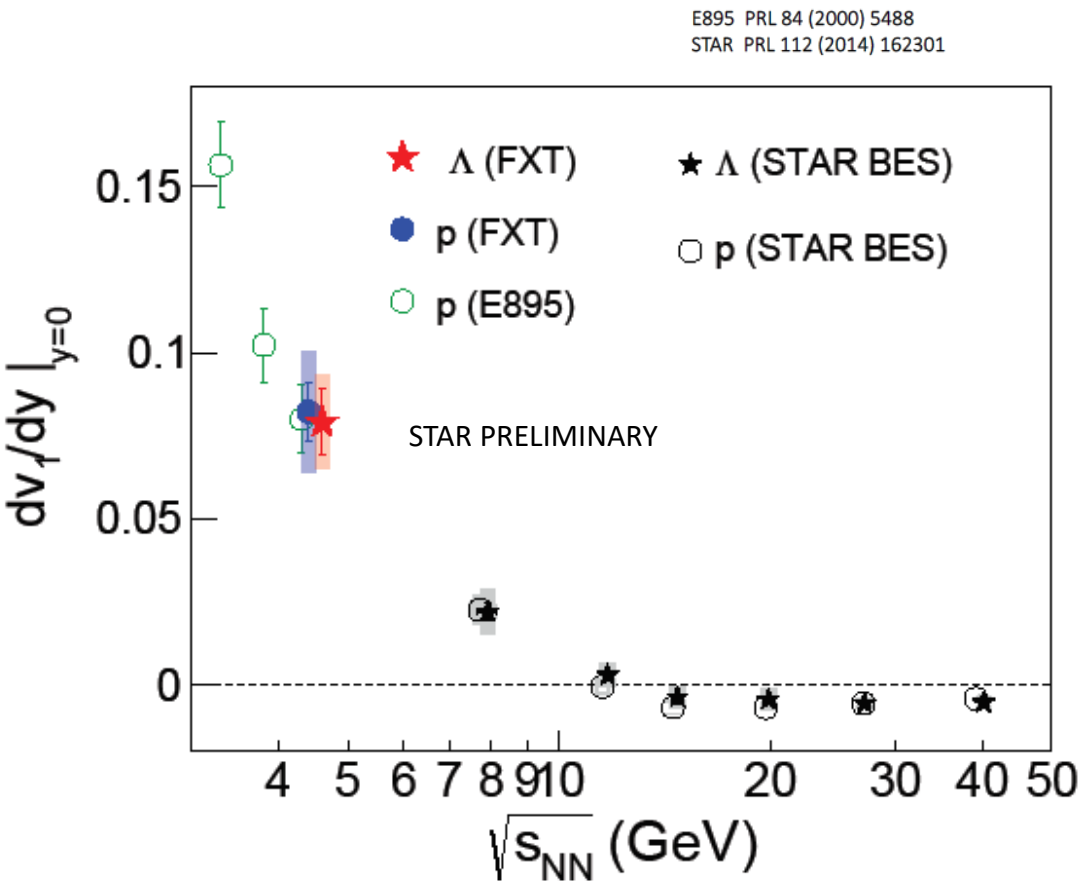


Consistent with proton results (*)

# FXT Results: meson directed flow

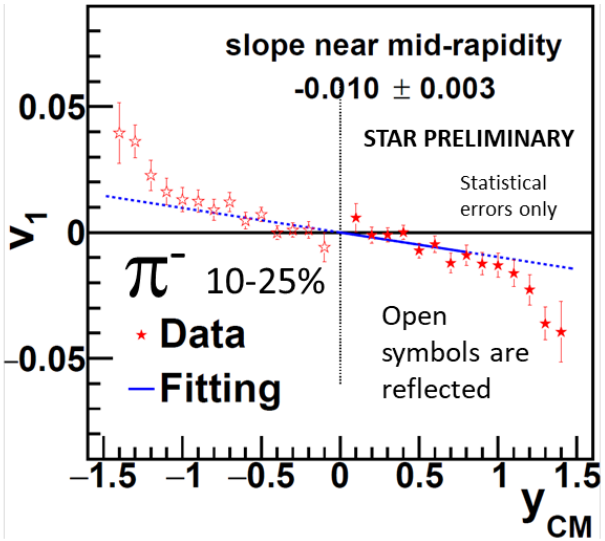


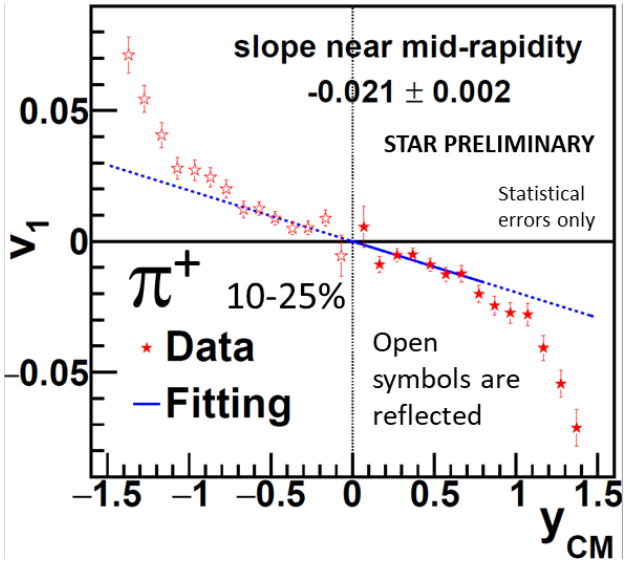


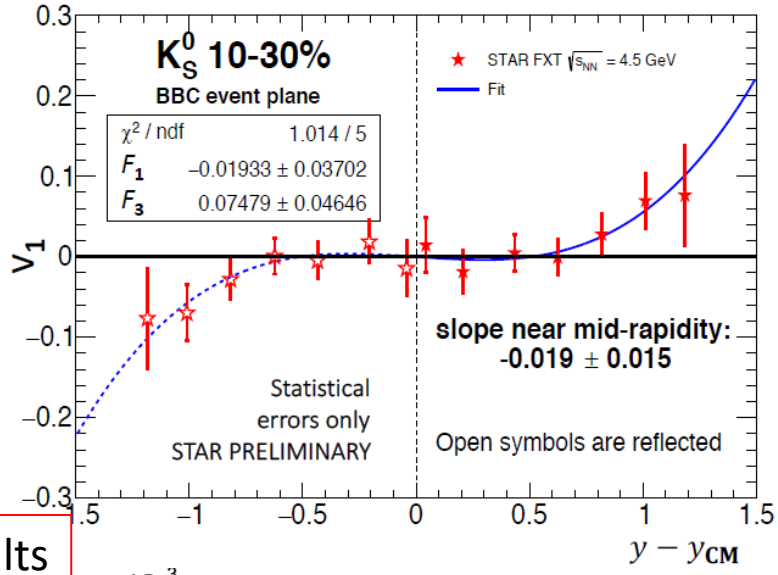


No AGS results

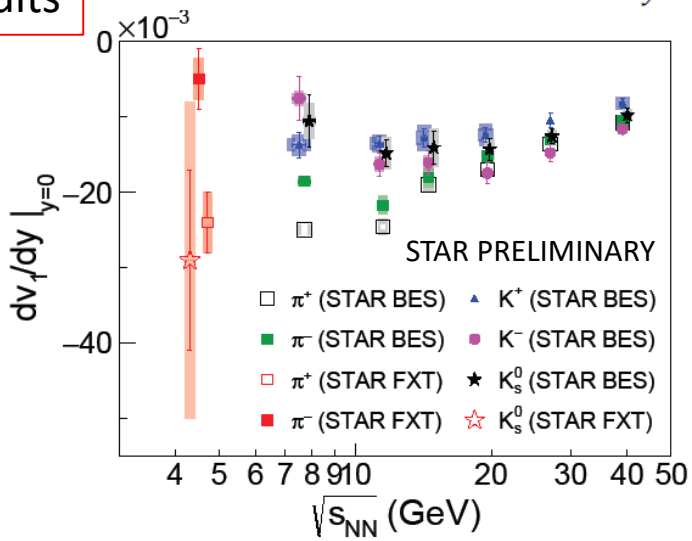

# FXT Results: proton elliptic flow

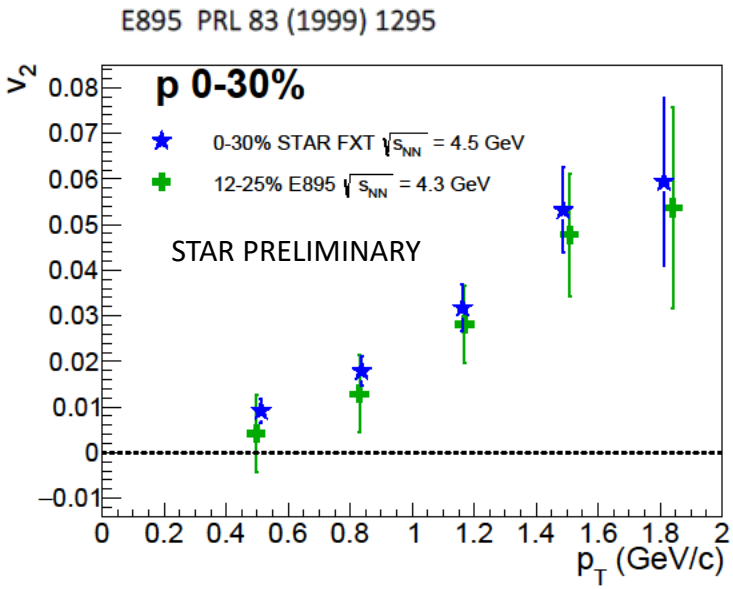


Consistent with AGS results

Consistent with AGS proton results
No AGS pion results

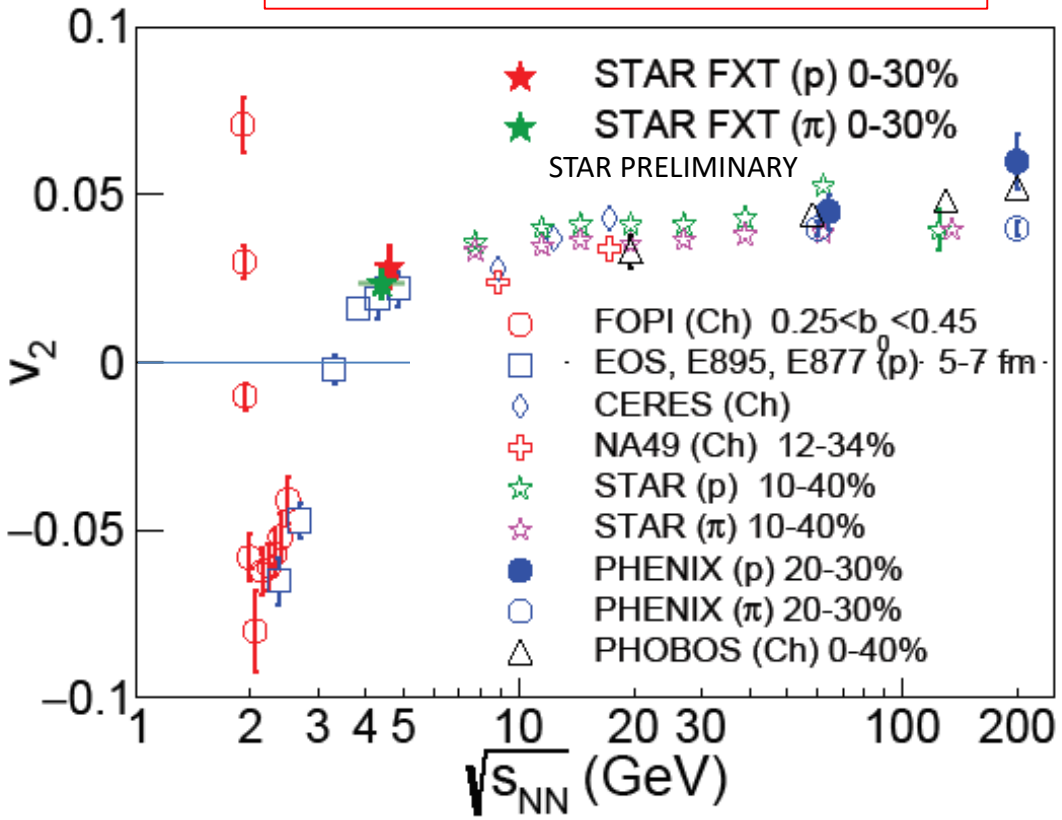

# FXT Results: HBT

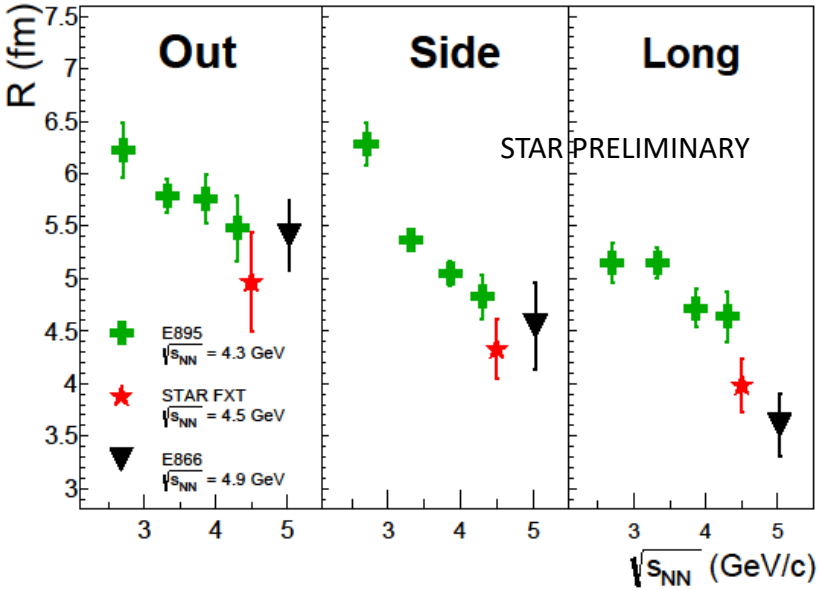


Consistent with AGS results

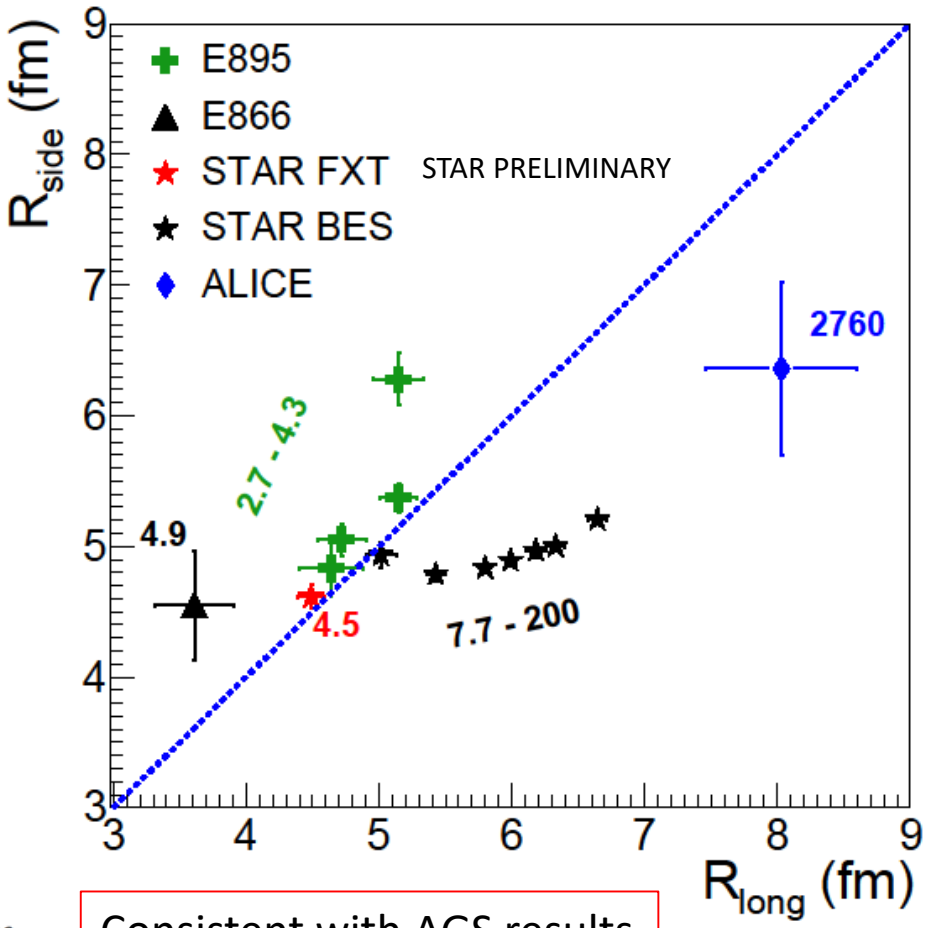


Consistent with AGS results

E866 PRC 66 (2002) 054096
E895 PRL 84 (2000) 2798
ALICE PRB 696 (2011) 328
STAR PRC 92 (2015) 14904

# 2018 ➔ 3.85 GeV Au+Au ($\sqrt{s_{NN}}$ = 3.0 GeV) Data Set

Data taking started: Thursday 31 May 2018  03:19 EDT with Run 19151029

Data taking completed: Monday 04 June 2018  07:48 EDT with Run 19155021

Total hours of beam: 60

Total physics triggers: 340 Million

Total good events: 309 Million

Tigger efficiency: 90%

First FXT Physics Run
Result should be available soon

(*Also, we took 7.2 GeV Au+Au FXT data for 72 hours, for a total of 237 M triggers*)

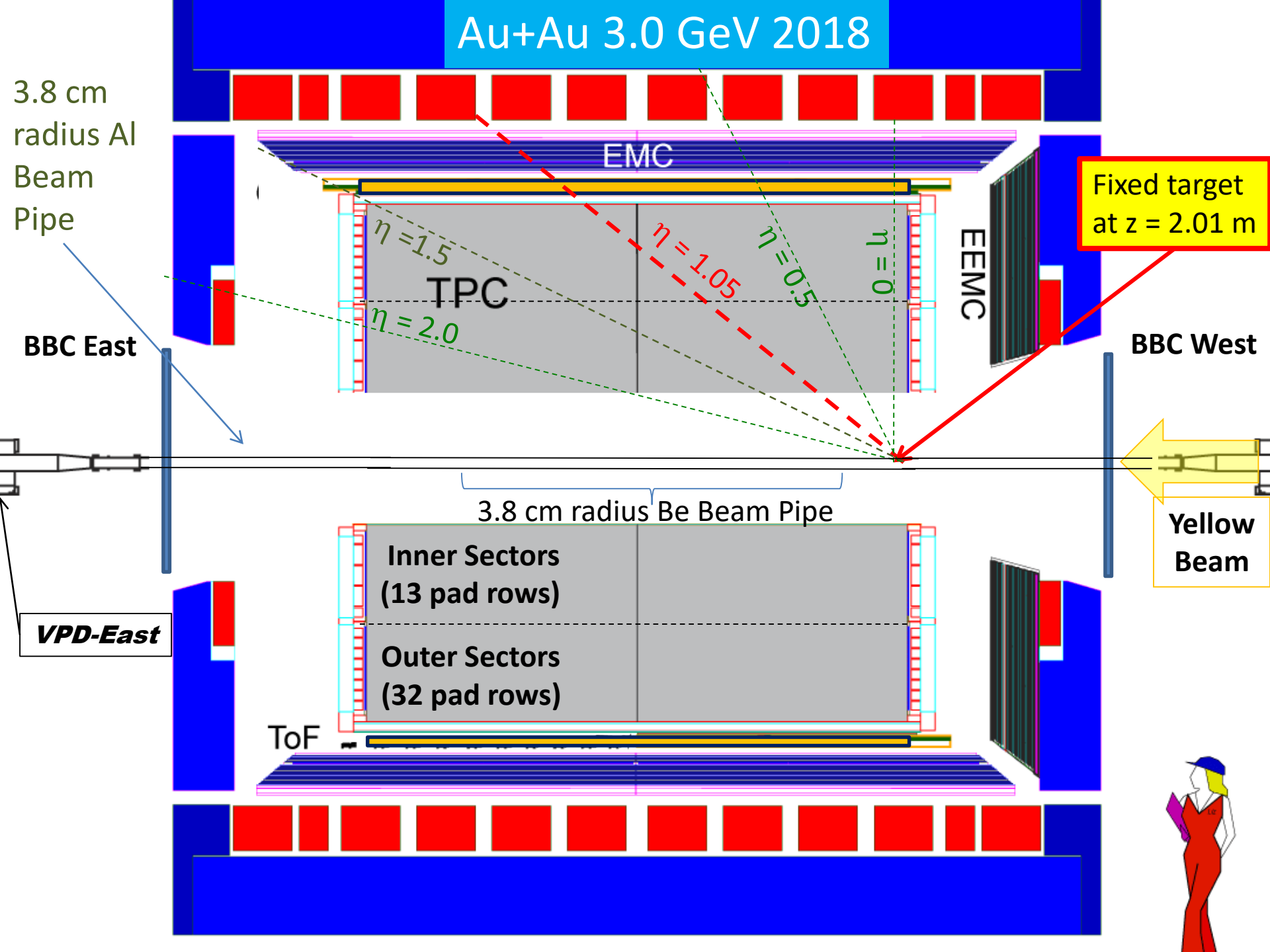
Au+Au 3.0 GeV 2018
3.8 cm radius Al Beam Pipe
EMC
EEMC
Fixed target at z = 2.01 m
η =1.5
η = 1.05
η =0.5
η = 0
TPC
η = 2.0
BBC East
BBC West
3.8 cm radius Be Beam Pipe
Yellow Beam
Inner Sectors (13 pad rows)
Outer Sectors (32 pad rows)
VPD-East
ToF

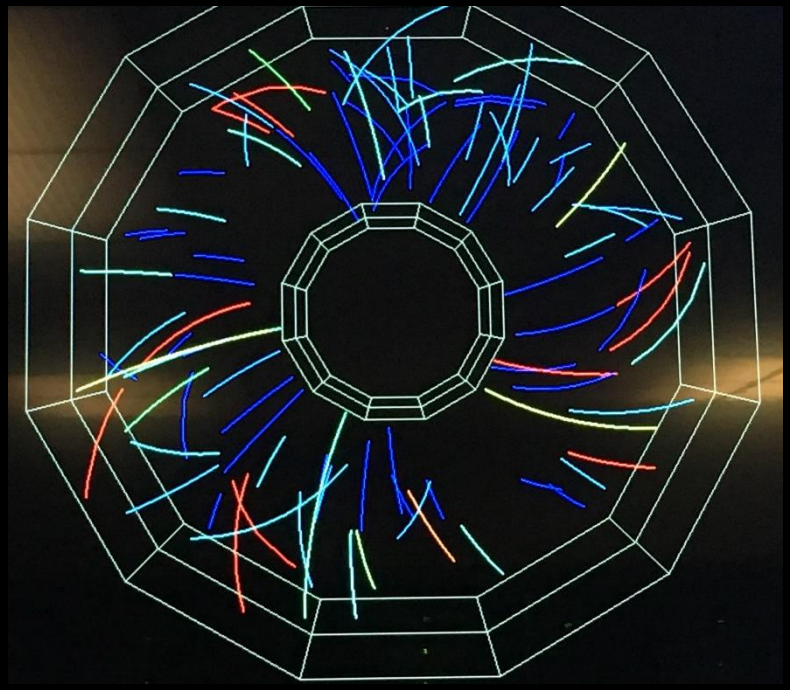

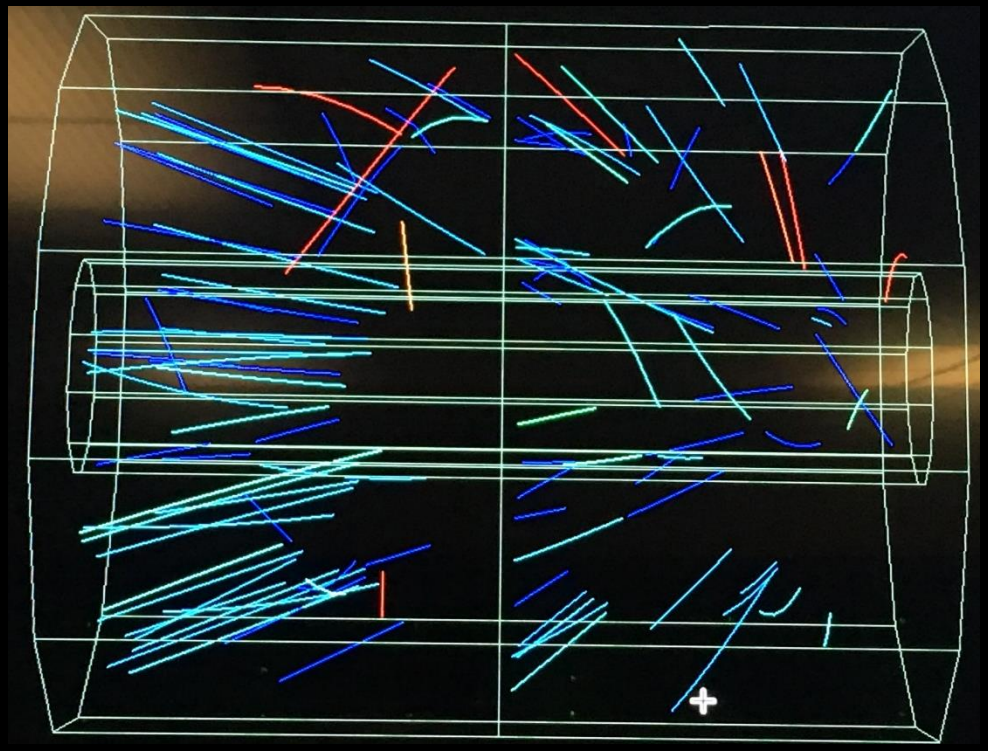

**Well centered beam spot; no background**

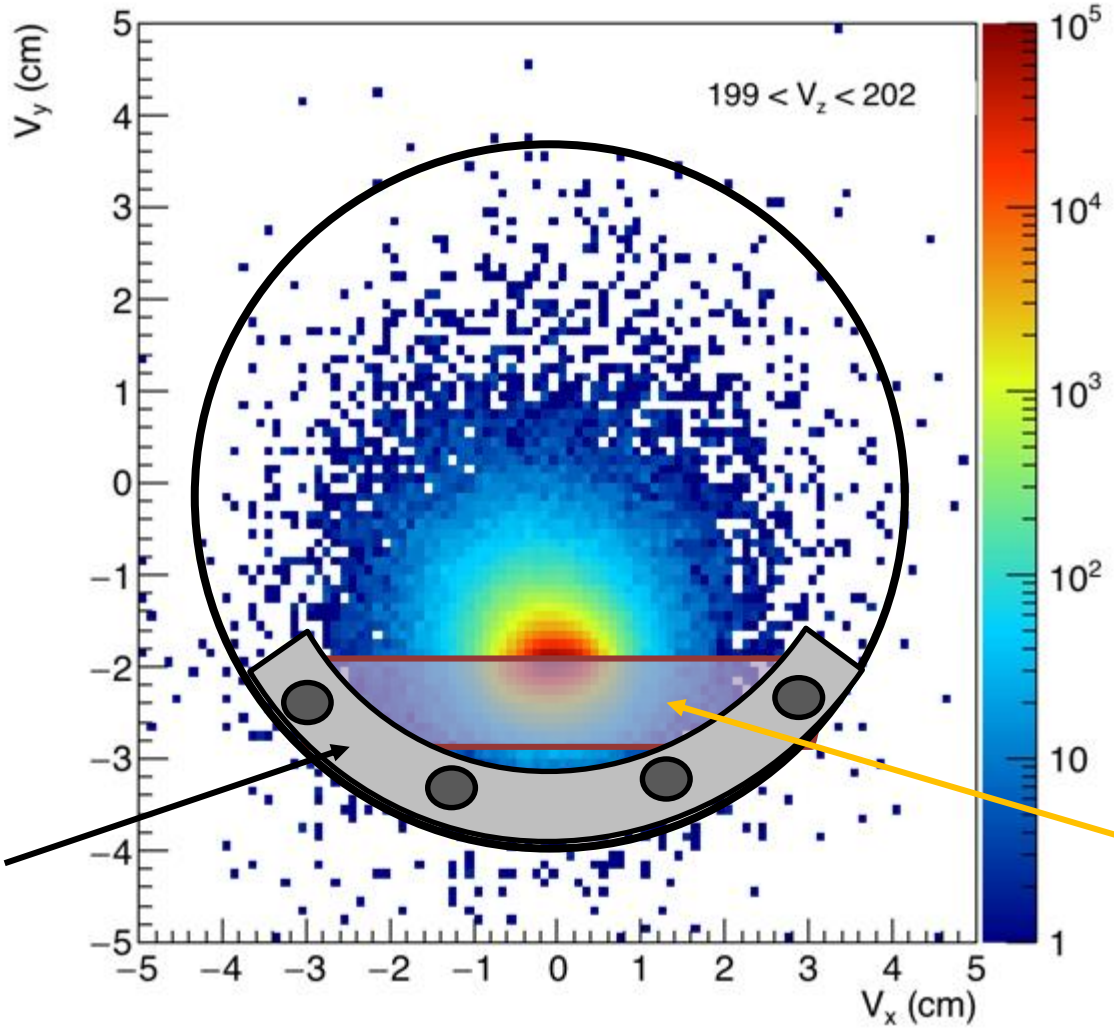

**Centrality ➔ established minimum bias trigger**

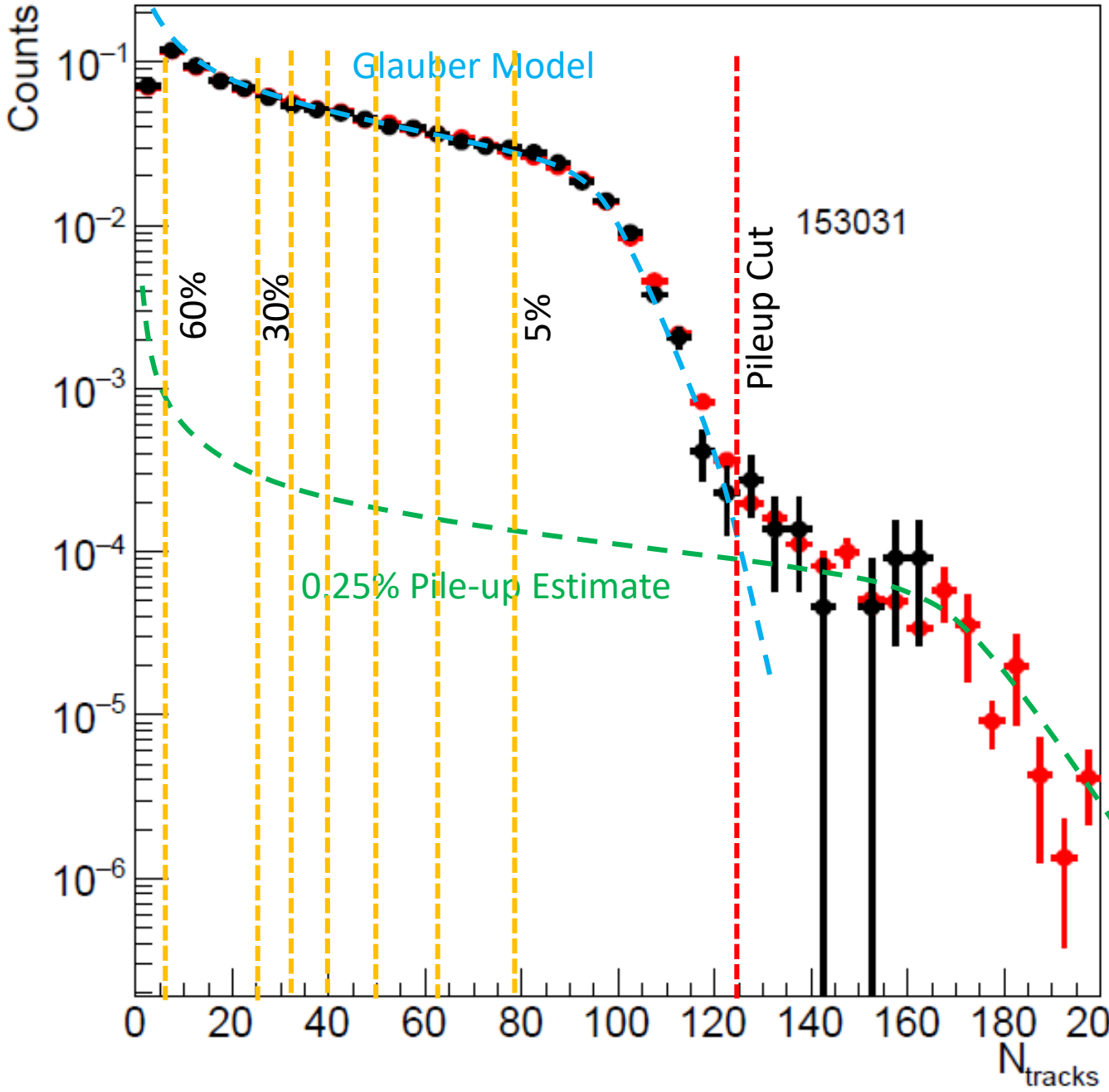

# Physics Goals of the FXT Program

**The Onset of Deconfinement:**

- High $p_T$ suppression
- $N_{CQ}$ scaling of Elliptic Flow
- LPV through three particle correlators (CME)
- Balance Functions
- Strangeness Enhancement

**Compressibility ➔ First Order Phase Transition**

- Directed flow
- Tilt angle of the HBT source
- The Volume of the HBT source
- The width of the pion rapidity distributions (Dale)
- The zero crossing of the elliptic flow (~6 AGeV)
- Volume measures from Coulomb Potential

**Criticality:**

- Higher moments
- Particle Ratio Fluctuations

**Chirality:**

- Dilepton studies

No measurements in this energy range

**Hypernuclei:** ➔ Lifetime of the hypertriton

**What a STAR FXT Program will not do:**

- Omega's
- Charm
- Doublely Hyper nuclei
- p+p scan
- p+A scan
- peripheral collisions
- > 200 Million event per energy
- > two weeks of beam time

# Plans for the Future 2019-2021

- Full FXT proposal was included in the May 2018 Beam Use Request
- Approved to run three energies in 2019
- Additional energies will be scheduled in 2020 and 2021

# FXT Program

| Collider Energy | Fixed-Target Energy | Single beam AGeV | Center-of-mass Rapidity | $\mu_B$ (MeV) | Year to complete |
|---|---|---|---|---|---|
| 62.4 | 7.7 | 30.3 | 2.10 | 420 | 2019 |
| 39 | 6.2 | 18.6 | 1.87 | 487 | 2021? |
| 27 | 5.2 | 12.6 | 1.68 | 541 | 2021? |
| 19.6 | 4.5 | 8.9 | 1.52 | 589 | 2019 |
| 14.5 | 3.9 | 6.3 | 1.37 | 633 | 2019 |
| 11.5 | 3.5 | 4.8 | 1.25 | 666 | 2020 |
| 9.1 | 3.2 | 3.6 | 1.13 | 699 | 2020 |
| 7.7 | 3.0 | 2.9 | 1.05 | 721 | 2018 |

- Data rate is DAQ limited
- Would need 100 Million Events at each energy to make the sensitivity of BES-II
- Roughly one to two days per energy

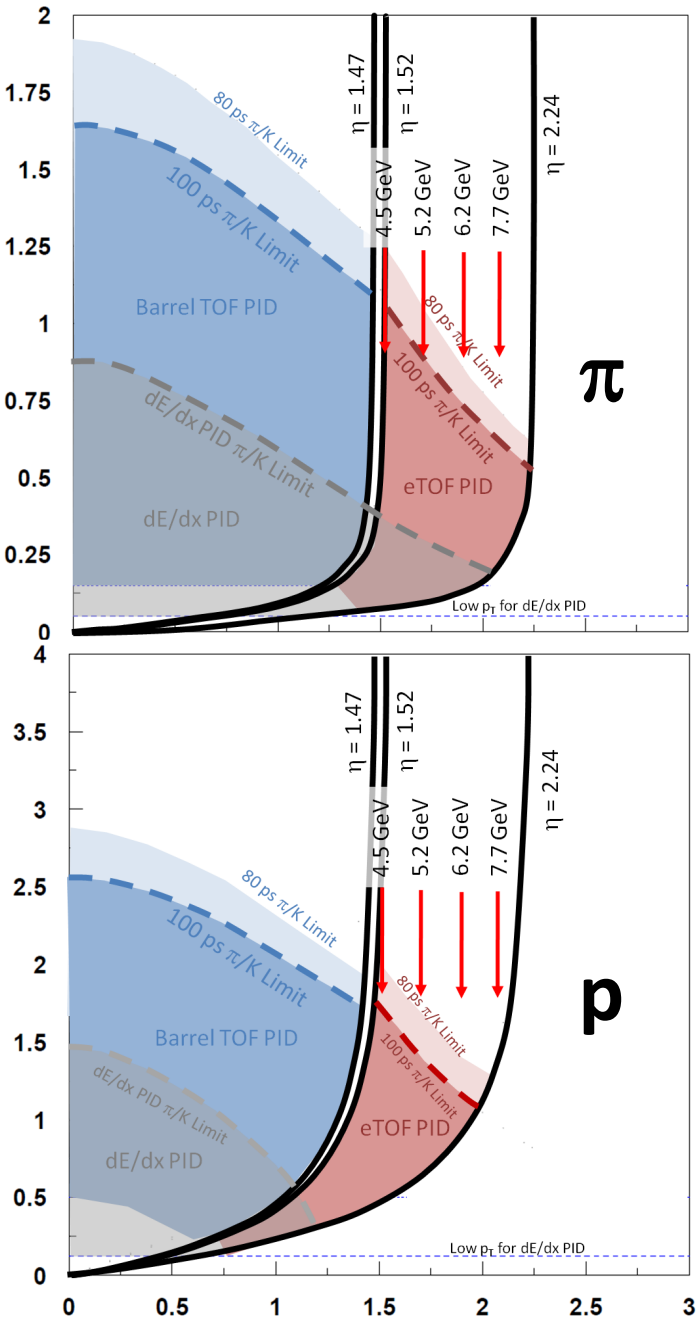

# Conclusions

- AGS Program provided extensive results at the top energy, but left many observables unmeasured across the energy scan.

- FXT program will allow for comprehensive measurements below 7.7 GeV

- Acceptance and physics have been demonstrated in test runs and other studies

# Extras

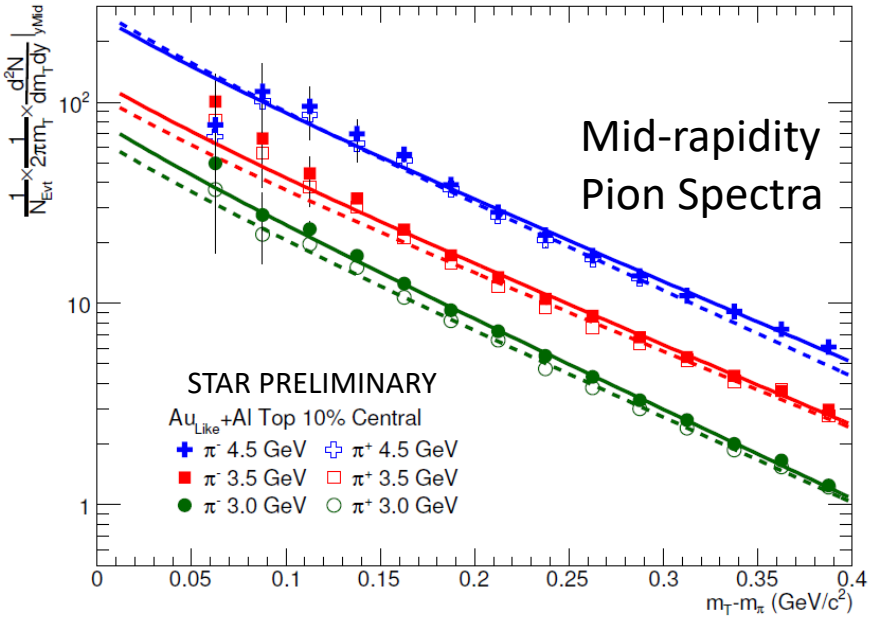
Mid-rapidity
Pion Spectra
STAR PRELIMINARY
Au_Like+Al Top 10% Central
π⁻ 4.5 GeV
π⁺ 4.5 GeV
π⁻ 3.5 GeV
π⁺ 3.5 GeV
π⁻ 3.0 GeV
π⁺ 3.0 GeV
m_T-m_π (GeV/c²)

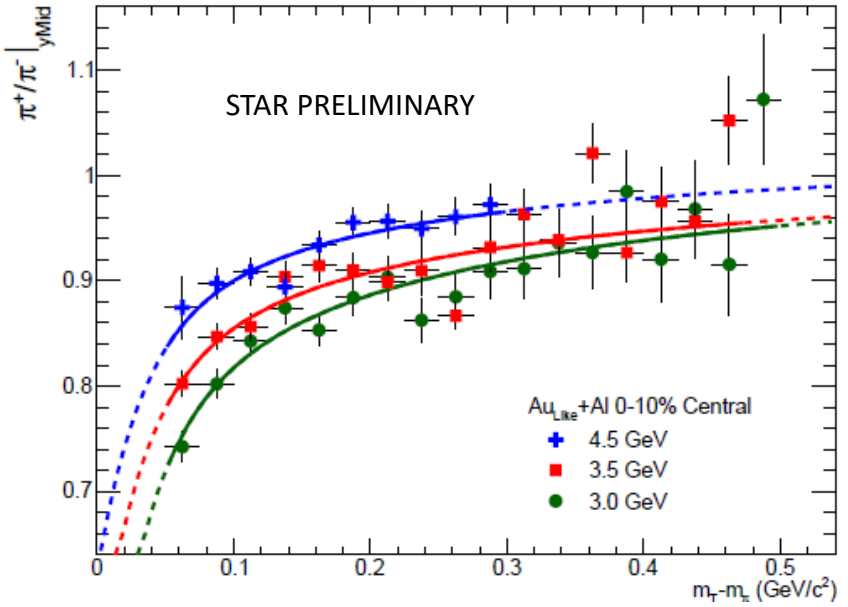
STAR PRELIMINARY
Au_Like+Al 0-10% Central
4.5 GeV
3.5 GeV
3.0 GeV
m_T-m_π (GeV/c²)

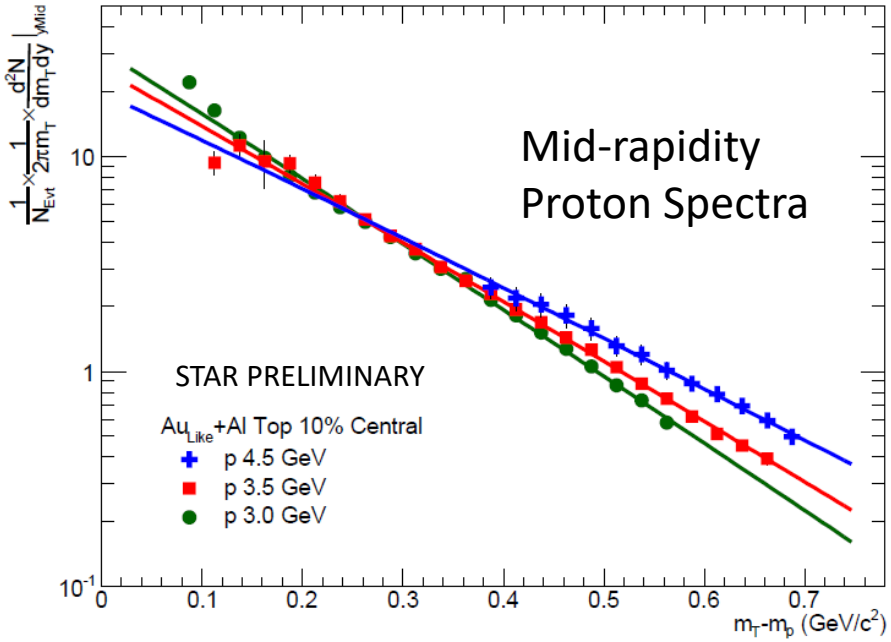
Mid-rapidity
Proton Spectra
STAR PRELIMINARY
Au_Like+Al Top 10% Central
p 4.5 GeV
p 3.5 GeV
p 3.0 GeV
m_T-m_p (GeV/c²)

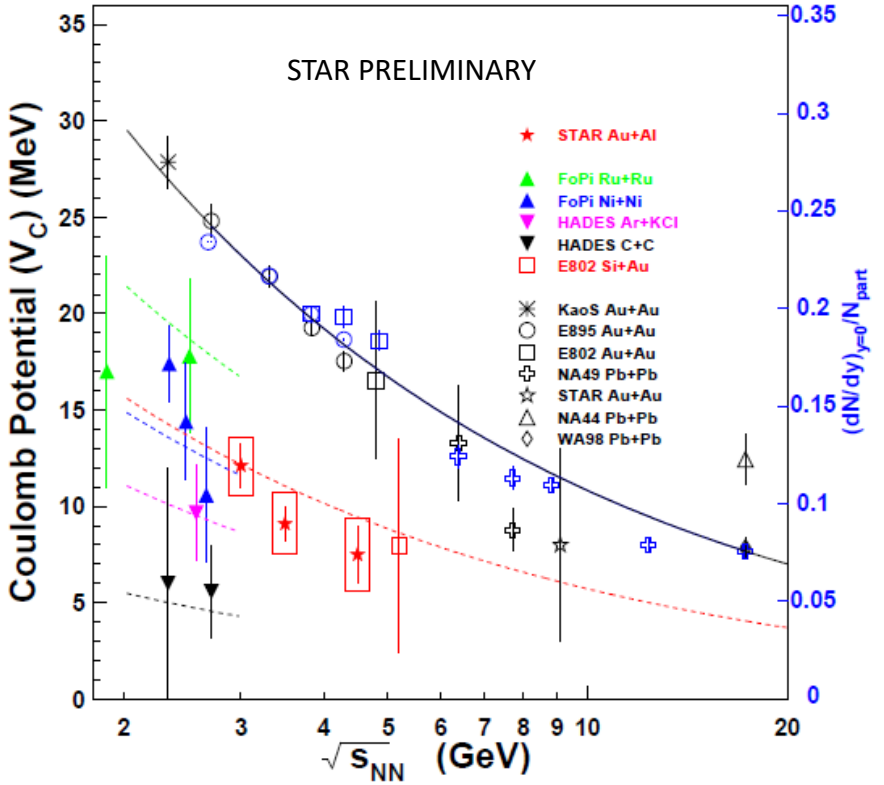
STAR PRELIMINARY
STAR Au+Al
FoPi Ru+Ru
FoPi Ni+Ni
HADES Ar+KCl
HADES C+C
E802 Si+Au
KaoS Au+Au
E895 Au+Au
E802 Au+Au
NA49 Pb+Pb
STAR Au+Au
NA44 Pb+Pb
WA98 Pb+Pb
Coulomb Potential (V_C) (MeV)
√s_NN (GeV)

May 20th, 2015

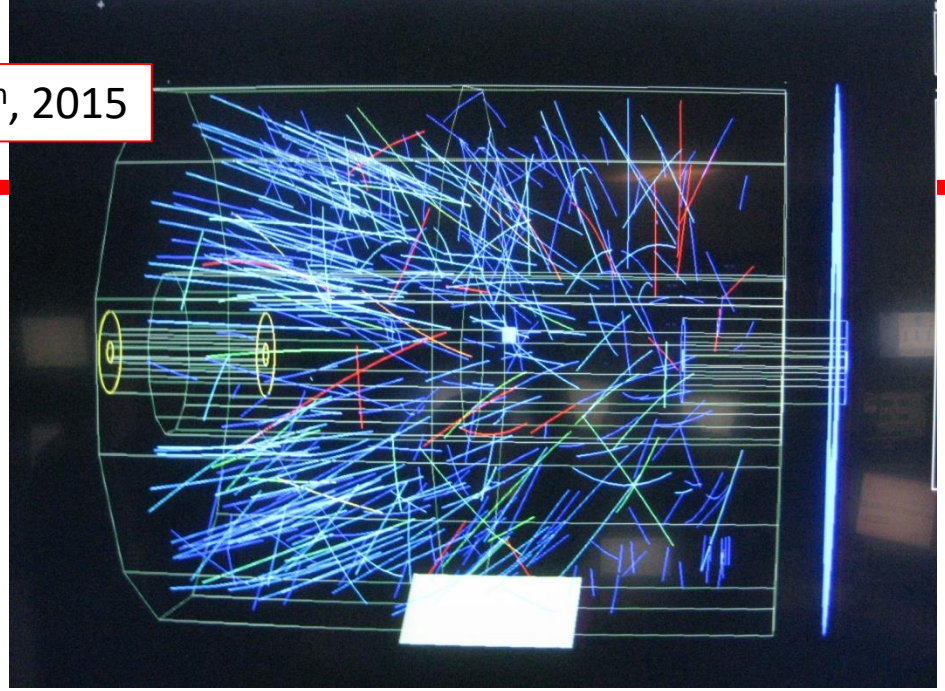

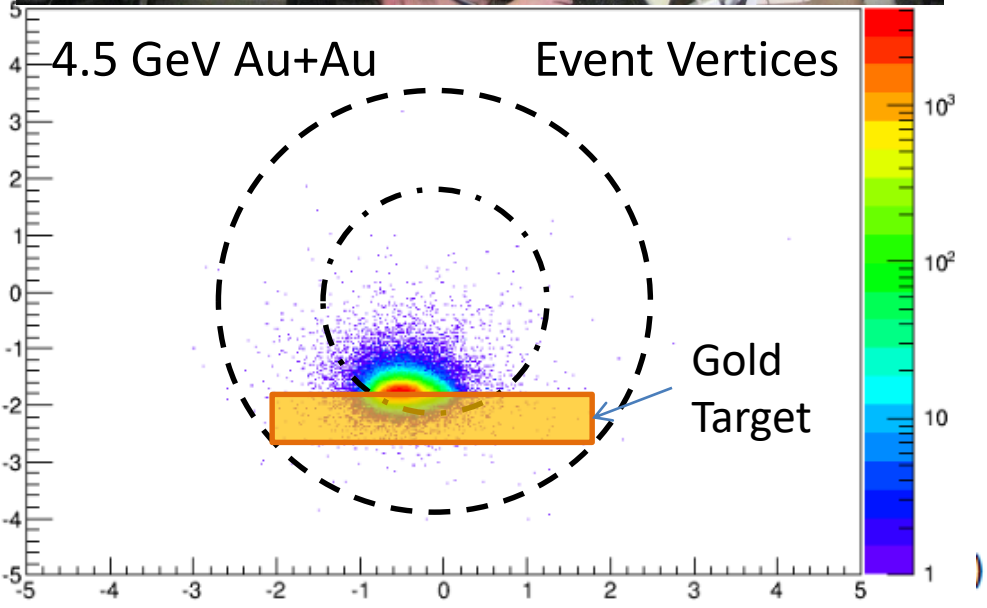


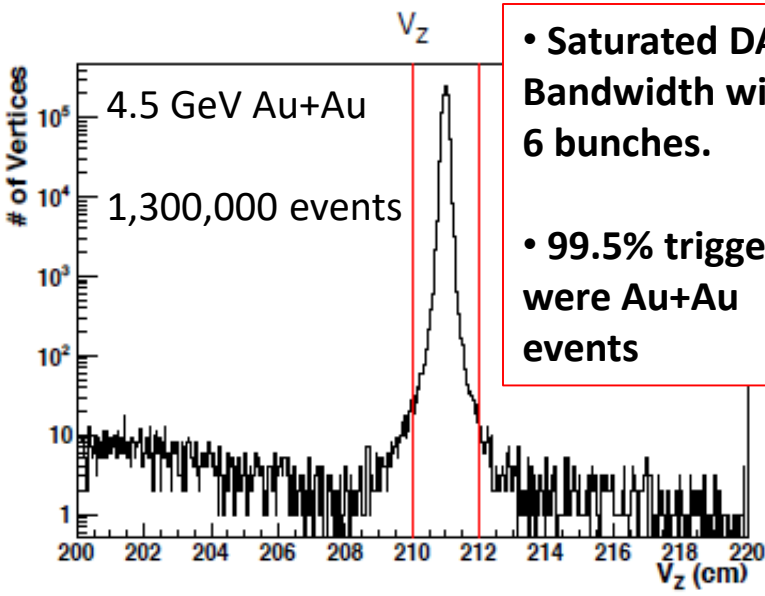


- **Saturated DAQ Bandwidth with 6 bunches.**
- **99.5% triggers were Au+Au events**

# Low Energy Electron Cooling at RHIC

Improve luminosity for low energy beams with electron cooling

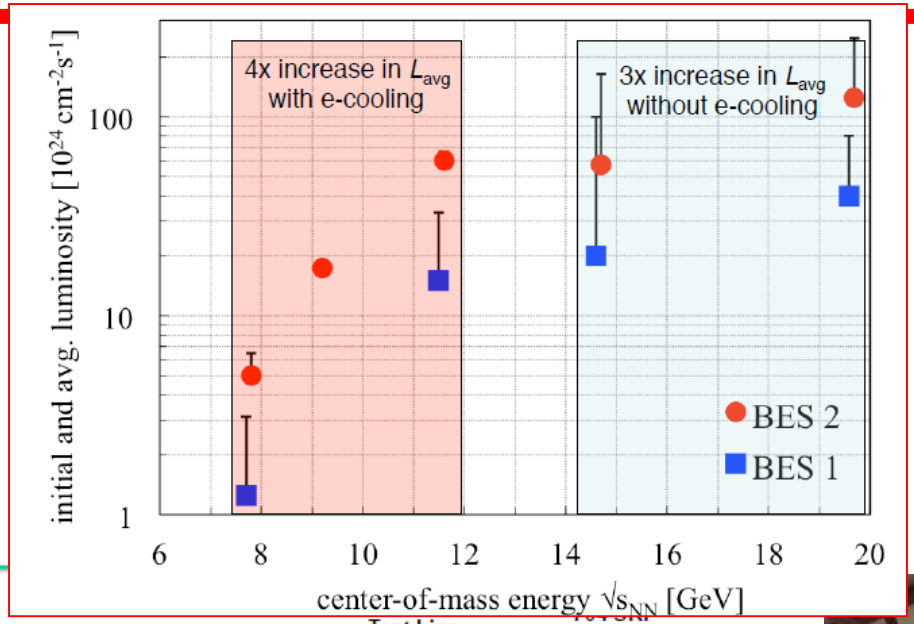


- Start with 14.5 and 19,6 3X improvement
- Following year, 7.7, 9.1, and 11.5. 4X improvement with eCooling
- Run 24 weeks

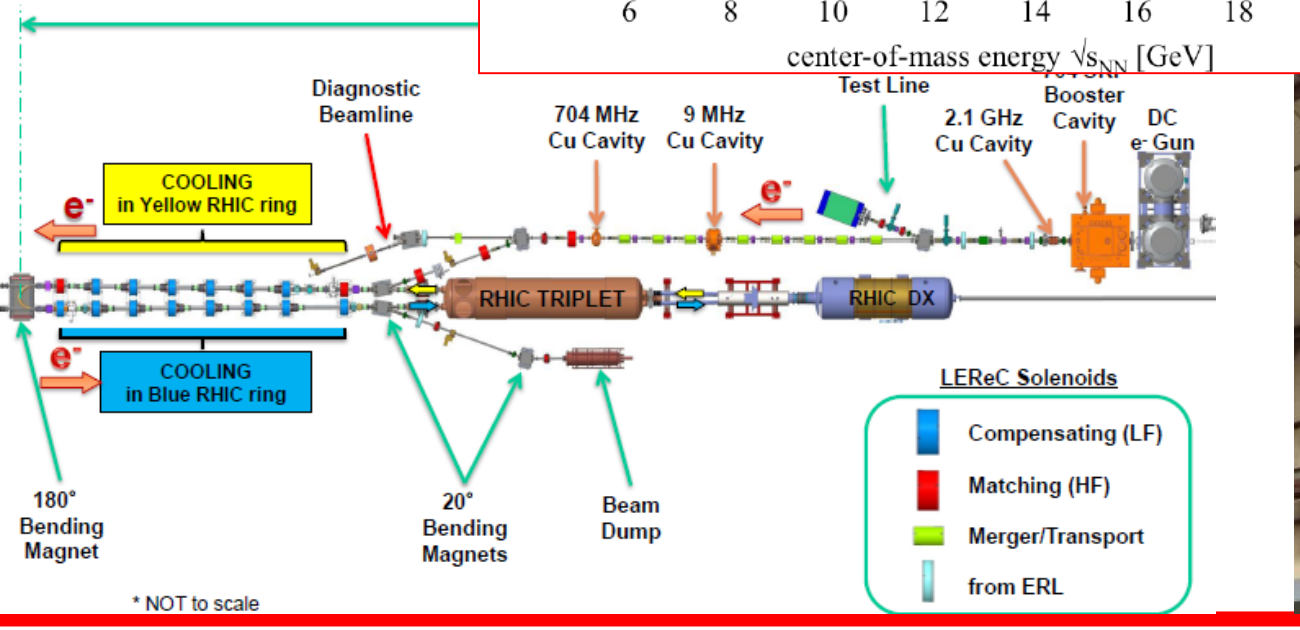


# The STAR Upgrades and the FXT program

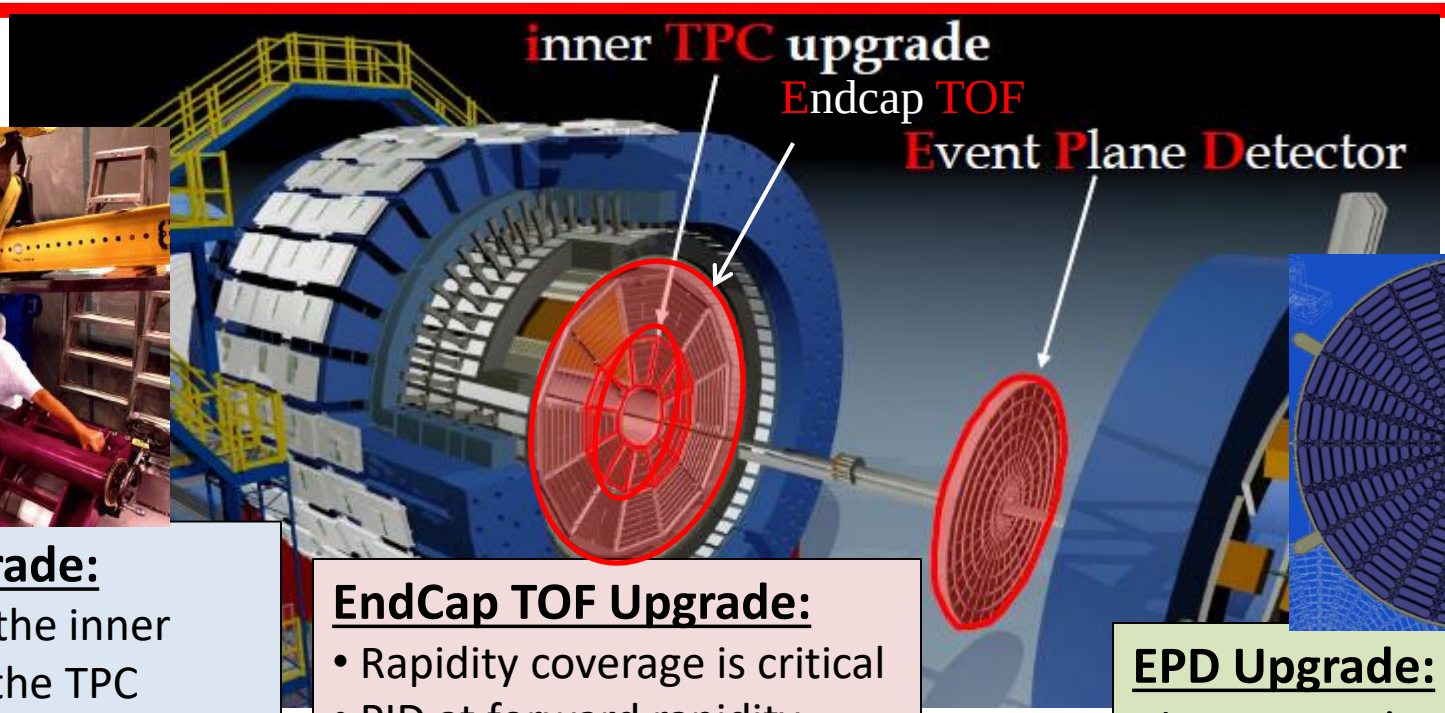



**iTPC Upgrade:**

- Rebuilds the inner sectors of the TPC
- Continuous Coverage
- Improves dE/dx
- Extends η coverage from 1.5 to 2.2
- Lowers $p_T$ cut-in from 125 MeV/c to 60 MeV/c
- Ready in 2019

**EndCap TOF Upgrade:**

- Rapidity coverage is critical
- PID at forward rapidity
- Allows higher energy range of FXT program
- Ready 2019

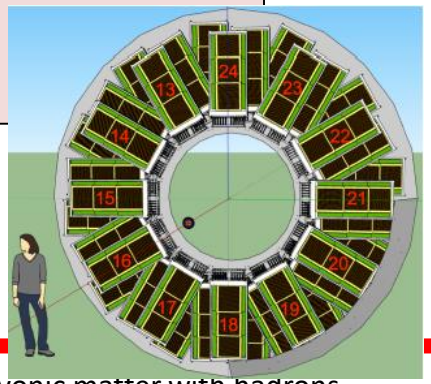


**EPD Upgrade:**

- Improves trigger
- Reduces background
- Allows a better and independent reaction plane measurement critical to BES physics
- Ready 2018

# Internal Fixed Target PseudoRapidity Considerations

eTOF:
Z = -270 cm
ΔZ = 480 cm
$R_{min}$ = 110 cm
$R_{max}$ = 220 cm

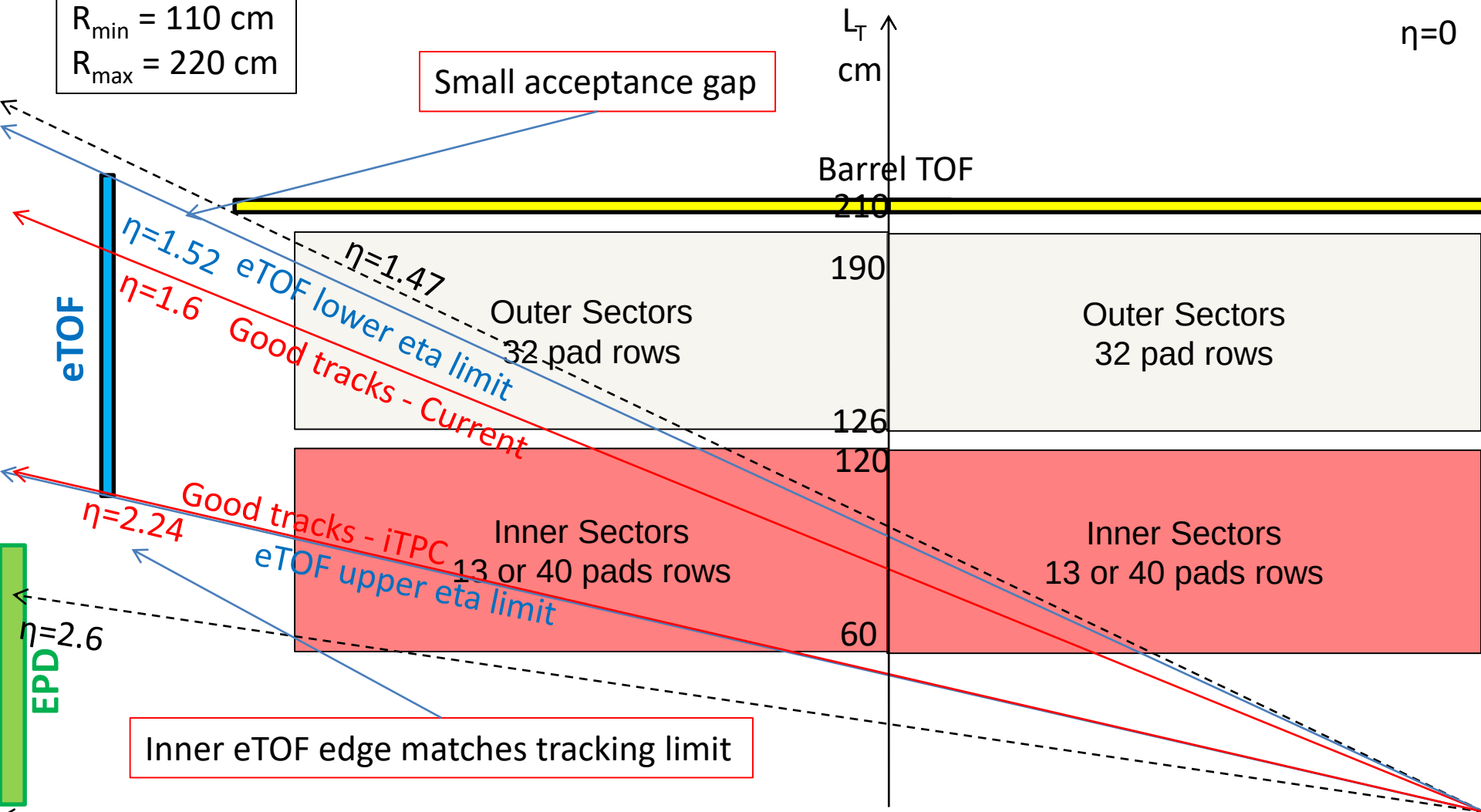

# Comparison of Facilities

| Facilty | RHIC BESII | SPS | NICA | SIS-100<br>SIS-300 | J-PARC HI |
|---|---|---|---|---|---|
| Exp.: | STAR<br>+FXT | NA61 | MPD<br>+ BM@N | CBM | JHITS |
| Start: | 2019-20<br>2018 | 2009 | 2020<br>2017 | 2022 | 2025 |
| Energy:<br>$\sqrt{s_{NN}}$ (GeV) | 7.7– 19.6<br>2.5-7.7 | 4.9-17.3 | 2.7 - 11<br>2.0-3.5 | 2.7-8.2 | 2.0-6.2 |
| Rate:<br>At 8 GeV | 100 HZ<br>2000 Hz | 100 HZ | <10 kHz | <10 MHZ | 100 MHZ |
| Physics: | CP&OD | CP&OD | OD&DHM | OD&DHM | OD&DHM |
| | Collider<br>Fixed Target | Fixed Target<br>Lighter ion collisions | Collider<br>Fixed Target | Fixed Target | Fixed Target |

**CP = Critical Point**
**OD = Onset of Deconfinement**
**DHM = Dense Hadronic Matter**

# Prospects for Higher Moments

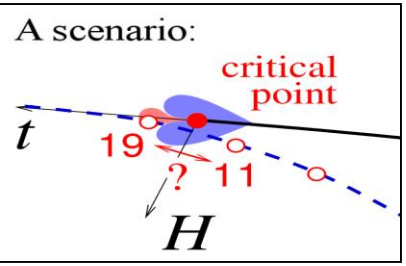


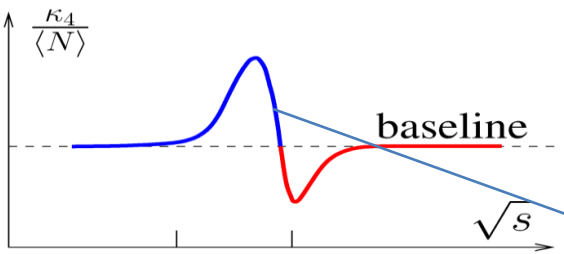


New HADES results

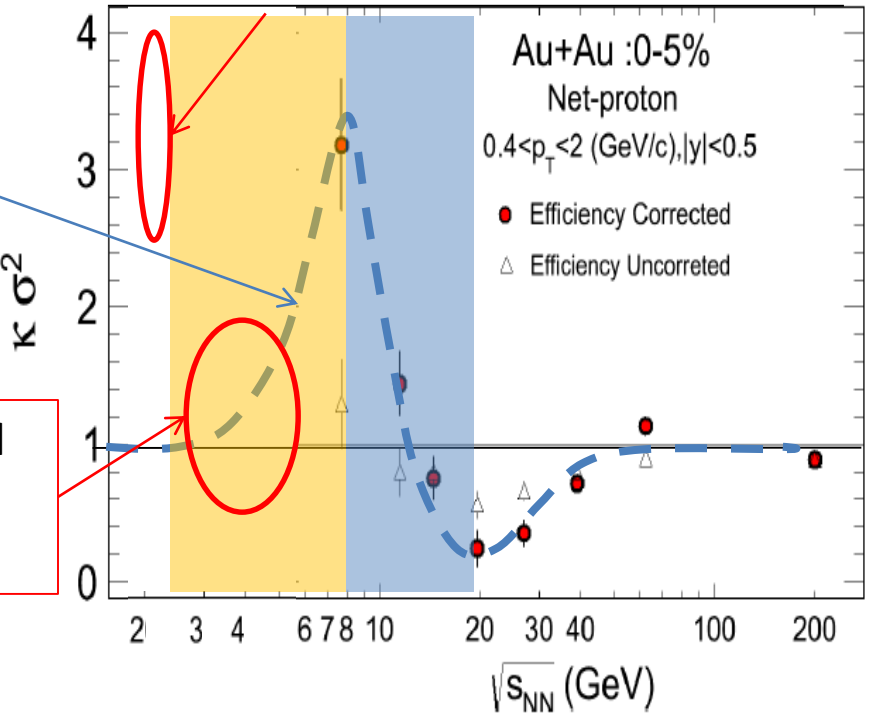


Need data here

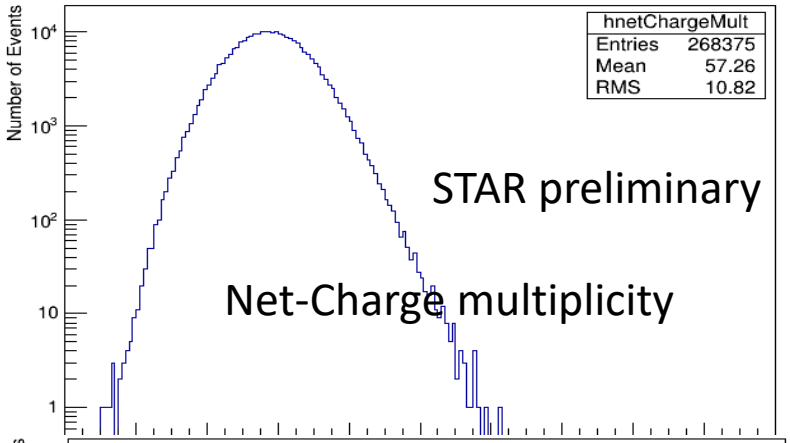


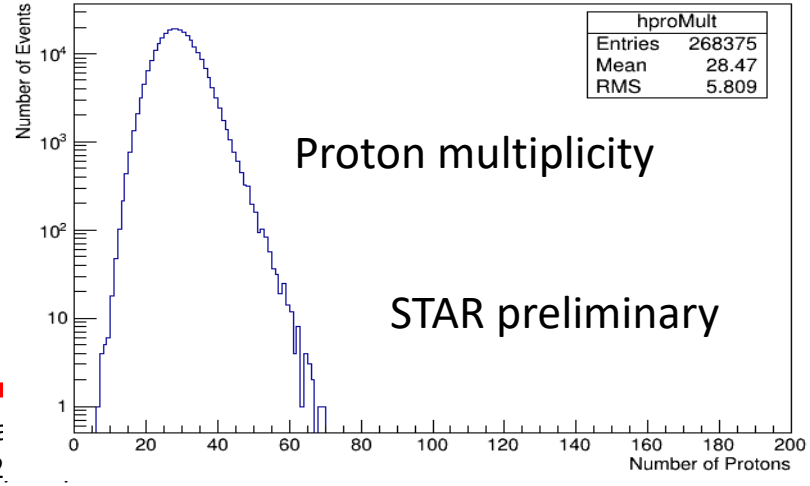


- Expect to have a sensitivity roughly comparable to the 7.7 GeV data point
- Analysis has not yet started
- Goal is to have preliminary result ready by April 2017 for use in the Beam Use Request

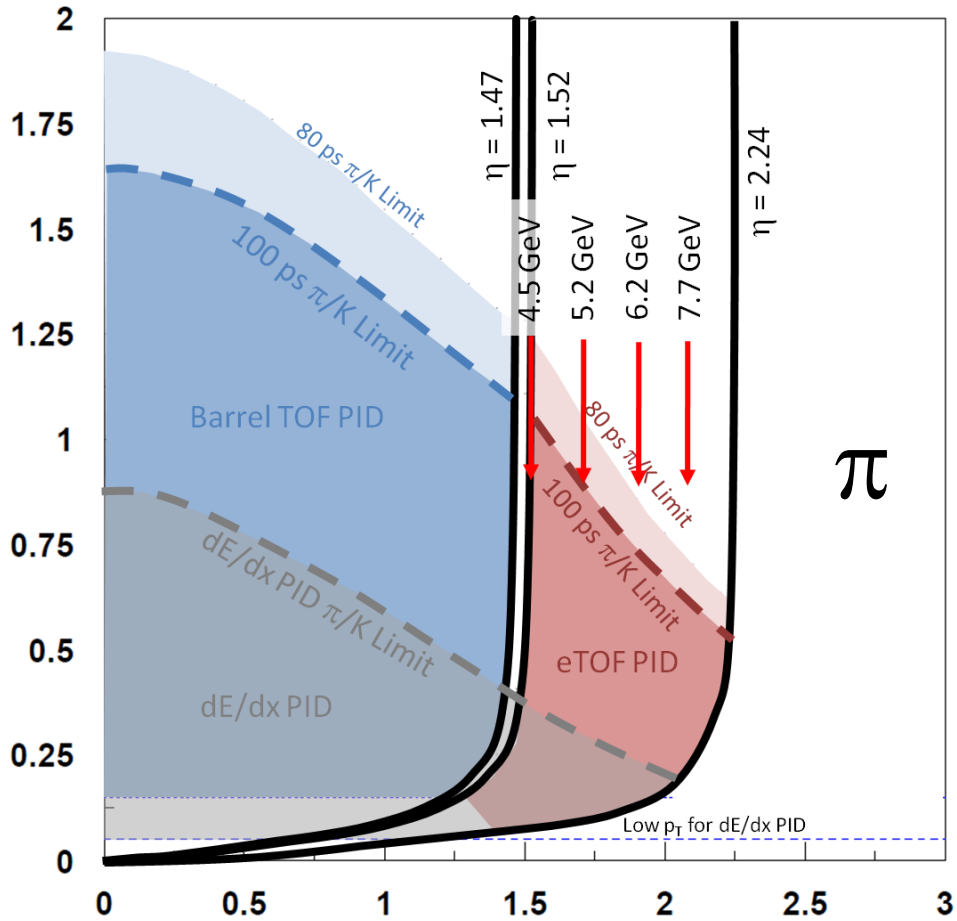
80 ps π/K Limit
100 ps π/K Limit
Barrel TOF PID
dE/dx PID π/K Limit
dE/dx PID
η = 1.47
η = 1.52
η = 2.24
4.5 GeV
5.2 GeV
6.2 GeV
7.7 GeV
80 ps π/K Limit
100 ps π/K Limit
eTOF PID
Low $p_T$ for dE/dx PID
π

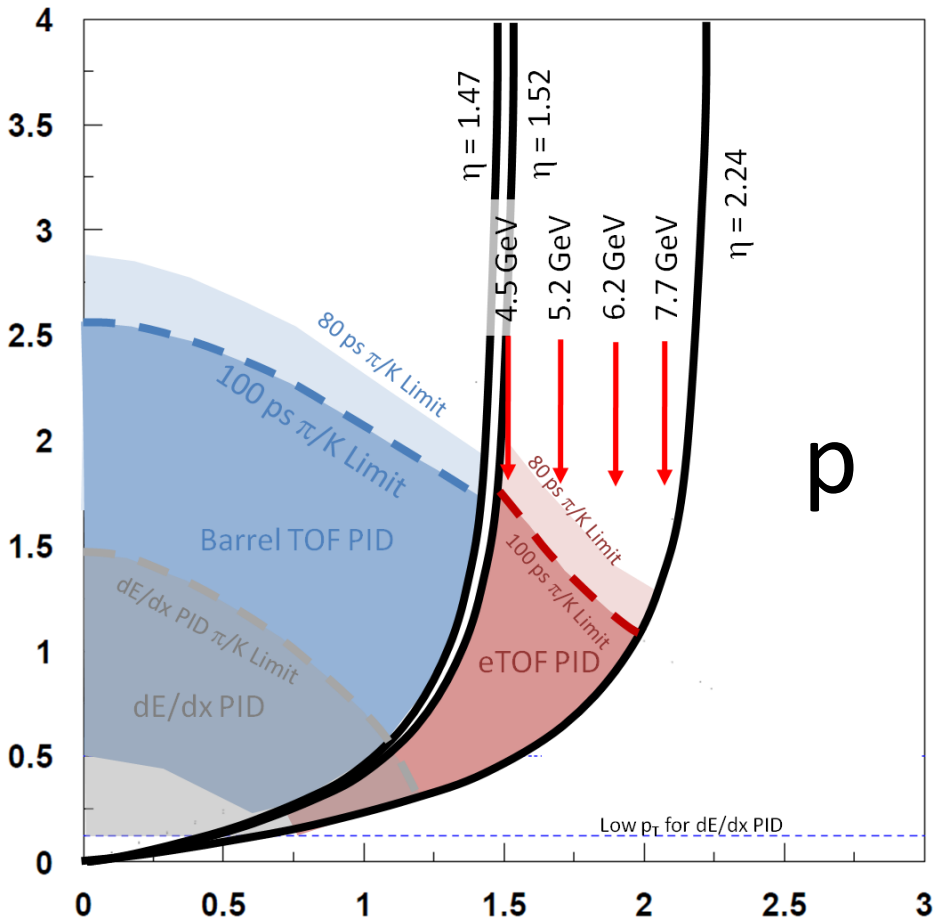
80 ps π/K Limit
100 ps π/K Limit
Barrel TOF PID
dE/dx PID π/K Limit
dE/dx PID
η = 1.47
η = 1.52
η = 2.24
4.5 GeV
5.2 GeV
6.2 GeV
7.7 GeV
80 ps π/K Limit
100 ps π/K Limit
eTOF PID
Low $p_T$ for dE/dx PID
p

| Collision Energy (GeV) | Single Beam Energy | Fixed Target Root s | Single Beam Rapidity | Center of Mass Rapidity | Chemical Potential $\mu_B$ | Events (Millions) |
|---|---|---|---|---|---|---|
| 200 | 100 | 13.713 | 5.369 | 2.685 | 0.276 | NA |
| 130 | 65 | 11.083 | 4.938 | 2.469 | 0.325 | NA |
| 62.4 | 31.2 | 7.737 | 4.204 | 2.102 | 0.420 | 100 |
| 39 | 19.5 | 6.170 | 3.734 | 1.867 | 0.487 | 100 |
| 27 | 13.5 | 5.185 | 3.366 | 1.683 | 0.541 | 100 |
| 19.6 | 9.8 | 4.468 | 3.042 | 1.521 | 0.589 | 100 |
| 14.5 | 7.25 | 3.904 | 2.741 | 1.370 | 0.633 | 100 |
| 11.5 | 5.75 | 3.528 | 2.507 | 1.253 | 0.666 | 100 |
| 9.1 | 4.55 | 3.196 | 2.269 | 1.134 | 0.699 | 100 |
| 7.7 | 3.85 | 2.985 | 2.097 | 1.049 | 0.721 | 100 |
| 5.0 | 2.50 | 2.320 | 1.644 | 0.822 | 0.774 | 100 |

# Run 14 and 15 Setup

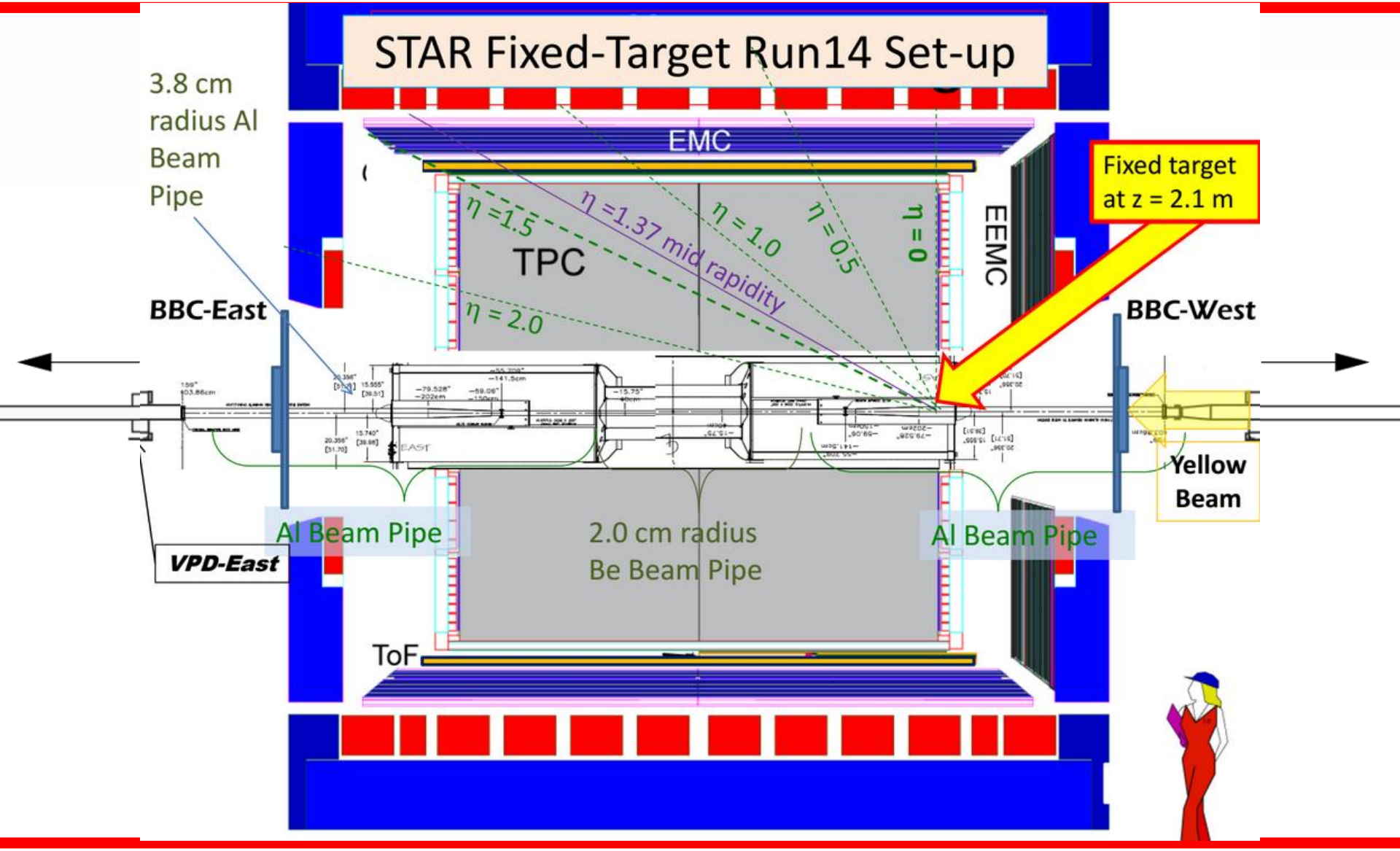

# BES Phase II Proposal

BES Phase II is planned for runs in 2019, 2020, and 2021

| $\sqrt{s_{NN}}$ (GeV) | 7.7 | 9.1 | 11.5 | 14.5 | 19.6 |
|---|---|---|---|---|---|
| $\mu_B$ (MeV) | 420 | 370 | 315 | 250 | 205 |
| BES I (MEvts) | 4.3 | --- | 11.7 | 24 | 36 |
| Rate(MEvts/day) | 0.25 | | 1.7 | 2.4 | 4.5 |
| BES I $\mathcal{L}$ ($1\times10^{25}$/cm$^2$sec) | 0.13 | | 1.5 | 2.1 | 4.0 |
| BES II (MEvts) | 100 | 160 | 230 | 300 | 400 |
| Improvement (X) | 4 | 4 | 4 | 3 | 3 |
| Beam Time (weeks) | **12** | **9.5** | **5.0** | **5.5** | **4.5** |

**Revised estimates**

# AGS E896 Experiment

E896 -- **Spokesperson:** Crawford, Henry J.; Hallman, Tim J.

- Forward spectrometer
- TOF & neutrons

**Main Results:**
Did not find the
$H^0$ di-baryon

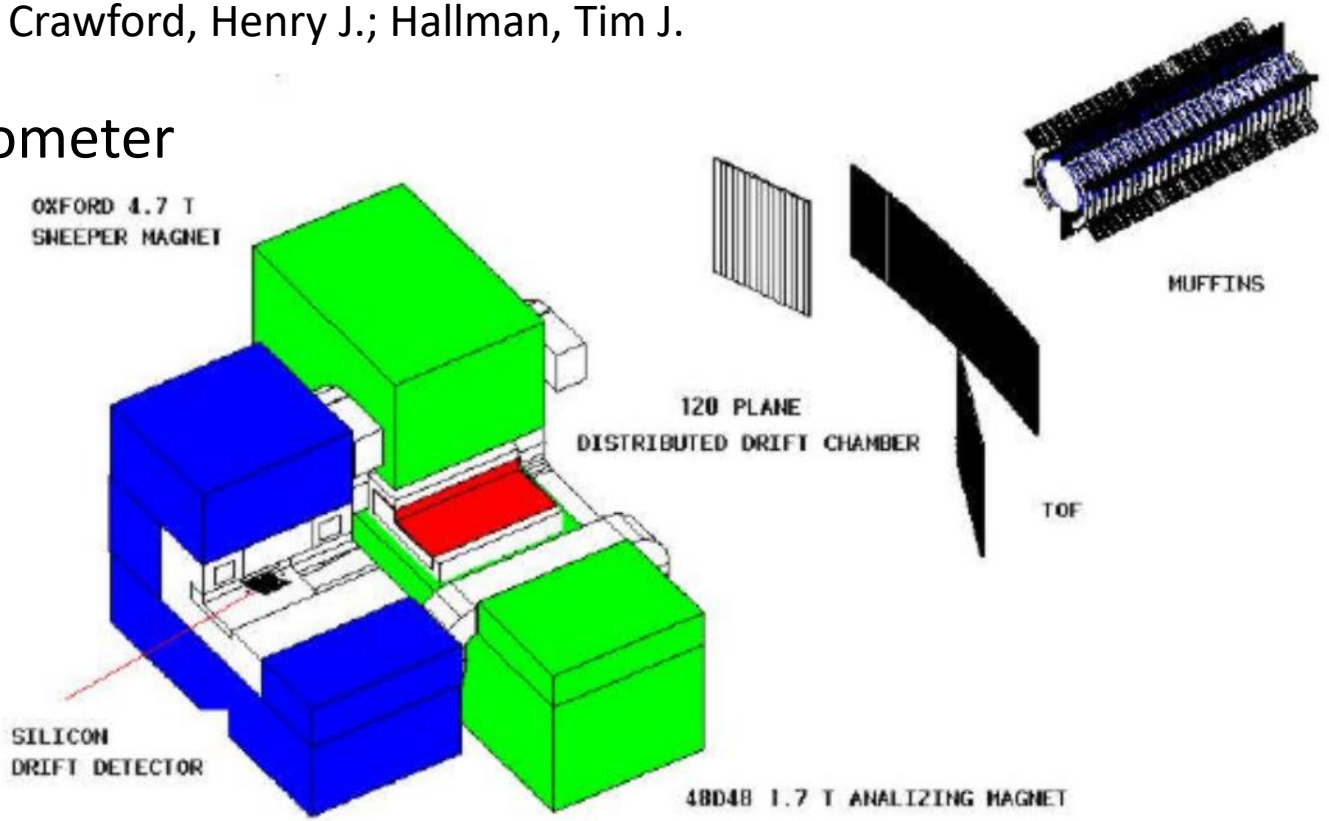

# Spectra

## Spectra -- pions

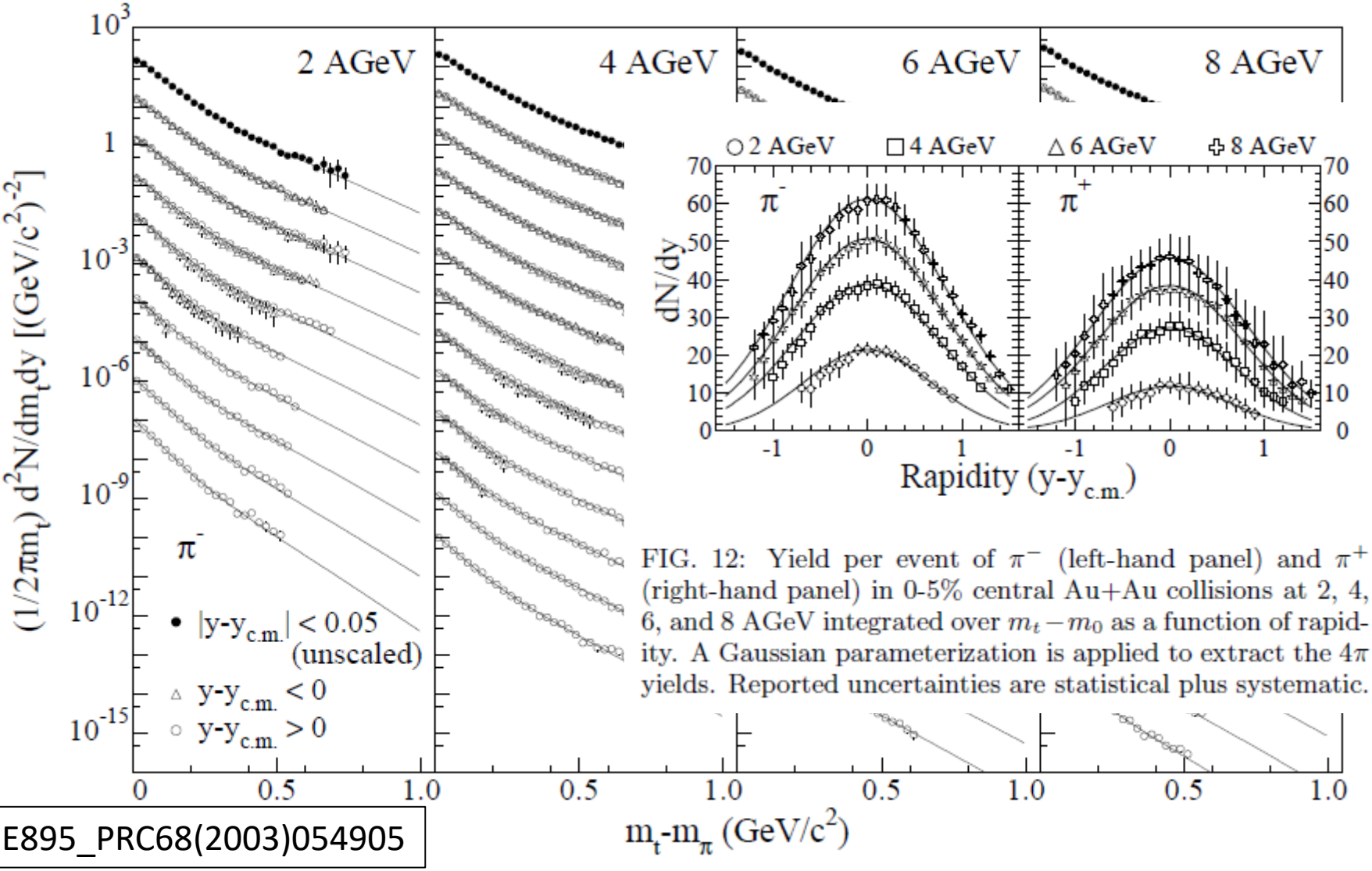


FIG. 12: Yield per event of $\pi^-$ (left-hand panel) and $\pi^+$ (right-hand panel) in 0-5% central Au+Au collisions at 2, 4, 6, and 8 AGeV integrated over $m_t - m_0$ as a function of rapidity. A Gaussian parameterization is applied to extract the $4\pi$ yields. Reported uncertainties are statistical plus systematic.

E895_PRC68(2003)054905

**Spectra -- pions**

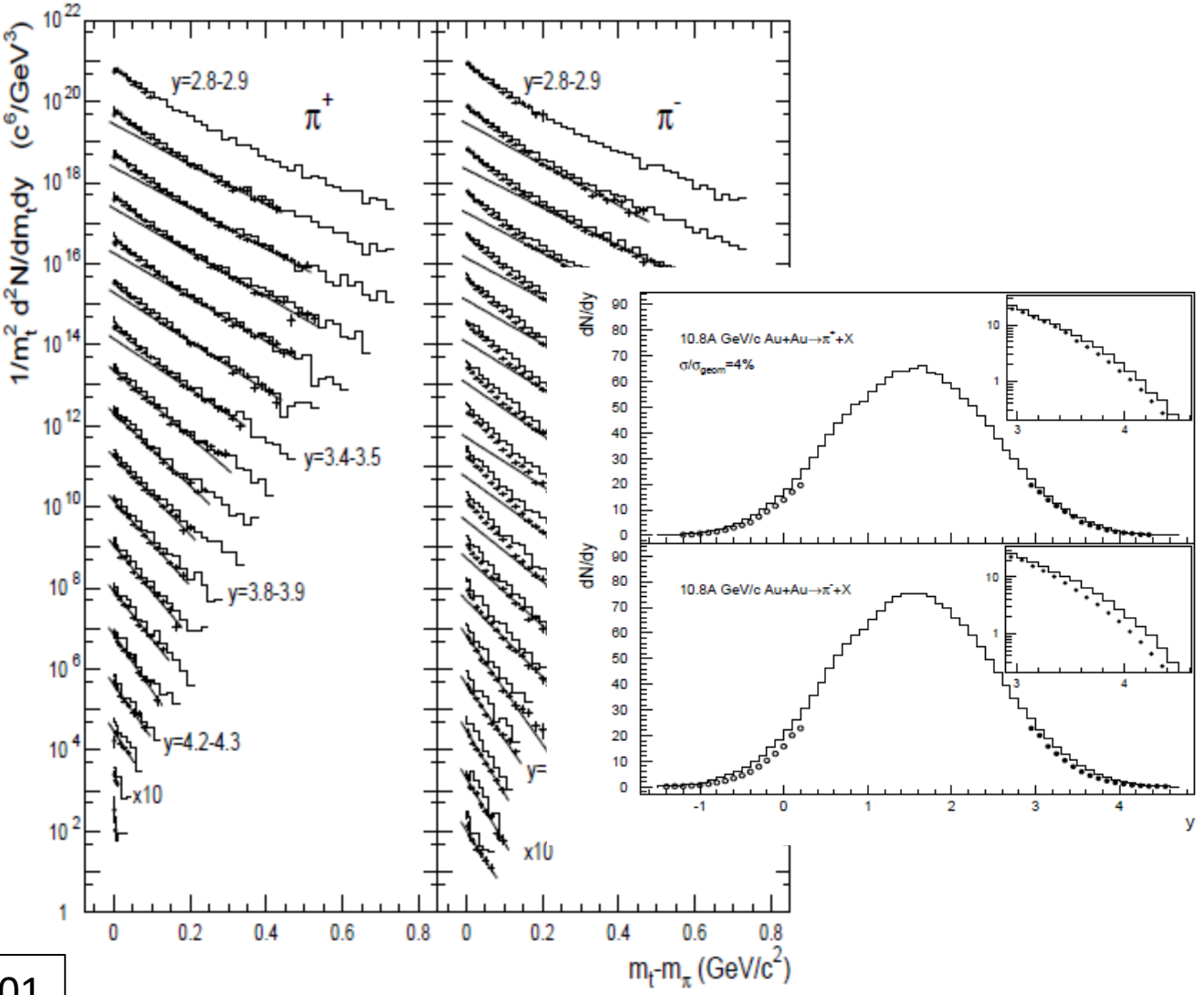


E877_PRC62(2000)024901

FIG. 6. Pion transverse mass spectra for central ($\sigma_{central}/\sigma_{geom}$=0.04) Au+Au collisions. Beginning with y=4.4-4.5, the spectra have been multiplied by successively increasing factors of ten. Full lines are the results of Boltzmann fits to the data over a limited range (see text). The histograms are ROMD predictions.

# Spectra -- pions

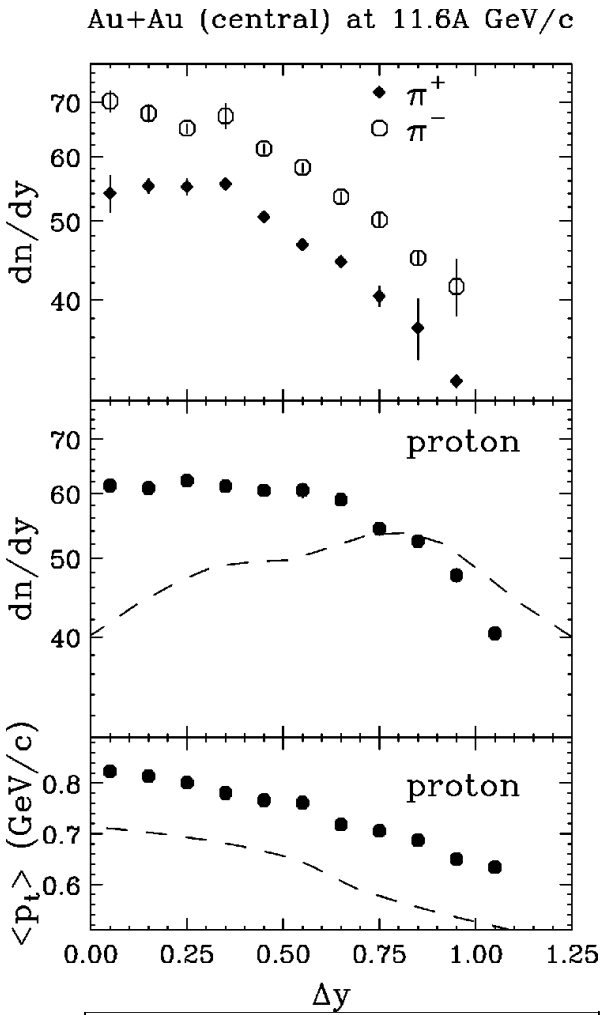


E802_PRC57(1998)R466

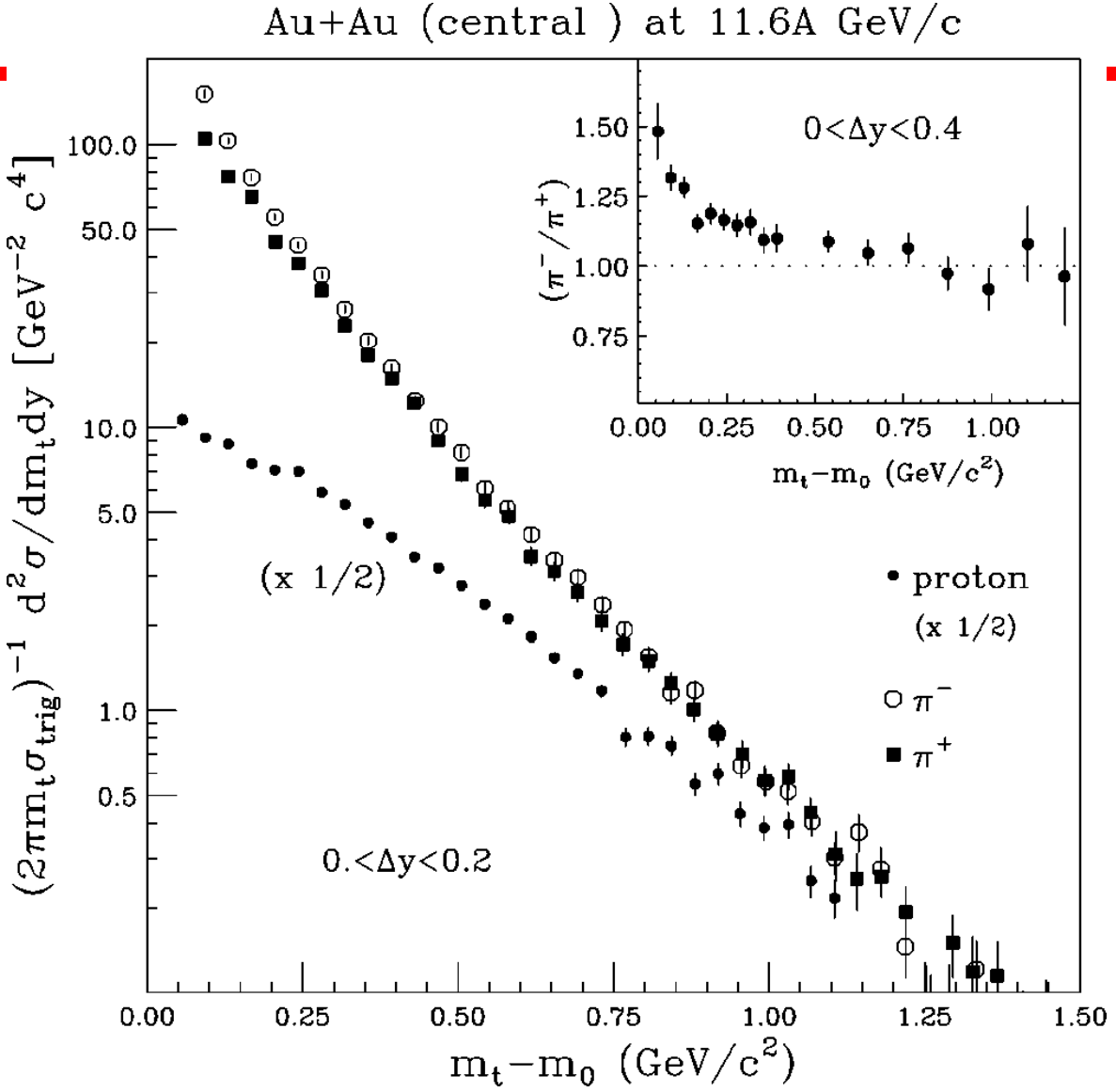

## Spectra -- pions

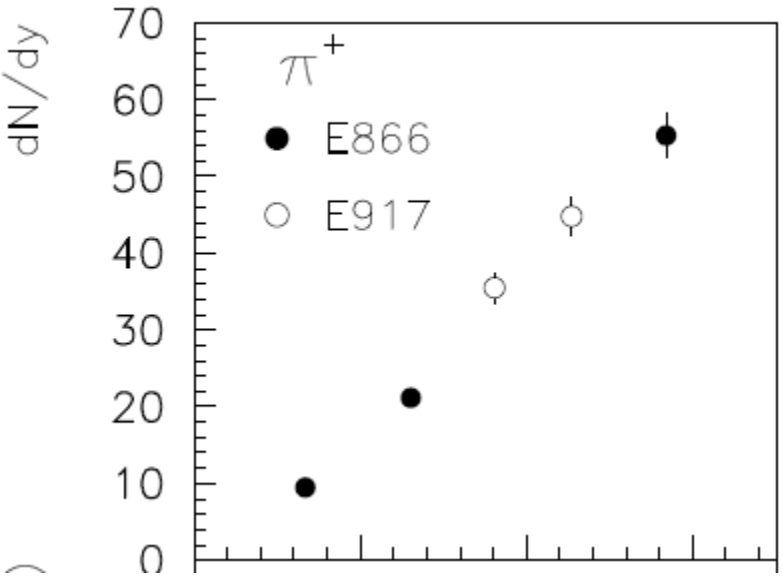


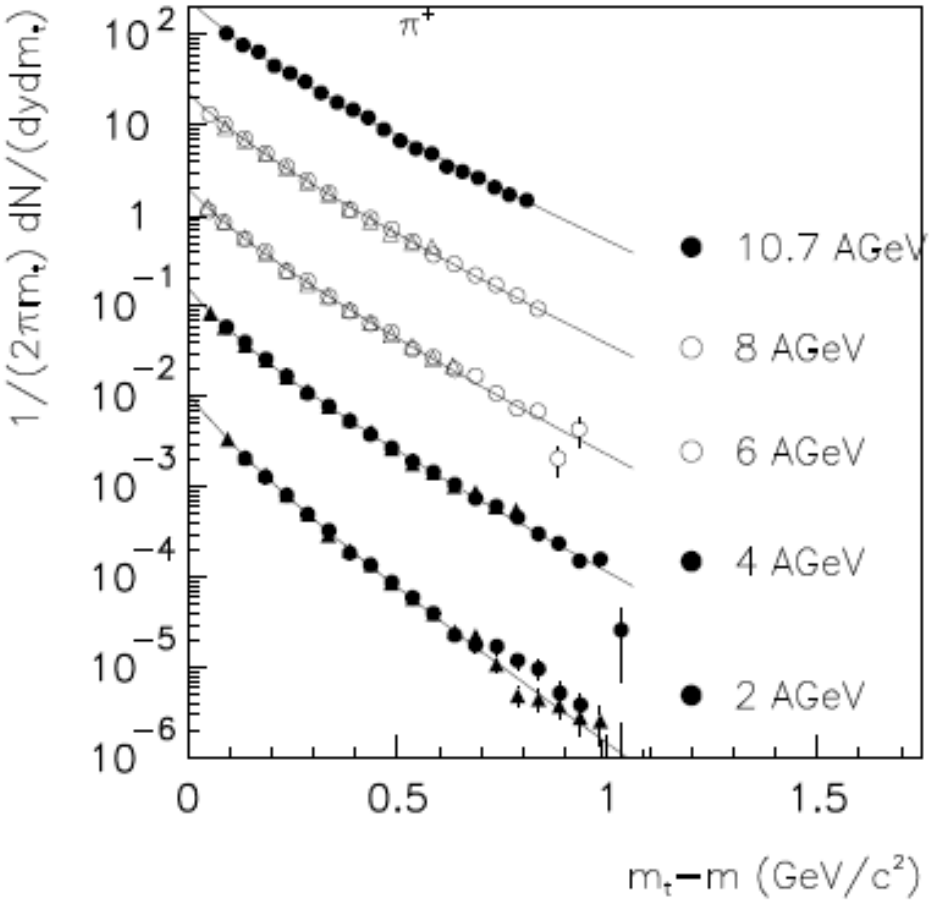


E917_PLB476(2000)1

# Spectra - Kaons

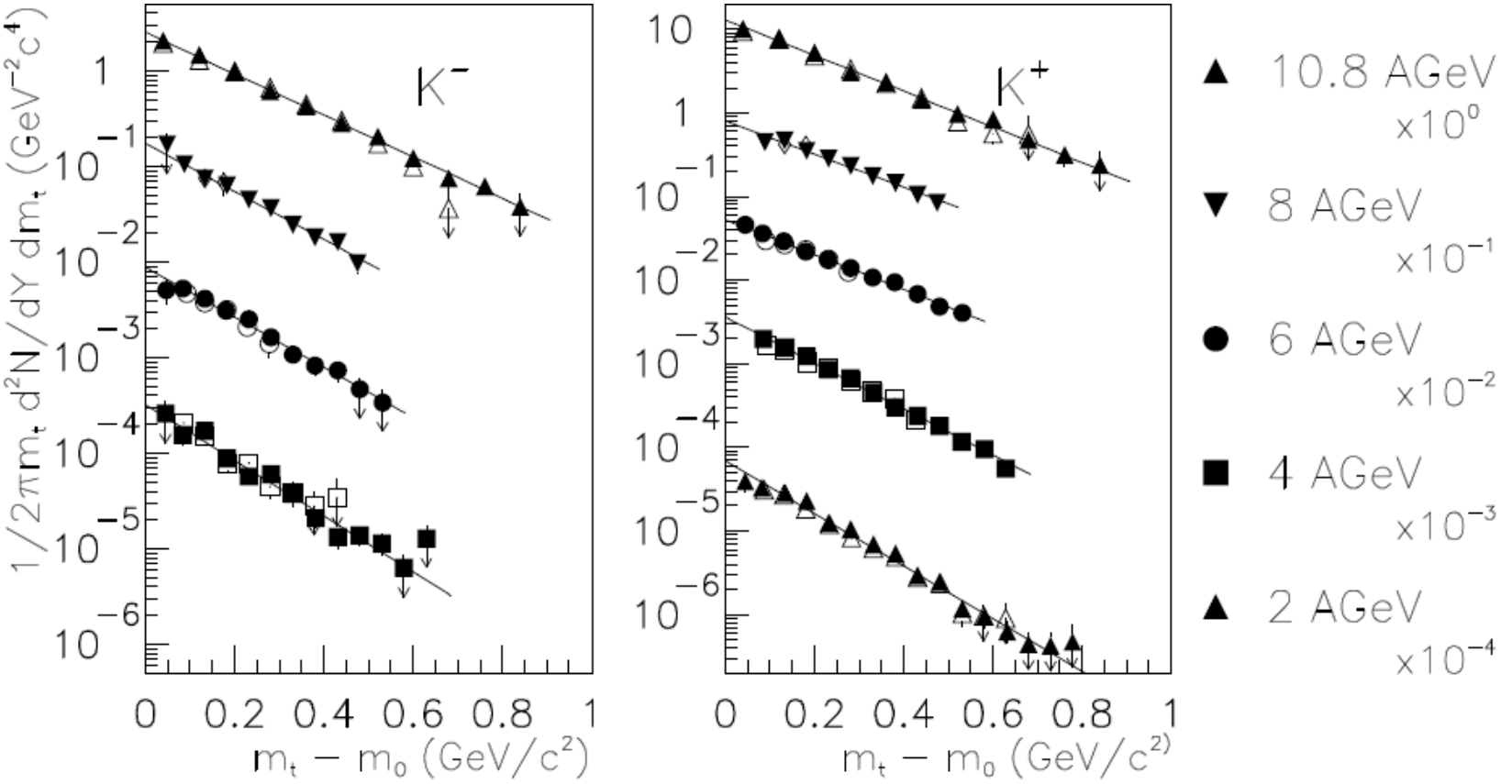


FIG. 1. The invariant yields of kaons plotted as a function of $m_t$ fro
only), 4, 6, 8, 10.7 AGeV. The left panel shows $K^-$ spectra the right panel s
mid-rapidity is shown with filled symbols, the spectrum just above mid-rap
and 10.7 AGeV are from E866 and the data at 6, and 8 AGeV are from E91
to zero cross-section. The data at 10.7 AGeV are shown on the correct s
successive powers of ten for clarity. The plotted errors are only statistical.

E866_PLB490(2000)53

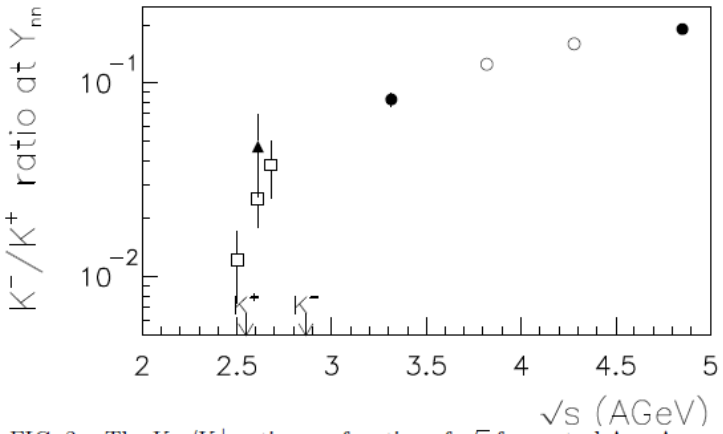

# Spectra -- Kaons

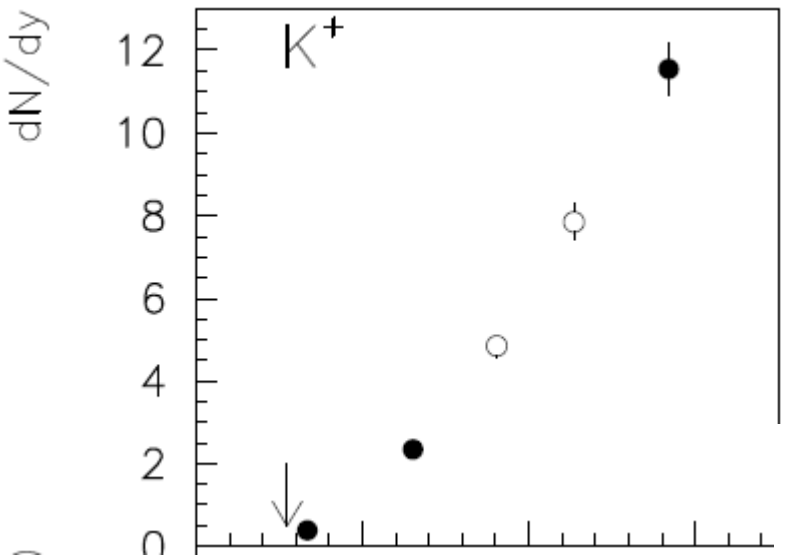


E917_PLB476(2000)1

E917_PLB490(2000)53

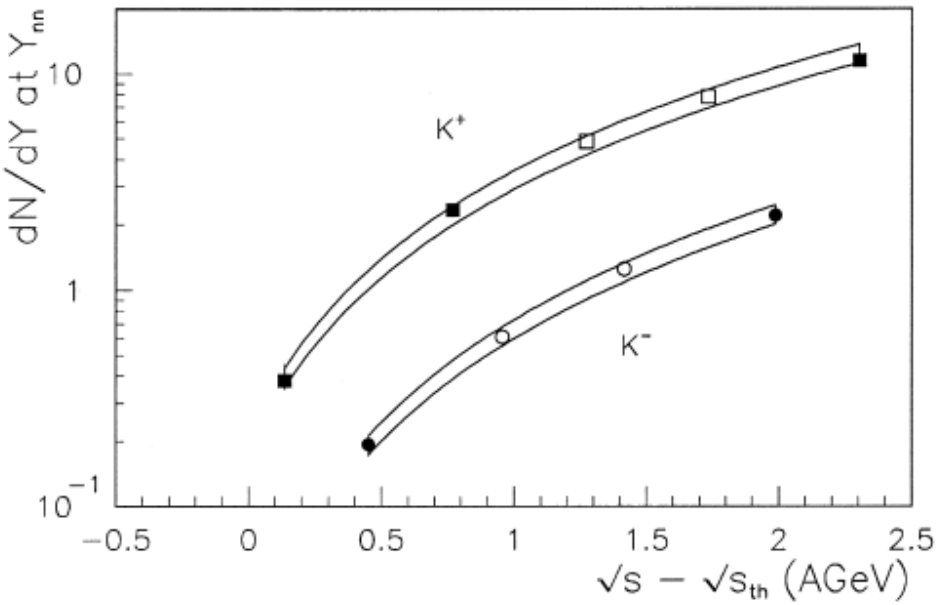

# Spectra -- Kaons

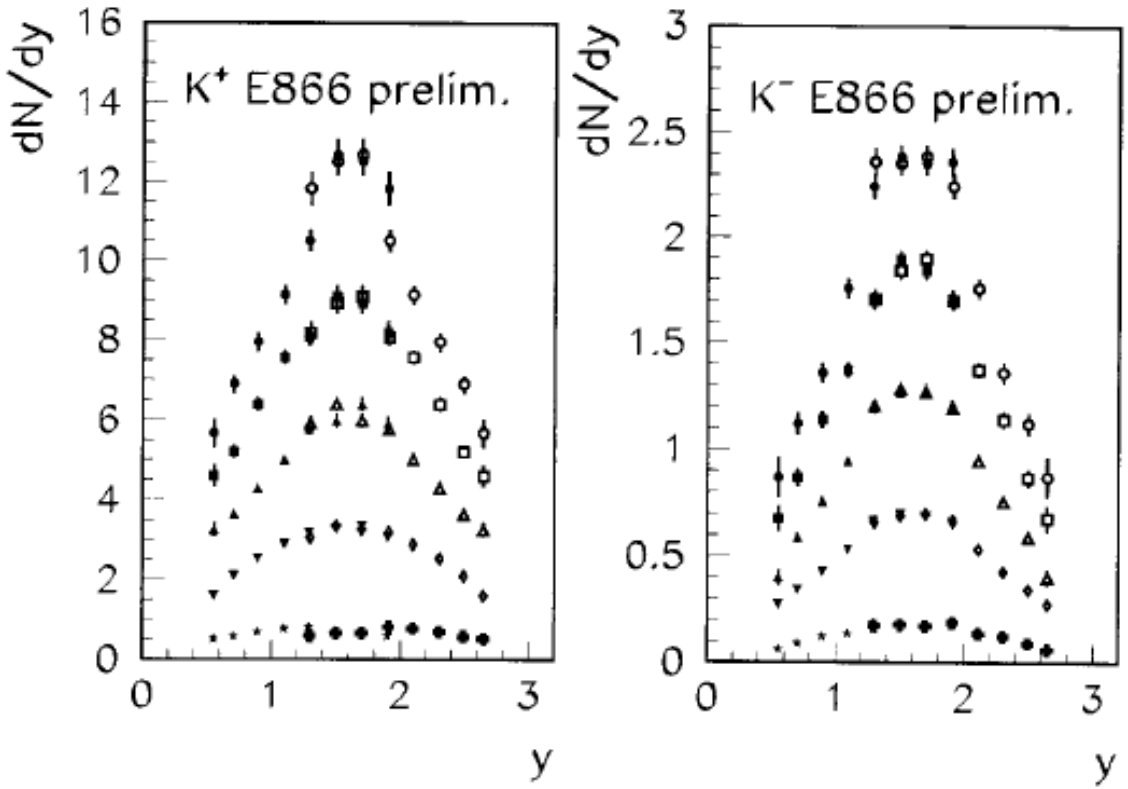


E866_NPA630(1998)571c

# Spectra - Protons

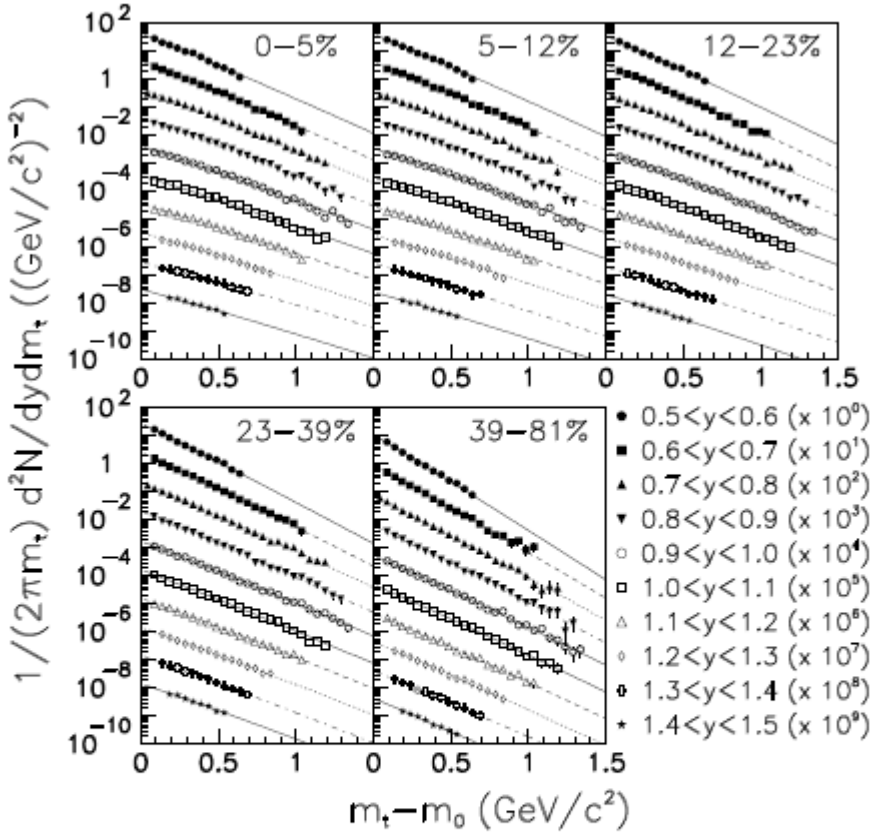


FIG. 1. Invariant yields of protons as a function of trans verse mass for ten rapidity intervals for each centrality clas of Au+Au collisions at 8 GeV/nucleon. The most backwar rapidity in each panel is plotted on the correct scale, whil successive spectra have been divided by ten for clarity. Th errors are statistical only. The curves are Boltzmann fits d scribed in the text.

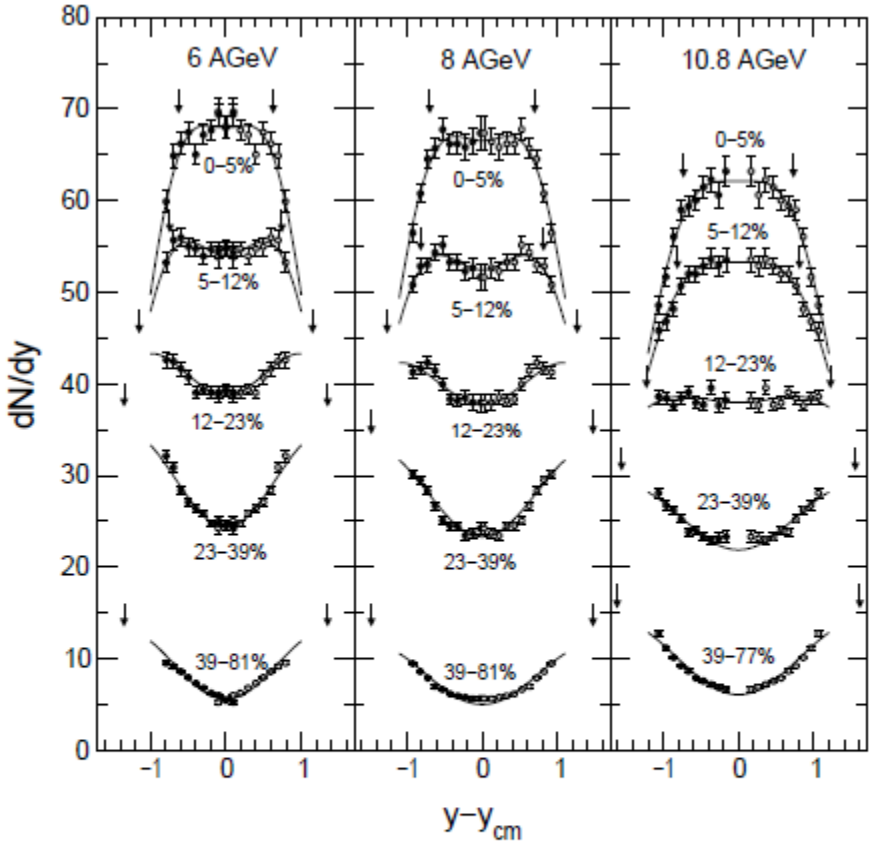


FIG. 2. Proton rapidity distributions for all centrality classes at all three beam energies from Boltzmann fits to the invariant cross sections. The open symbols are the data reflected about mid-rapidity. The errors are statistical only. The curves represent double Gaussian fits to the data (see text), the centroids of which are indicated by the arrows.

E917 PRL86(2001)1970

# Spectra -- protons

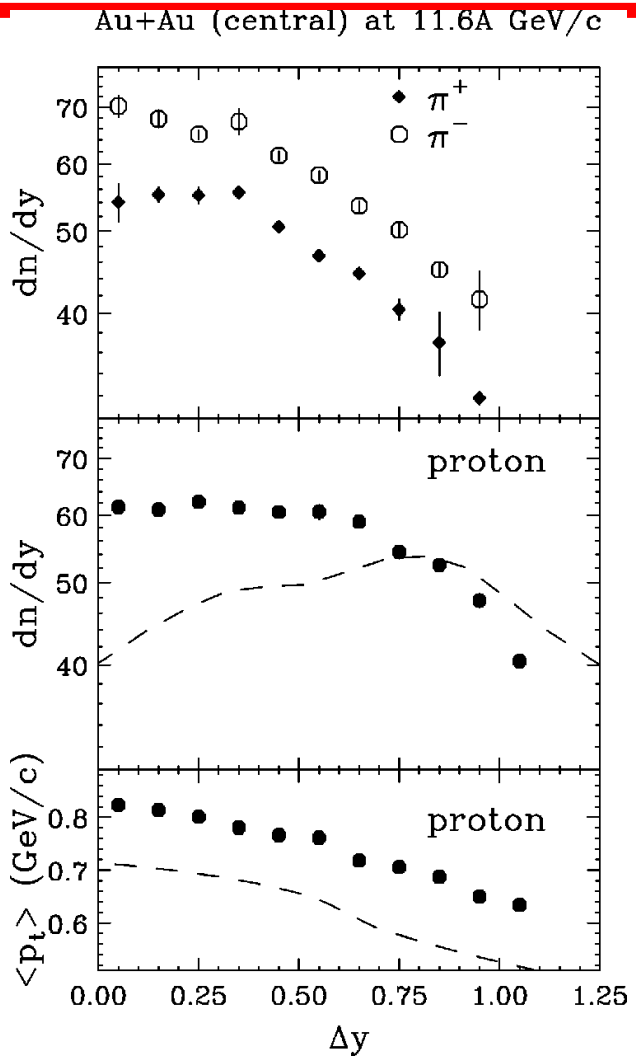


E802_PRC57(1998)R466

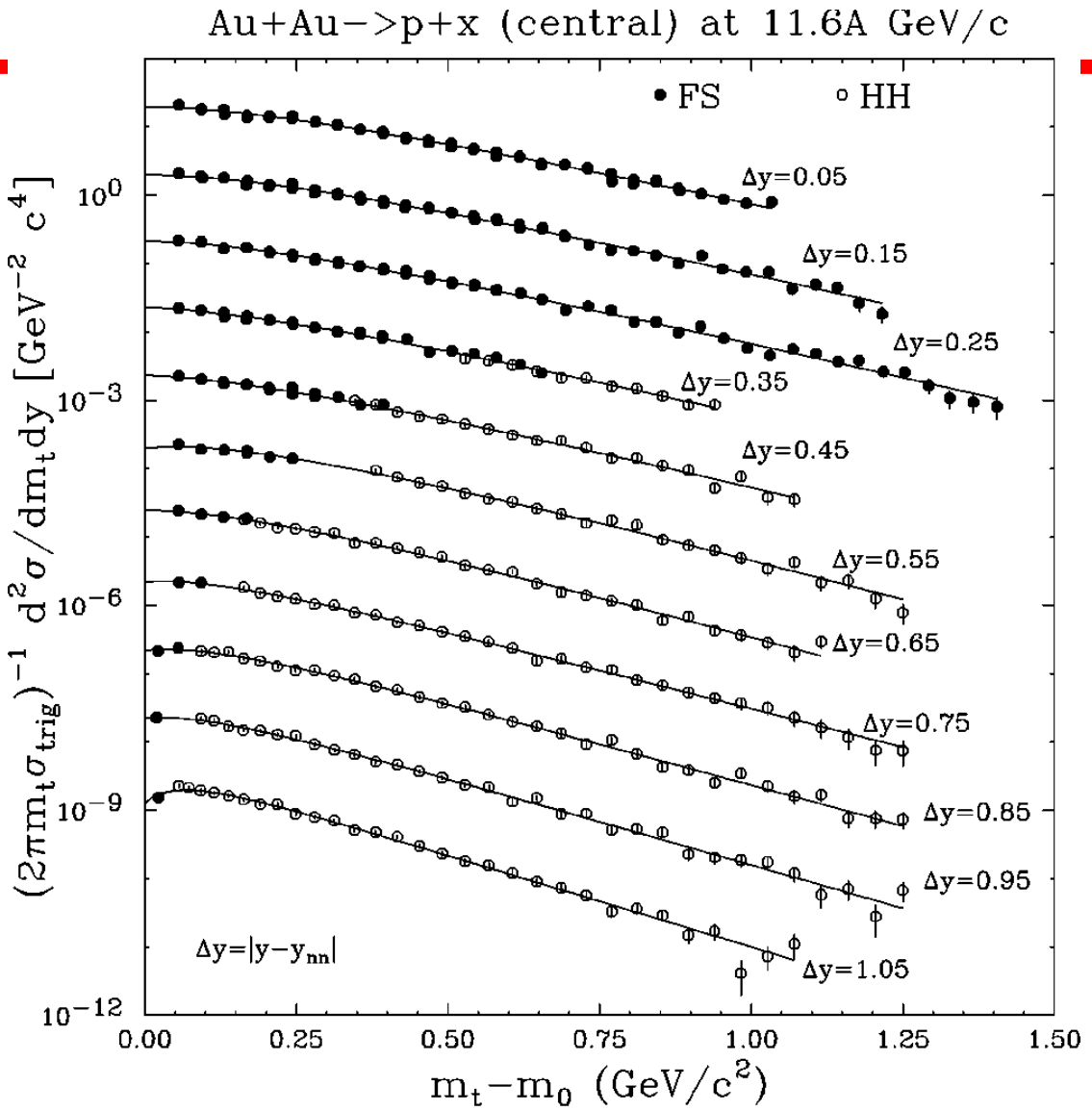

# Spectra -- protons

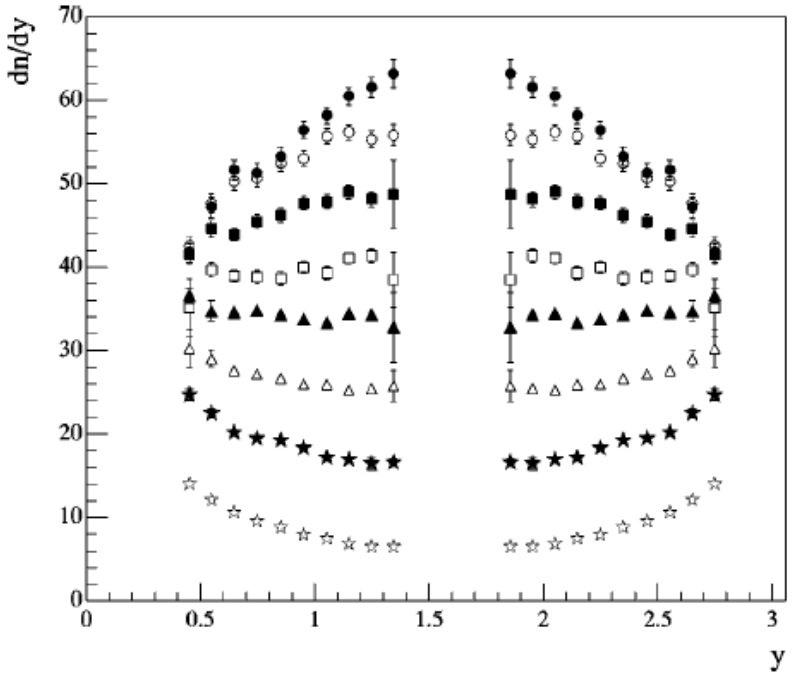


E802_PRC60(1999)064901

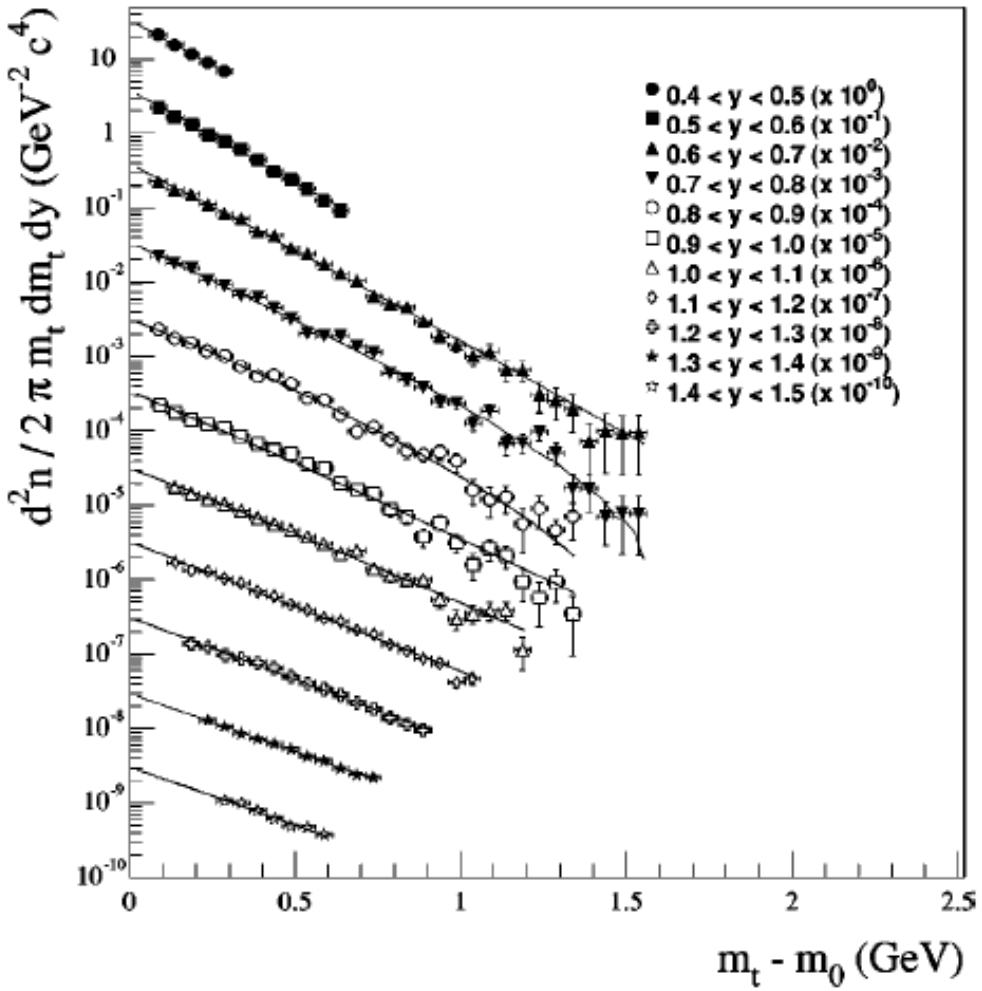


FIG. 5. Measured double differential yield for protons, in different rapidity intervals as a function of transverse kinetic energy $m_t - m_0$. This spectra is for the 0–3 % centrality cut. The lines are fits to Eq. (4) (see text). The error bars are only statistical; the systematic errors are discussed in the text.

# Spectra -- protons

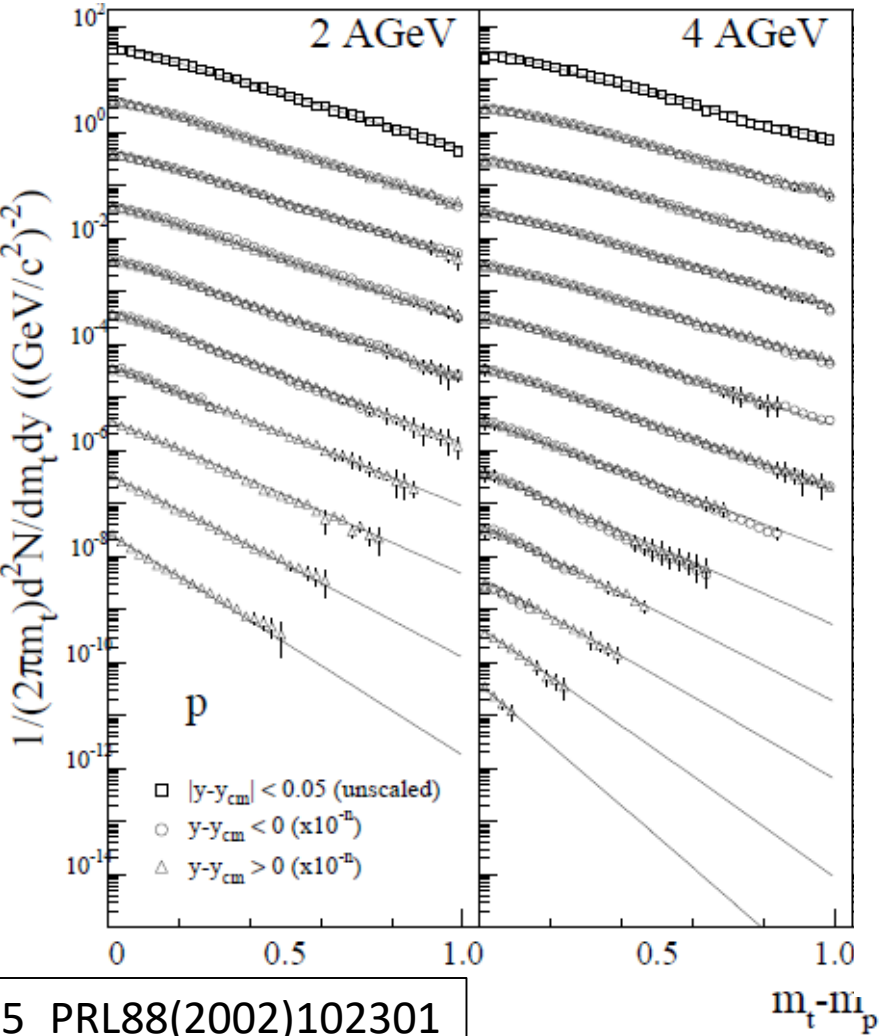


E895_PRL88(2002)102301

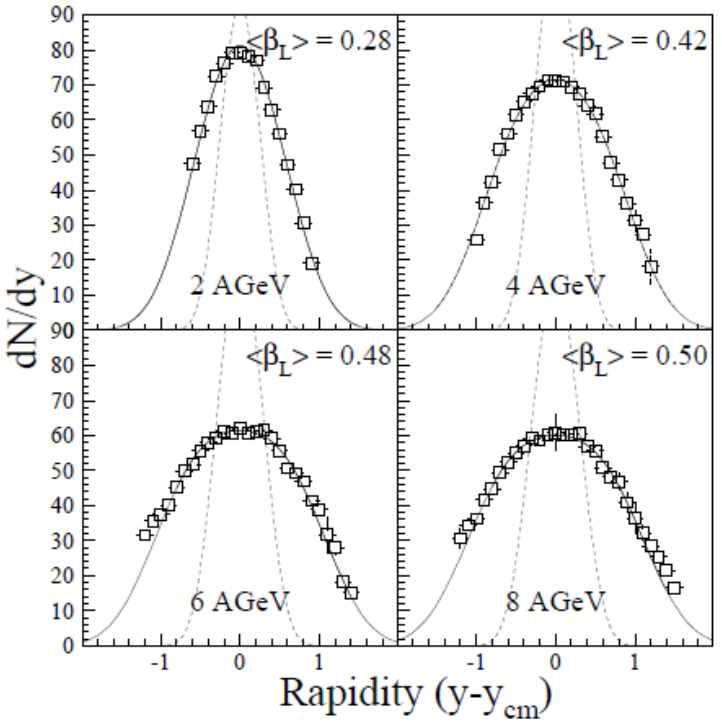


FIG. 2: Proton rapidity distributions in central Au+Au collisions at 2, 4, 6, and 8 AGeV. The dashed curves correspond to isotropic emission from a stationary thermal source with temperatures given by the mid-rapidity inverse slope parameters from the transverse mass fits (Eq. (2)), whereas the solid curves indicate fits with longitudinal flow (Eq. (3)).

FIG. 1: Invariant yield per event as a function of $m_t$-$m_0$ for protons in central Au+Au collisions at 2, 4, 6, and 8 AGeV. Midrapidity is shown unscaled, while the 0.1 unit forward/backward rapidity slices are scaled down by successive factors of 10.

## Spectra -- protons

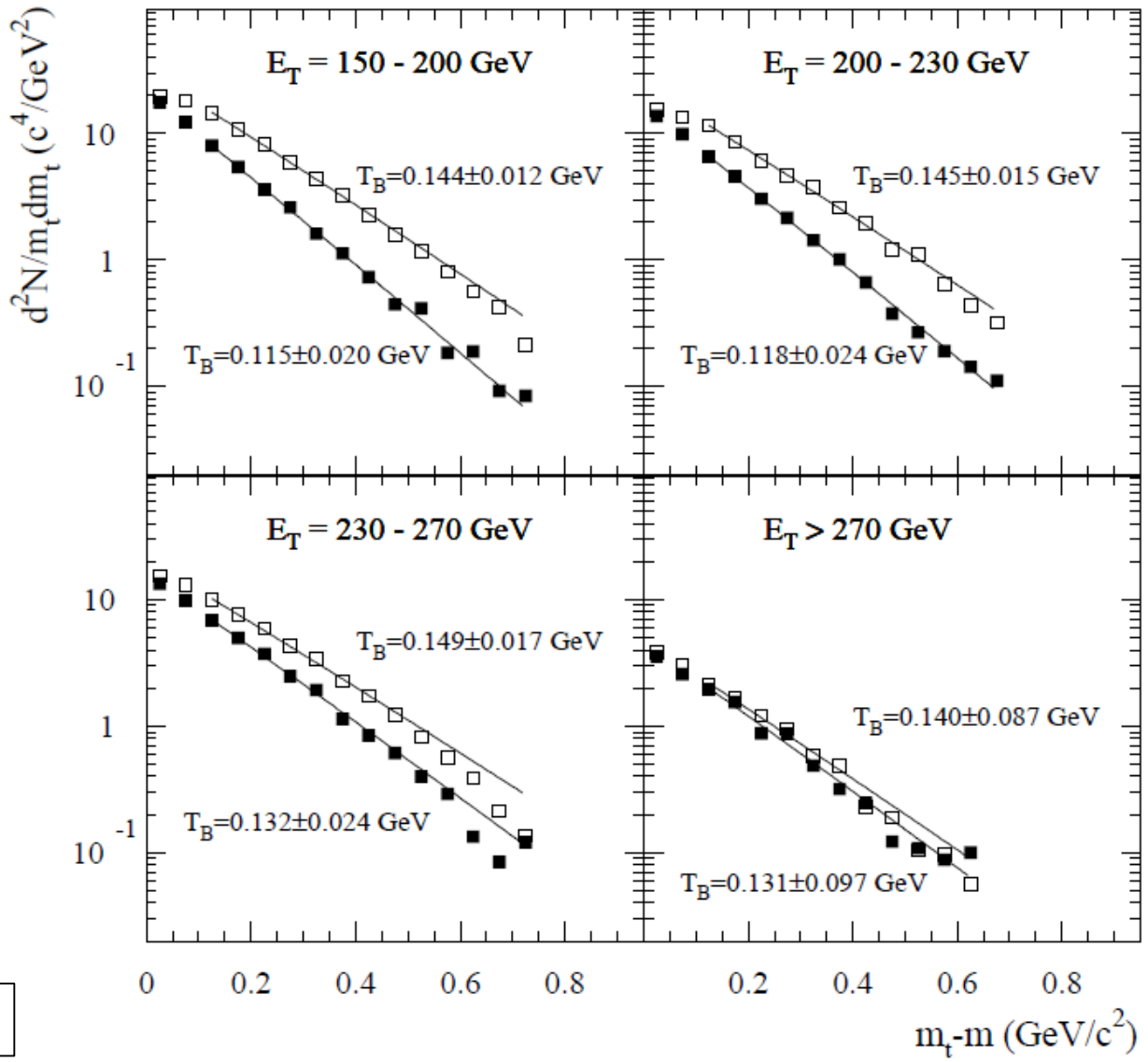


E877_PRC56(1997)3254

FIG. 2. Proton $m_t$ distributions in the rapidity interval $2.8 < y < 2.9$ for different centralities

# Spectra -- Protons

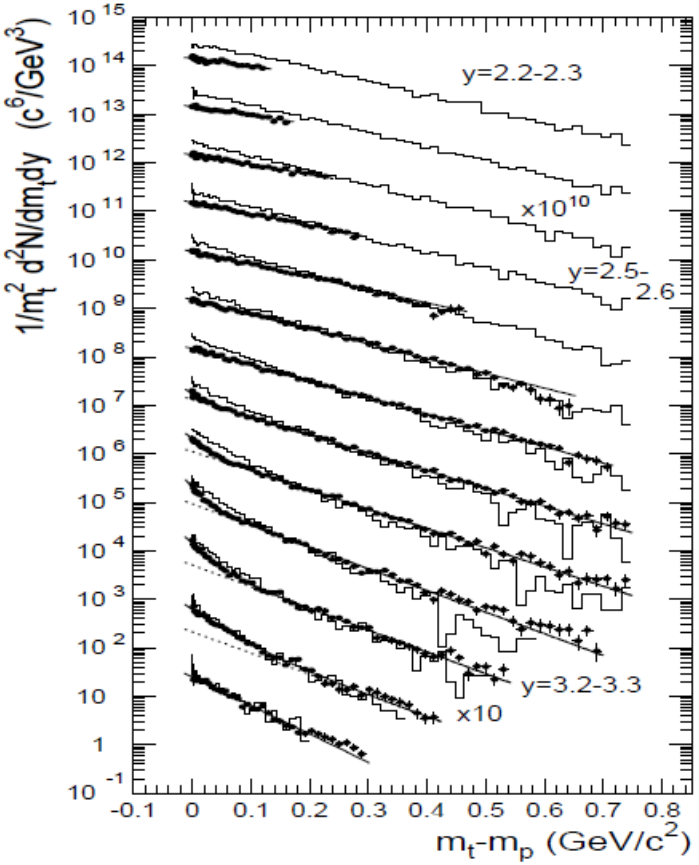


E877_PRC62(2000)024901

FIG. 1. Transverse mass spectra for protons produced in central ($\sigma_{central}/\sigma_{geom}$=0.04) Au+Au collisions. The dots correspond to constant $p_t$ bins of 20 MeV, and $y$ bins of 0.1 units. Beginning with rapidity bin $y$=3.3-3.4, spectra have been multiplied by successively increasing factors of ten. Full lines are two component exponential fits to the data. The histograms are RQMD predictions.

# Spectra -- Neutrons

E864_PRC60(2000)064903

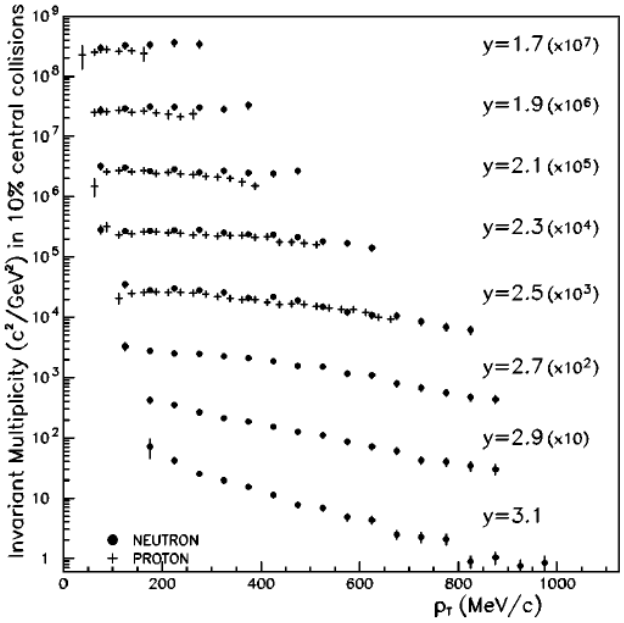


FIG. 5. Neutron invariant multiplicities in 10% most central Au+Pb collisions as a function of transverse momentum for rapidities from near center of mass ($y=1.6$) to beam ($y=3.2$). Each rapidity range is multiplied by a successive factor of 10 for presentational purposes. Proton multiplicities measured by E864 in central collisions are shown for comparison for rapidities 1.7 to 2.5.

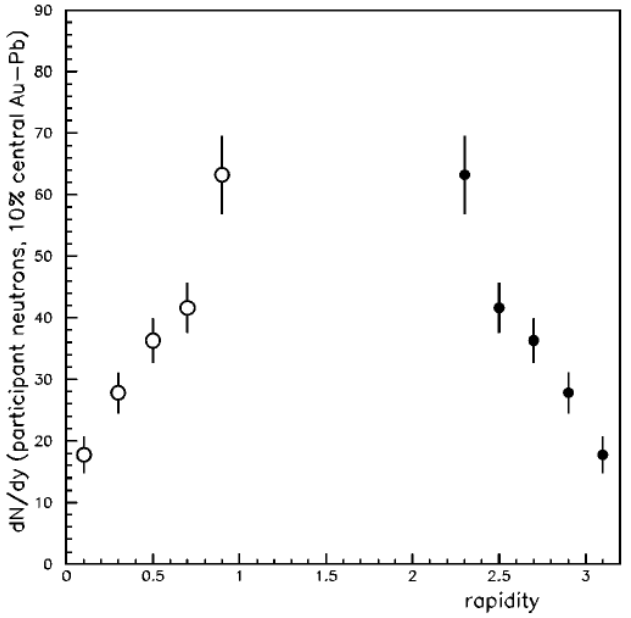


FIG. 10. $dN/dy$ measured for ''participant'' neutrons in central Au+Pb collisions. For those $m_T$ ranges not covered by direct measurements (or having a large contribution from spectator neutrons), a Boltzmann fit is used for the integration in $m_T$. Hollow points denote a reflection about center-of-mass rapidity.

# Spectra – Light Nuclei

E864_PRC61(2000)064908

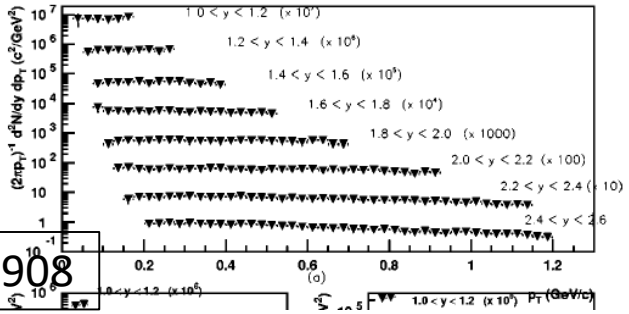


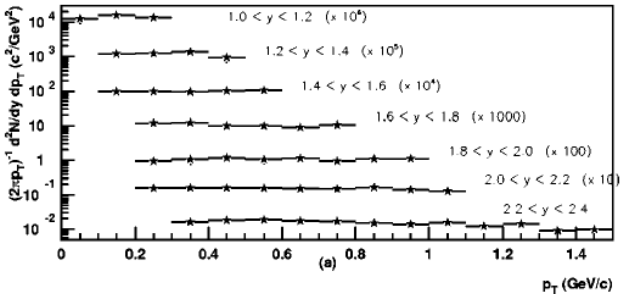


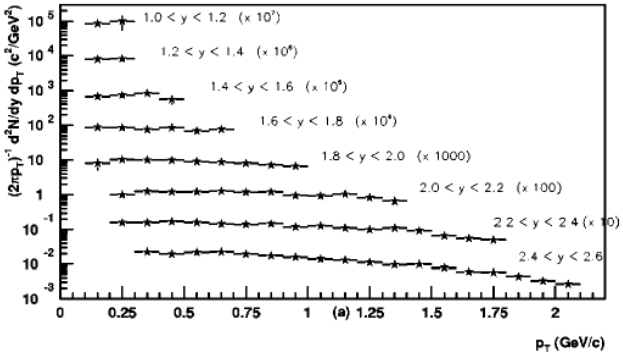


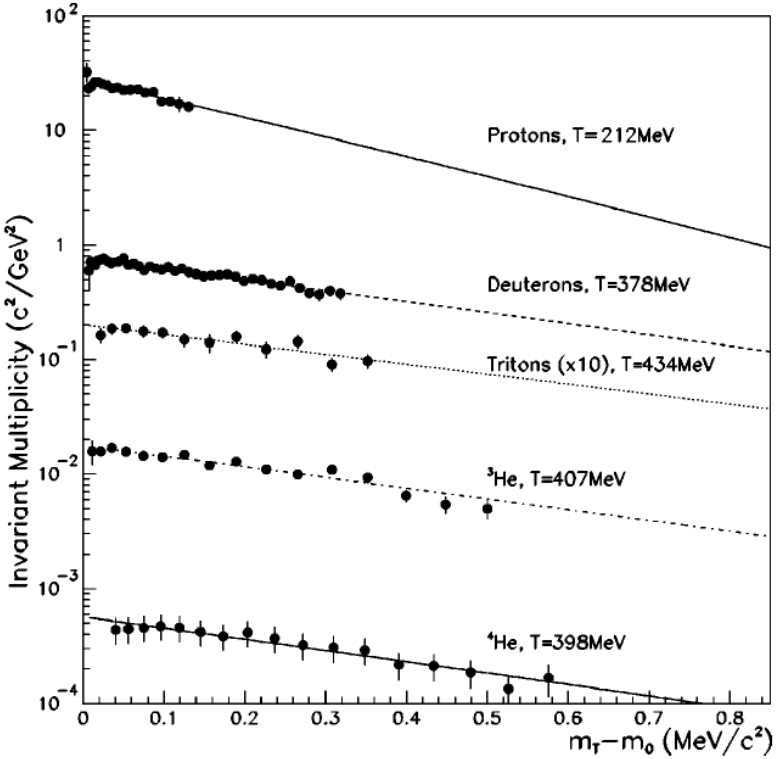


Comparison of the three experiments' measurements of deuterons and tritons shows close agreement and the measurements of E864 and E878 of $\alpha$ particle yields also agree within errors.

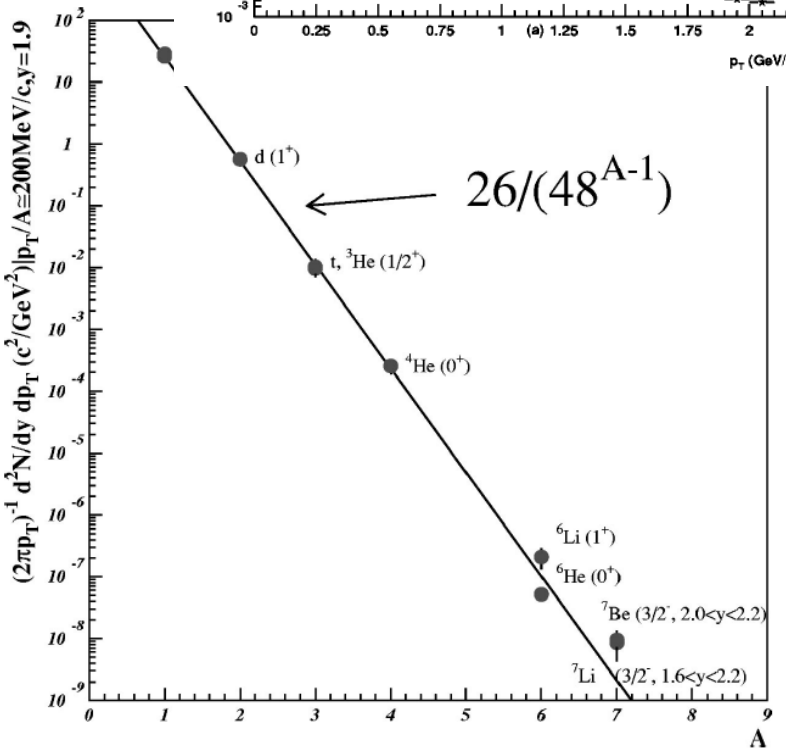

# Spectra – Light Nuclei

E864_PRC61(2000)064908

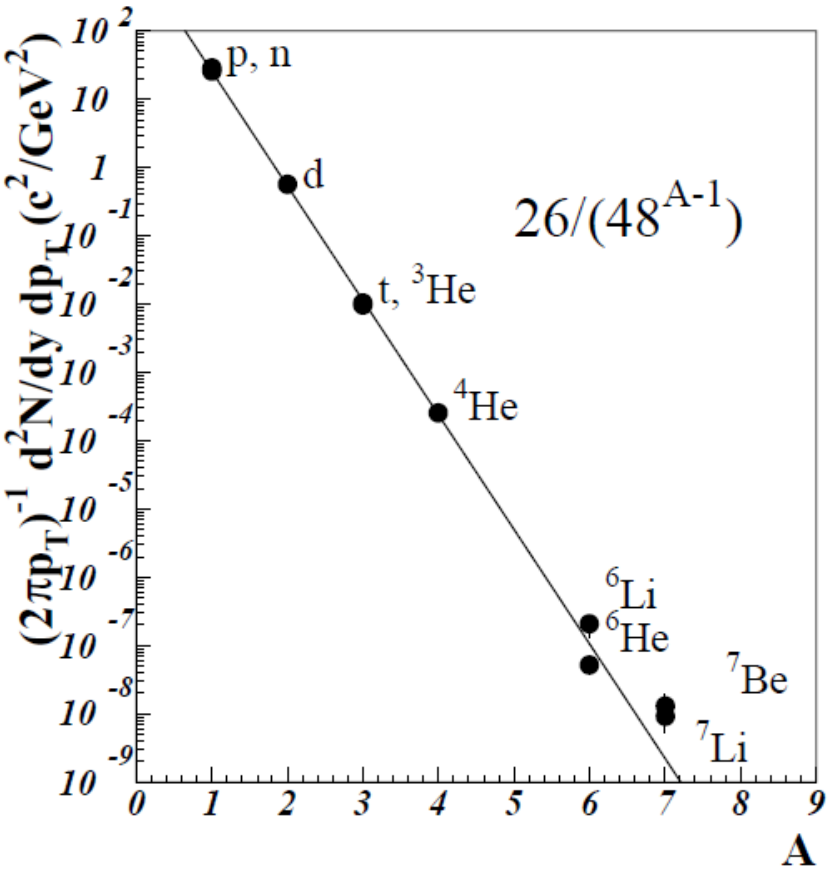


FIG. 1. Invariant yield as a function of nuclear number $A$. The bin size in rapidity is 0.2 (0.6 for $^7$Li). $p_T/A \leq 300$ MeV. The $J^P$'s of $p$, $n$, $d$, $^3$He, $t$, $^4$He, $^6$He, $^6$Li, $^7$Li, and $^7$Be are $\frac{1}{2}^+$, $\frac{1}{2}^+$, $1^+$, $\frac{1}{2}^+$, $\frac{1}{2}^+$, $0^+$,$0^+$, $1^+$, $\frac{3}{2}^-$, and $\frac{3}{2}^-$, respectively. The line is a fit to the data with $26/(48^{A-1})$.

## Spectra – anti-deuteron

E864_PRL85(2000)2685

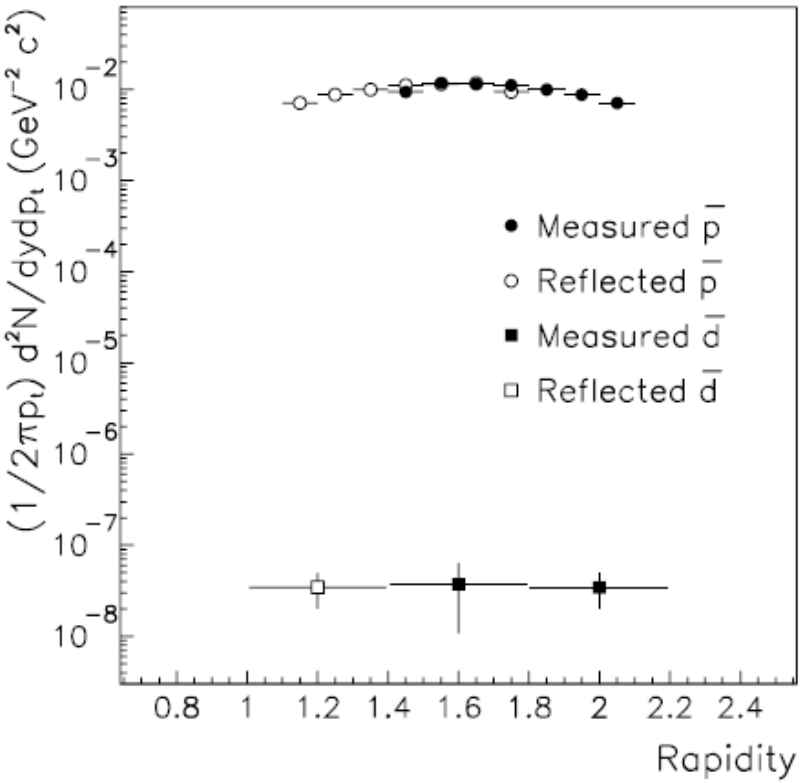


FIG. 3. Antimatter invariant yields measured by E864 in 10% central heavy ion collisions (statistical errors only).

# Spectra – hyper-nuclei

E864_PRC70(2004)024902

PHYSICAL REVIEW C 70, 024902 (2004)

## Production of $^{3}_{\Lambda}$H and $^{4}_{\Lambda}$H in central 11.5 GeV/$c$ Au+Pt heavy ion collisions

T. A. Armstrong,[8,*] K. N. Barish,[3] S. Batsouli,[13] S. J. Bennett,[12] M. Bertaina,[7,†] A. Chikanian,[13] S. D. Coe,[13,‡] T. M. Cormier,[12] R. Davies,[9,§] C. B. Dover,[1,‖] P. Fachini,[12,¶] B. Fadem,[5] L. E. Finch,[13] N. K. George,[13,**] S. V. Greene,[11] P. Haridas,[7,††] J. C. Hill,[5] A. S. Hirsch,[9] R. Hoversten,[5] H. Z. Huang,[2] H. Jaradat,[12] B. S. Kumar,[13,‡‡] T. Lainis,[10] J. G. Lajoie,[5] R. A. Lewis,[8] Q. Li,[12] B. Libby,[5,§§] R. D. Majka,[13] T. E. Miller,[11] M. G. Munhoz,[12] J. L. Nagle,[4] I. A. Pless,[7] J. K. Pope,[13,‖‖] N. T. Porile,[9] C. A. Pruneau,[12] M. S. Z. Rabin,[6] J. D. Reid,[11,¶¶] A. Rimai,[9,a] A. Rose,[11] F. S. Rotondo,[13,b] J. Sandweiss,[13] R. P. Scharenberg,[9] A. J. Slaughter,[13] G. A. Smith,[8] X. M. L. Tincknell,[9,c] W. S. Toothacker,[8,‖] G. Van Buren,[7,2,¶] F. K. Wohn,[5] and Z. Xu[13]
(E864 Collaboration)

# Spectra – anti-proton

E864_PRL79(1997)3351

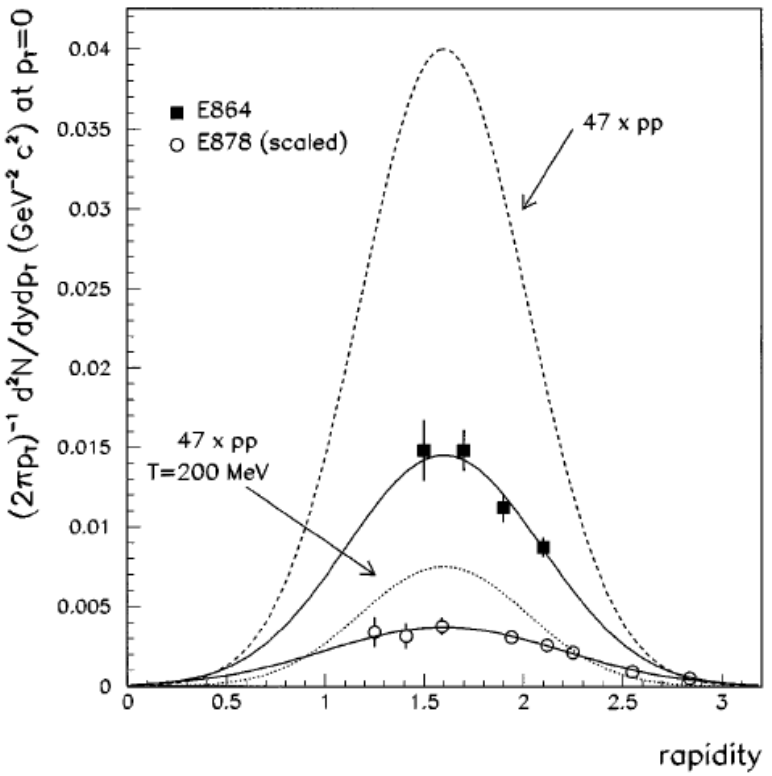


FIG. 3. $\overline{p}$ invariant multiplicities as extrapolated to $p_T = 0$ in E864 and measured in E878 (scaled to 11.5$A$ GeV/$c$), for 10% central Au + Pb and Au + Au collisions. Fits to the E864 and E878 data are also shown. The errors are statistical only. Two predictions based on first collision scaling (without annihilation) are also indicated.

# Spectra – Anti-protons and anti-Lambdas

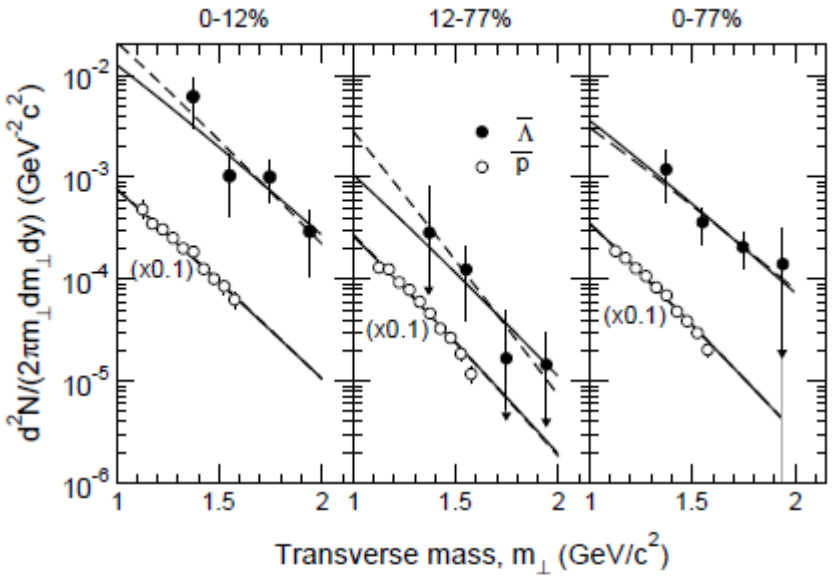


FIG. 1: Invariant spectra as a function of transverse mass $\bar{\Lambda}$ (solid circles) and $\bar{p}$ (open circles, multiplied by 0.1 for cl ity) in the three centrality classes. The error bars include a point-to-point systematic error due to acceptance correctio The solid lines are from the simultaneous fit as described the text and the dashed lines are from independent fits $\bar{\Lambda}$ and $\bar{p}$ spectra shown for comparison. Solid and dashed lines overlap for the $\bar{p}$ spectra.

E917_PRL(2001)242301

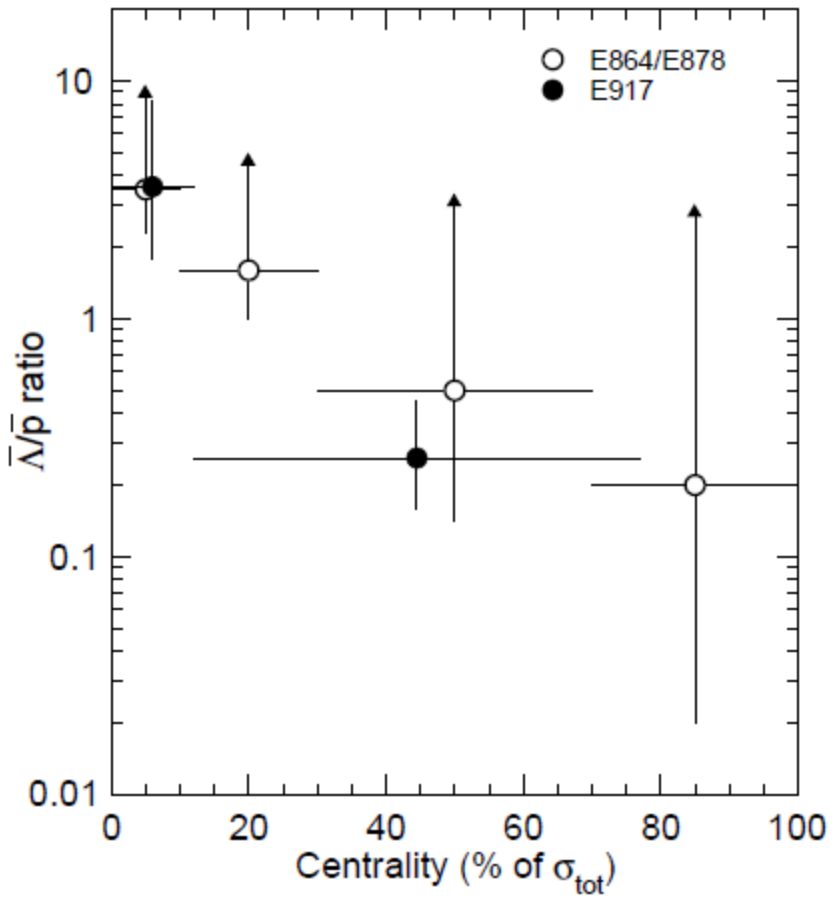


FIG. 3: The $\bar{\Lambda}/\bar{p}$ ratio is shown as a function of the centrality given in terms of the percentage of the total interaction cross section, $\sigma_{tot}$. The E917 data are integrated over all $p_\perp$ and $1.0 < y < 1.4$ and are shown as solid circles with $1\sigma$ statistical error bars for the $\bar{\Lambda}/\bar{p}$ ratio. The E864/E878 indirect results [15] are at $p_\perp \sim 0$ and y=1.6 and are shown as most probable values with the 98% confidence level of the minimum value indicated by the lower error bar. Upper limits are not given. Horizontal bars indicate bin widths.

## Spectra – anti-protons

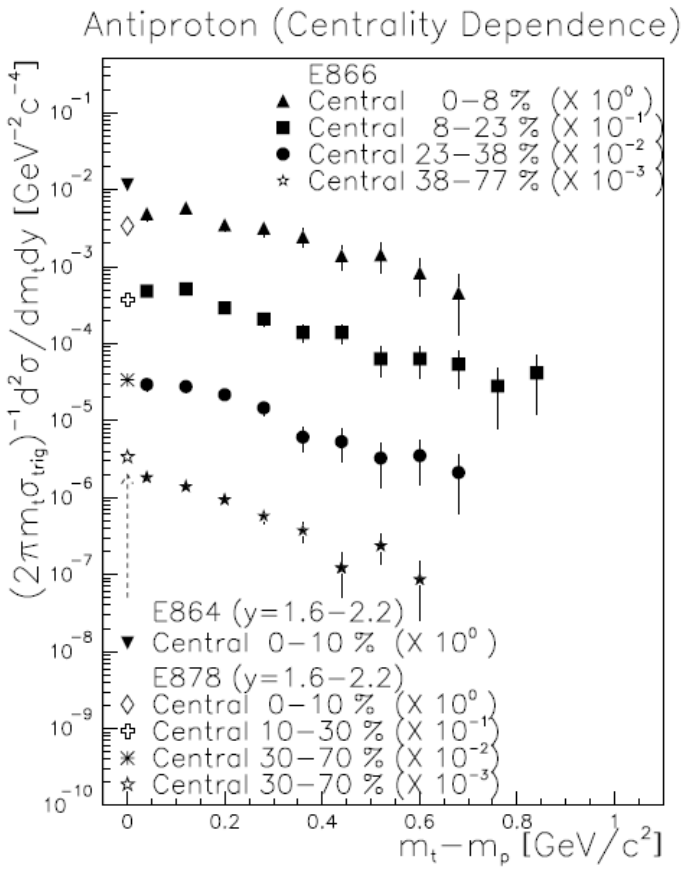


FIG. 2. Invariant differential yields of $\overline{p}$ in $1.0 < y < 2.2$ in four centrality windows, 0%–8%, 8%–23%, 23%–38%, and 38%–77%, from top to bottom. Data from other AGS experiments are also shown. Error bars are statistical. See text for details.

E802_PRL81(1998)2650

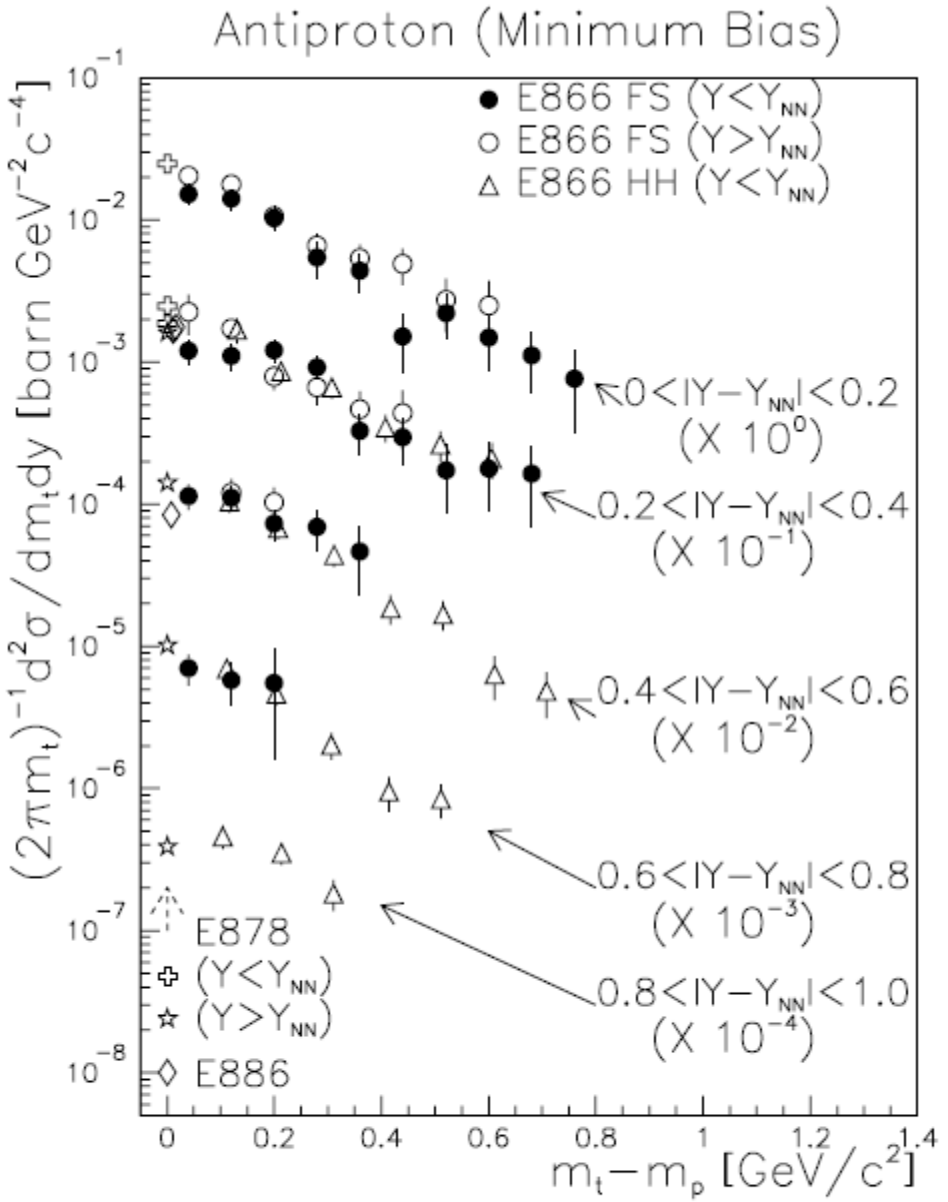


FIG. 1. Invariant differential cross sections of $\overline{p}$ as a function of $m_t - m_p$ for minimum-bias events at each rapidity range. Data from other AGS experiments are also shown. Error bars are statistical. See text for details.

## Spectra -- deuterons

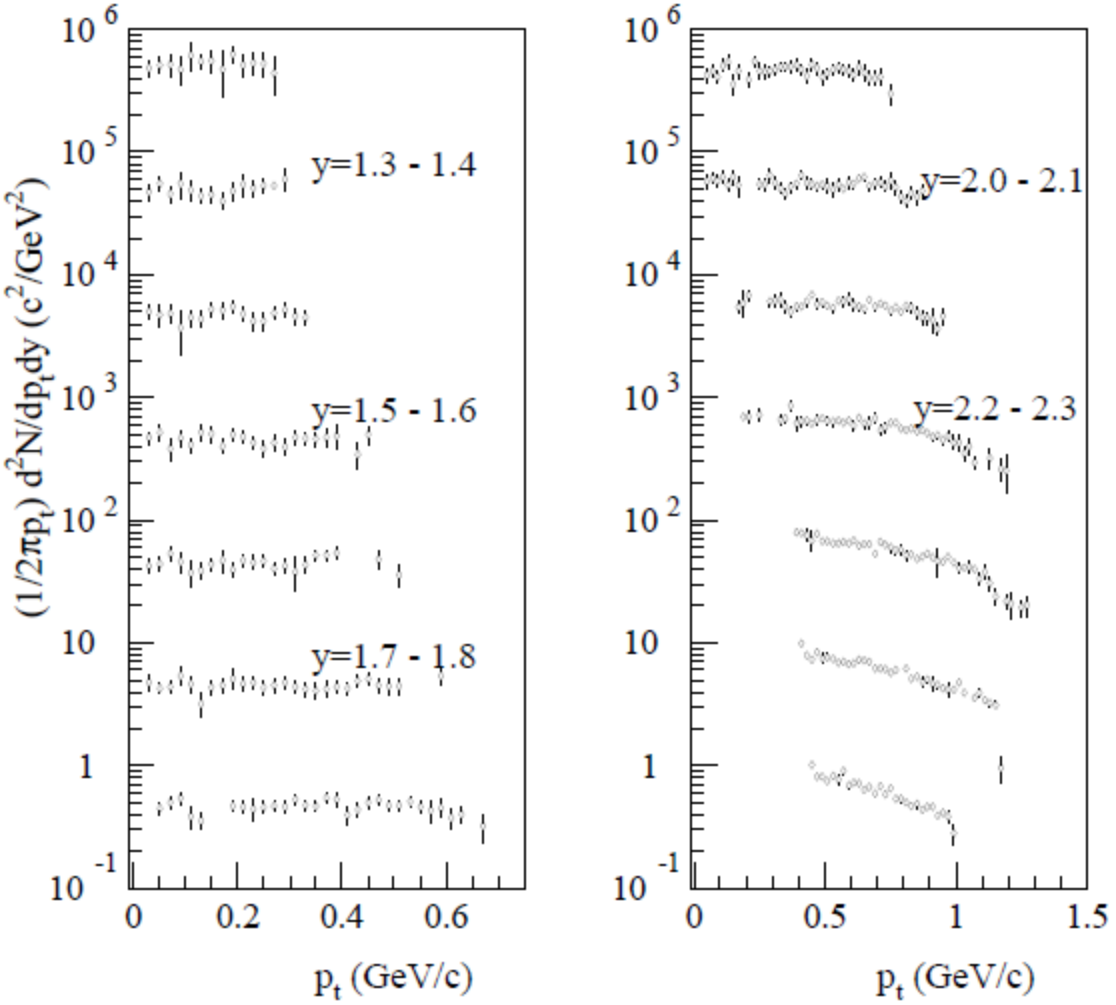


E814_PRC61(2000)044906

FIG. 7. Invariant multiplicities of deuterons for the 4% highest $E_t$ events. The spectra are binned in units of .1 in rapidity and 20 MeV in $p_t$. The $y = 2.5 - 2.6$ and $y = 1.8 - 1.9$ spectra are properly normalized and the yields for the lower rapidity bins are multiplied by successive powers of 10 for clarity of the presentation. *e.g.* The $y = 1.7 - 1.8$ bin is multiplied by a factor of 10, the $y = 1.6 - 1.7$ bin is multiplied by a factor of 100, etc. The error bars reflect the statistical uncertainties.

# Spectra -- deuterons

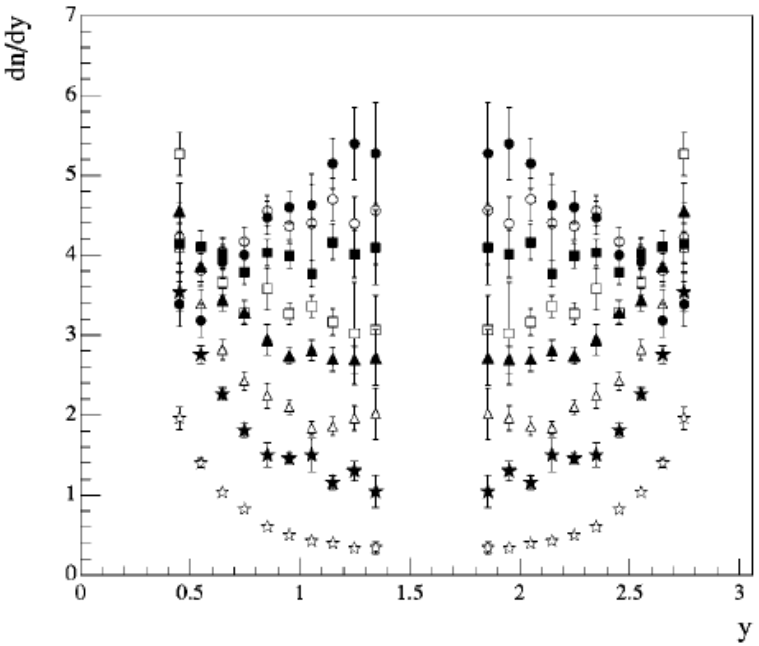


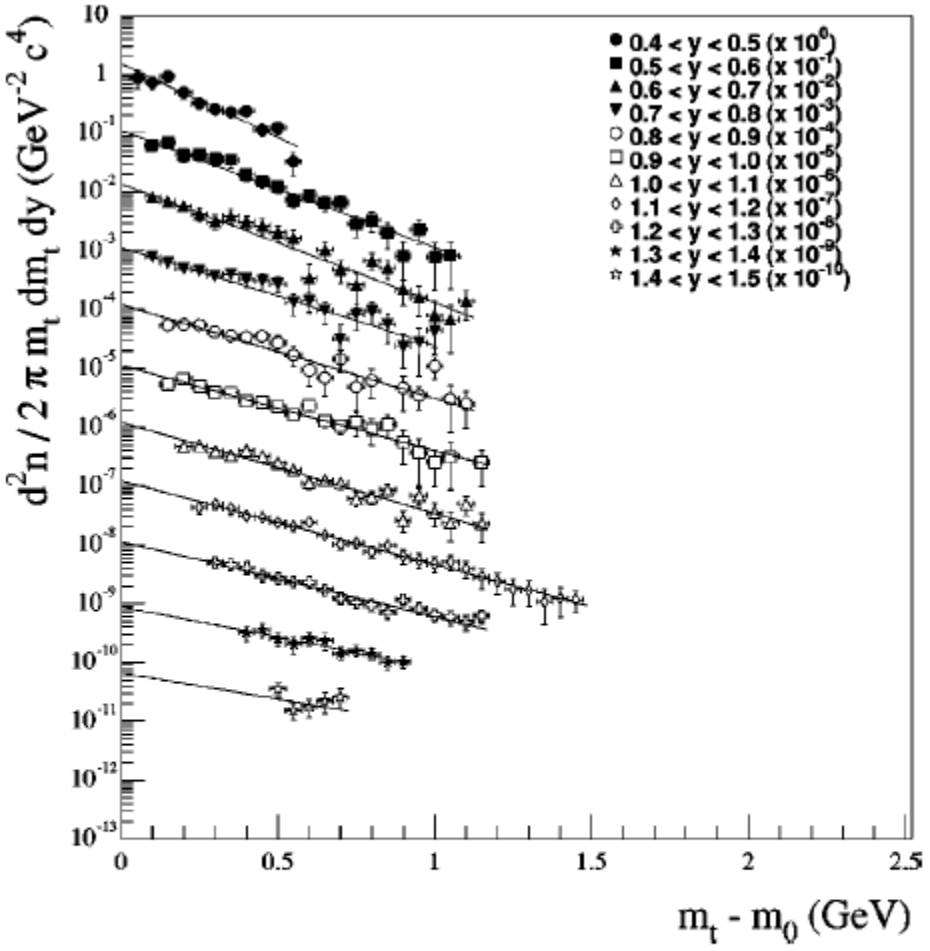


FIG. 6. Measured double differential yield for deuterons, in different rapidity intervals as a function of transverse kinetic energy $m_t - m_0$. These spectra are for the 0–3 % centrality cut. The lines are fits to Eq. (4) (see text). The error bars are only statistical; the systematic errors are discussed in the text.

E802_PRC60(1990)064901

# Spectra – tritons and helions

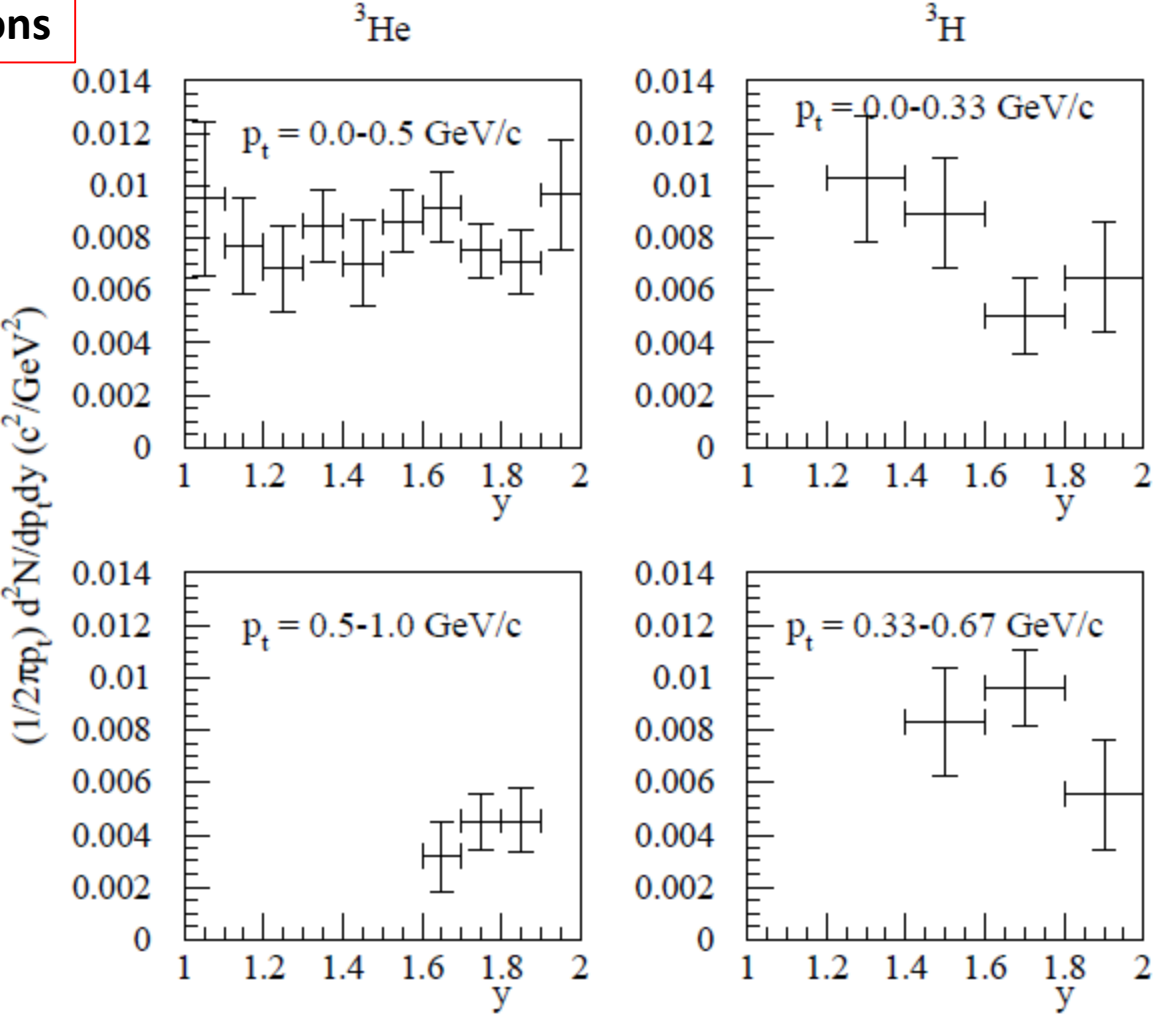


E814_PRC61(2000)044906

FIG. 8. Invariant multiplicities of $^3$He and $^3$H for the 4% inclusive $E_t$ bin. Plotted is the nvariant cross section at the center of the bin assuming an underlying thermal distribution similar o what is measured. Error bars reflect statistical uncertainties only.

# Spectra – d, t, h

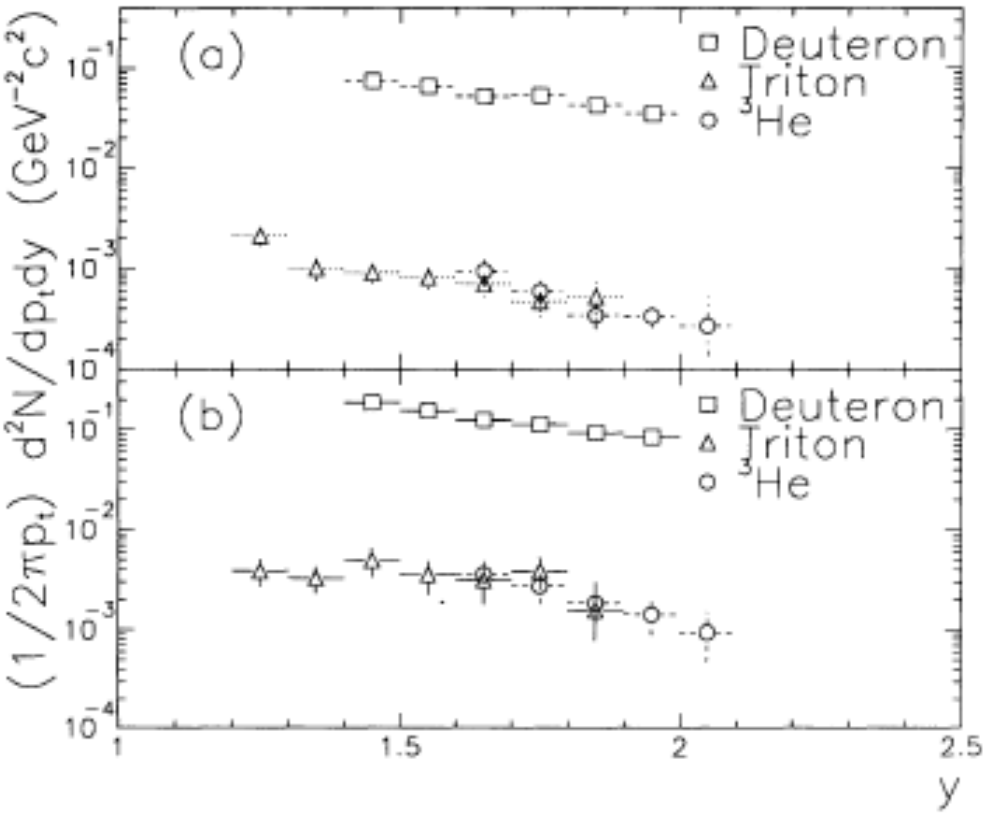


**FIG. 4. The invariant yields of deuterons, tritons, and $^3$He at $p_t = 0$ plotted as a function of rapidity for Si+Pb collisions. Multiplicity cuts correspond to (a) 89% and (b) 8% , respectively, of the geometrical cross section. The uncertainties shown are statistical only.**

E814_PRC50(1994)1077

# Spectra – anti-proton and anti-deuteron

E864_PRC59(1999)2699

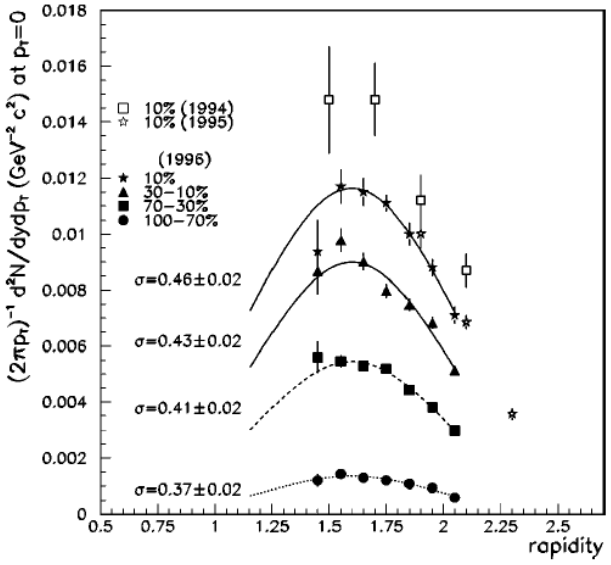


FIG. 6. Antiproton invariant multiplicities as a function of centrality showning the 1994, 1995, and 1996 data sets from E864. The error bars shown are statistical only. Systematic errors are estimated to be 20% on the 1994 data, 15% for the 1995 data, and 10% for the 1996 data, not including a 6% systematic error for the projection to $p_T = 0$. The fits are constrained to have a mean value at midrapidity ($y = 1.6$).

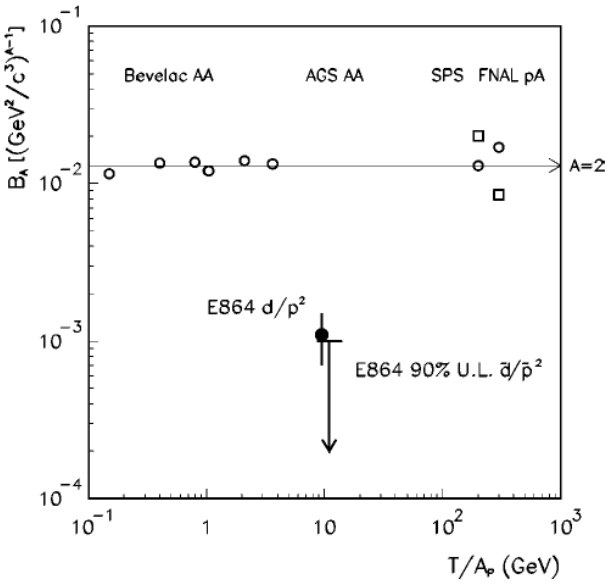


FIG. 16. Coalescence scale factors as a function of kinetic energy per nucleon of the colliding beam. The upper limit on $\overline{B_2}$ from E864 is shown as an arrow. The E864 value for deuterons $B_2$ is also shown. The simple coalescence level is shown as a line with low-energy AA and high-energy pA results.

# Strangeness

# Strangeness - Lambdas

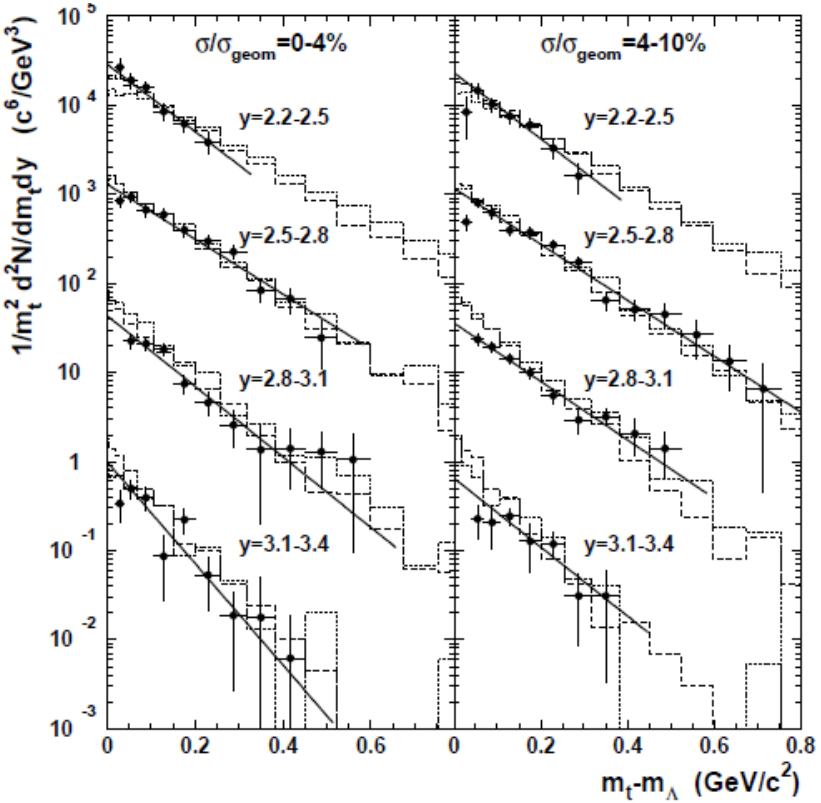


FIG. 5. Measured Λ transverse mass spectra for the most central ($0-4\%$ $\sigma_{geom}$-left side) semi-central ( $4-10\%$ $\sigma_{geom}$ - right side) Au+Au collisions. Beginning with rapidity bin $y$=3.1 spectra have been multiplied by successive factor of 10. The solid lines are the exponential Boltzmann fits to the data. The dashed lines and dotted lines are the predictions of RQMD v2.3 model run in *cascade* and *mean-field* modes, respectively.

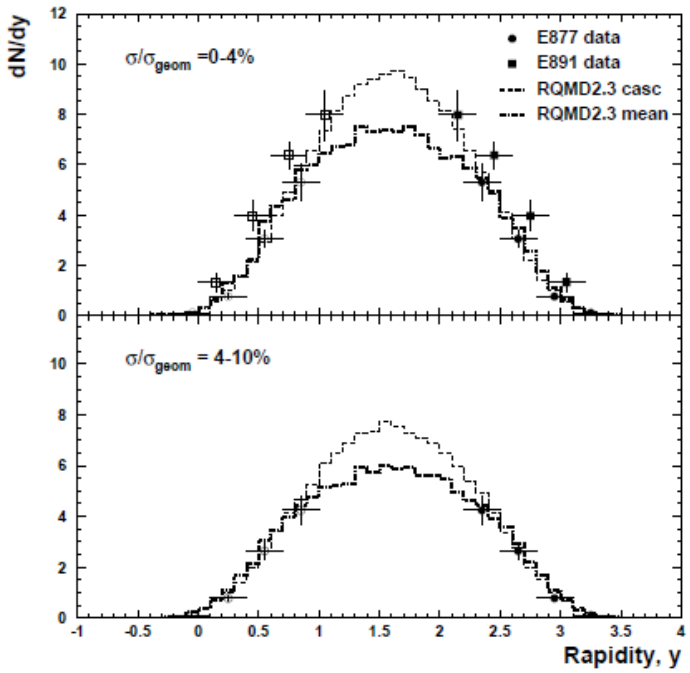


FIG. 7. Lambda rapidity distribution in the most central Au+Au collisions ($0-4\%$ $\sigma_{geom}$-upper pannel) and semi-central ( $4-10\%$ $\sigma_{geom}$ - lower pannel) Au+Au collisions. The data are represented by solid symbols and reflected about mid-rapidity (open symbols). The histograms correspond to RQMD v2.3 predictions.

E877_PRC63(2001)014902

# Strangeness – Phi meson

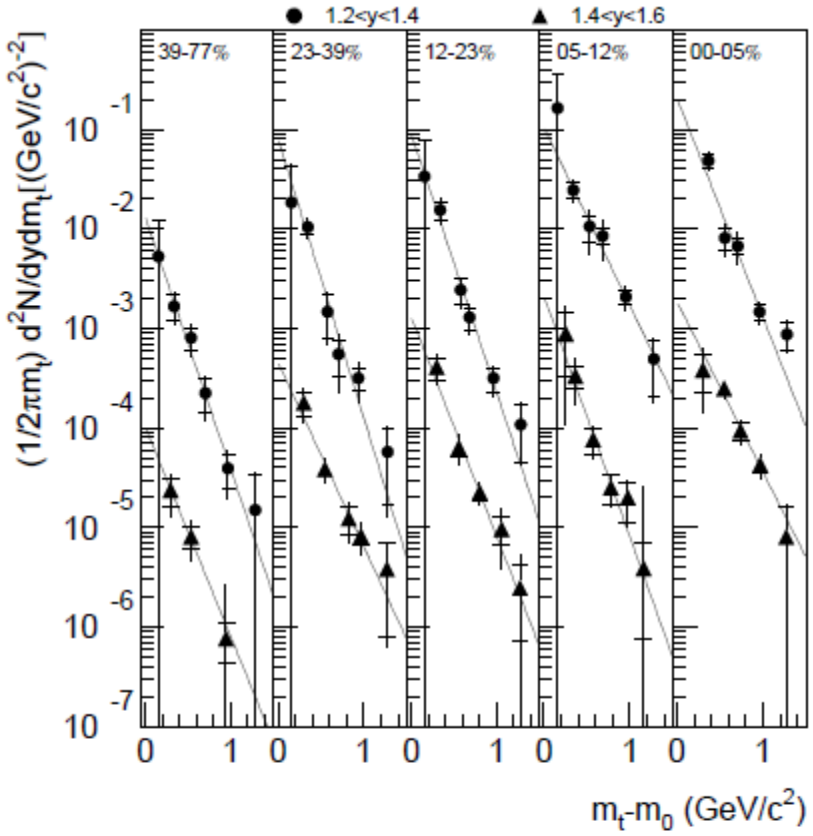


FIG. 4: The invariant yield of $\phi$'s as a function of transverse mass $(m_t - m_0)$ in five centrality bins labeled by $\sigma/\sigma_{\rm tot}$. In each panel, the top set of points (circles) is for $1.2 < y < 1.4$, while the second set of points (triangles) is for $1.4 < y < 1.6$ and is divided by 100 for presentation. The total errors are calculated as the quadrature sum of the systematic and statistical errors, while the magnitudes of the latter are indicated by the cross bars. The lines are the results of the exponential fits described in the text.

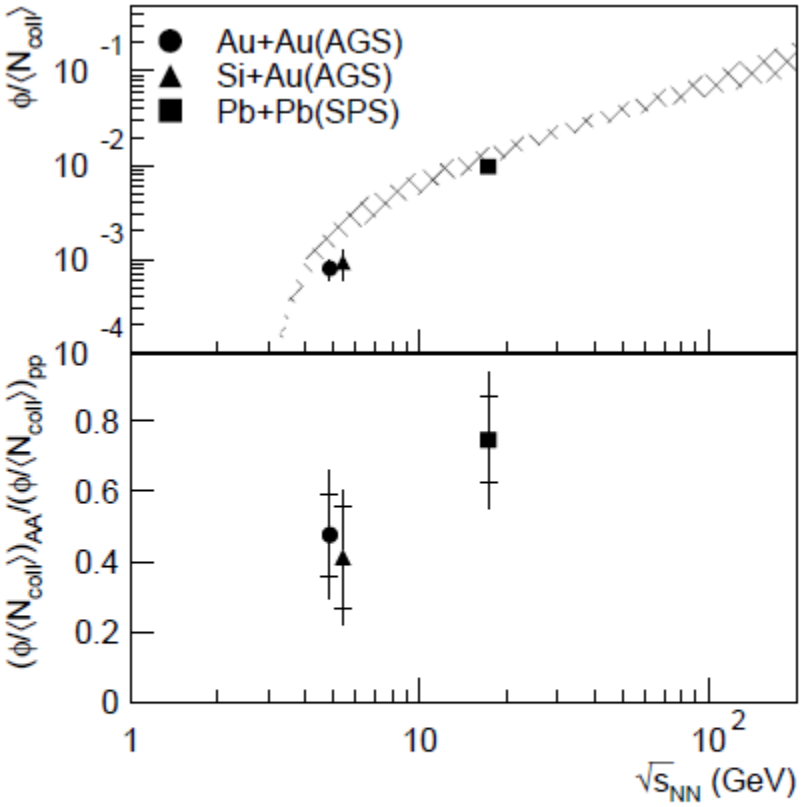


FIG. 13: Same as Fig. 10 for the ratios of $\phi/\langle N_{\rm coll}\rangle$, where $\langle N_{\rm coll}\rangle$ is the number of binary collisions. For the E917 data point, an estimated total $\phi$ yield is plotted as described in the text.

E917_PRC69(2004)054901

# Strangeness – Phi meson

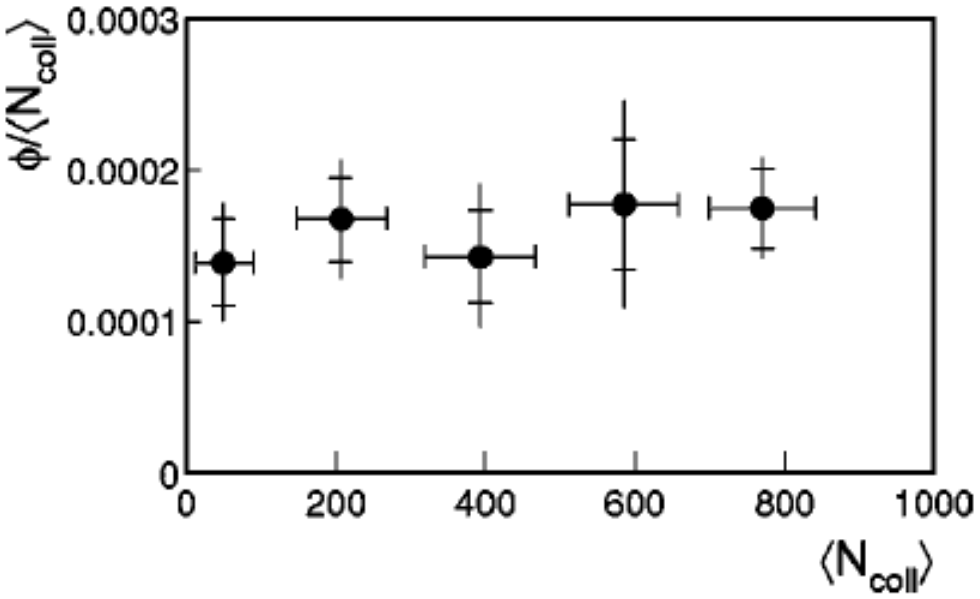


FIG. 9. The normalized fiducial yield of $\phi$ mesons per number of binary collisions $\langle N_{coll}\rangle$ as a function of $\langle N_{coll}\rangle$. The accepted rapidity region is $1.2 < y < 1.6$.

E917_PRC69(2004)054901

# Strangeness – Lambdas and Cascades

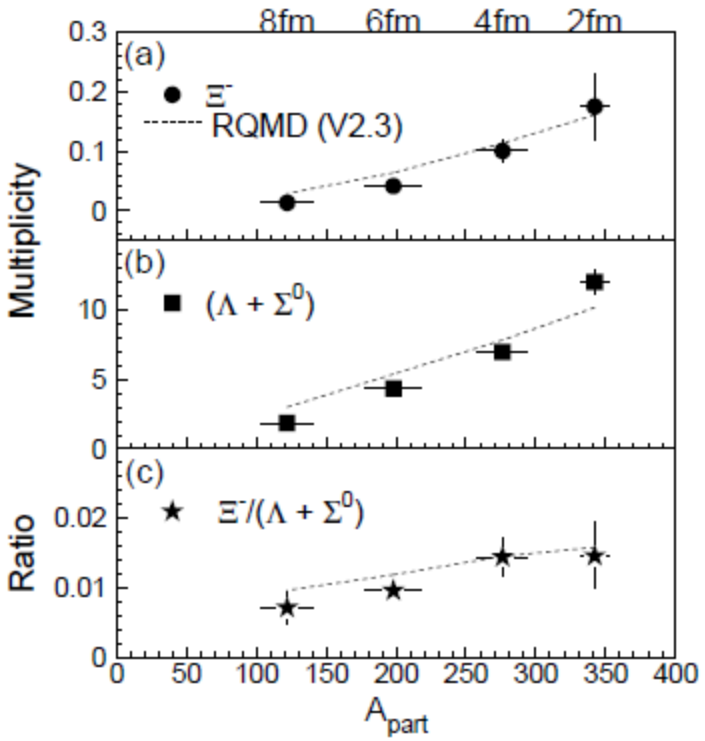


E895_PRL91(2003)202301

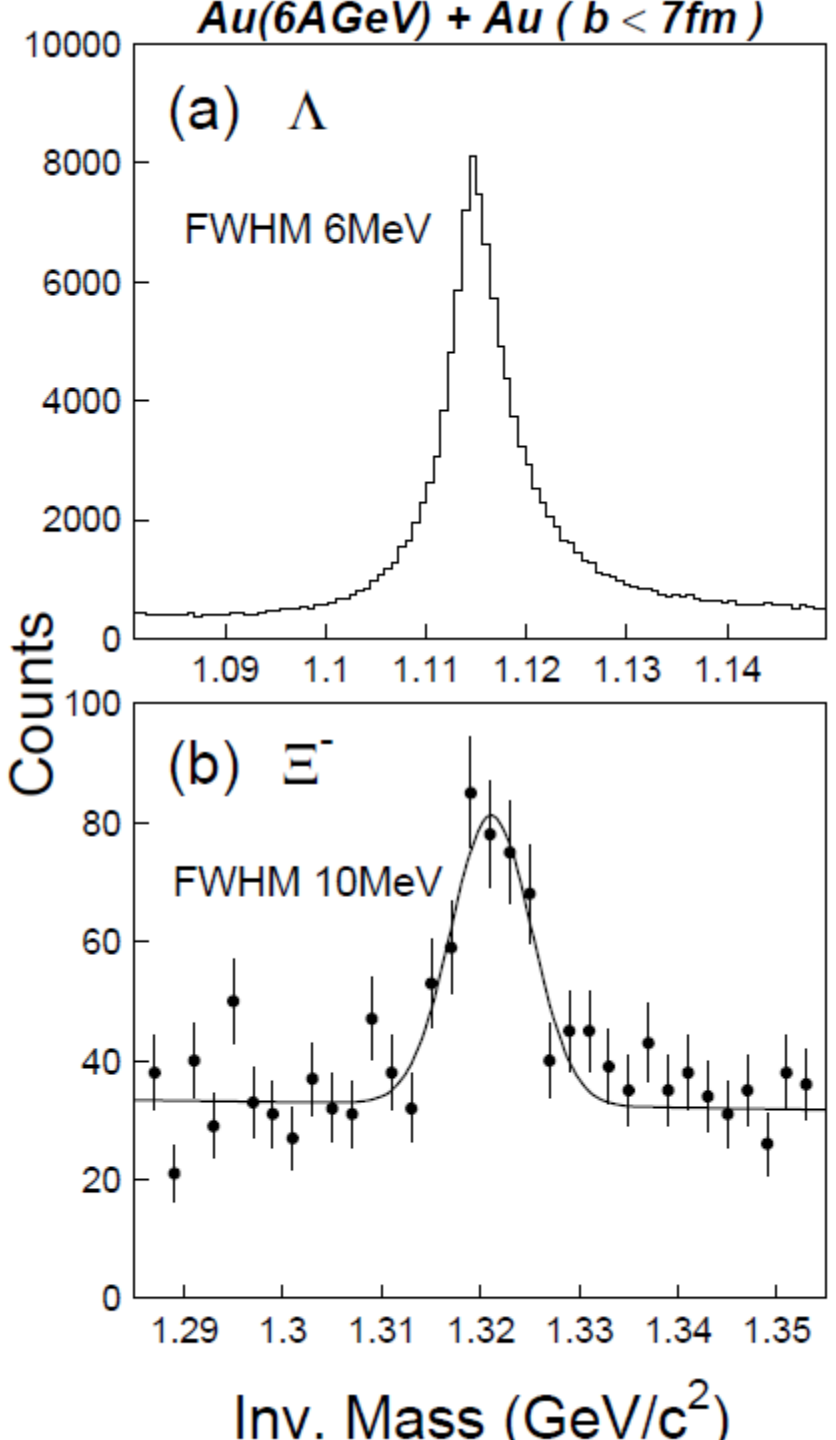

# Spectra – Anti-protons and anti-Lambdas

E917_PRL(2001)242301

| Bin | $dN_{\bar{p}\,\mathrm{total}}/dy$ ($\times 10^{-3}$) | $T_{\bar{p}\,\mathrm{total}}$ (GeV) | $T_{\bar{p}\,\mathrm{direct}}$ (GeV) | $dN_{\bar{\Lambda}}/dy$ ($\times 10^{-3}$) | $T_{\bar{\Lambda}}$ (GeV) | $\bar{\Lambda}/\bar{p}_{\mathrm{direct}}$ |
|---|---|---|---|---|---|---|
| 0%–12% | $17.7 \pm 0.5 \pm 1.8$ | $0.200 \pm 0.008 \pm 0.010$ | $0.23^{+0.15+0.1}_{-0.06-0.01}$ | $19^{+4+3}_{-5-2}$ | $0.22^{+0.04+0.01}_{-0.03-0.01}$ | $3.6^{+4.7+2.7}_{-1.8-1.1}$ |
| 12%–77% | $5.5 \pm 0.1 \pm 0.6$ | $0.175 \pm 0.004 \pm 0.008$ | $0.18^{+0.02+0.01}_{-0.01-0.01}$ | $1.2^{+0.7+0.2}_{-0.6-0.2}$ | $0.19^{+0.06+0.01}_{-0.03-0.01}$ | $0.26^{+0.19+0.5}_{-0.15-0.4}$ |
| 0%–77% | $7.4 \pm 0.1 \pm 0.7$ | $0.185 \pm 0.004 \pm 0.009$ | $0.183^{+0.017+0.014}_{-0.014-0.003}$ | $5.3^{+1.1+1.0}_{-1.1-1.0}$ | $0.218^{+0.026+0.020}_{-0.020-0.004}$ | $1.3^{+0.6+0.6}_{-0.4-0.3}$ |

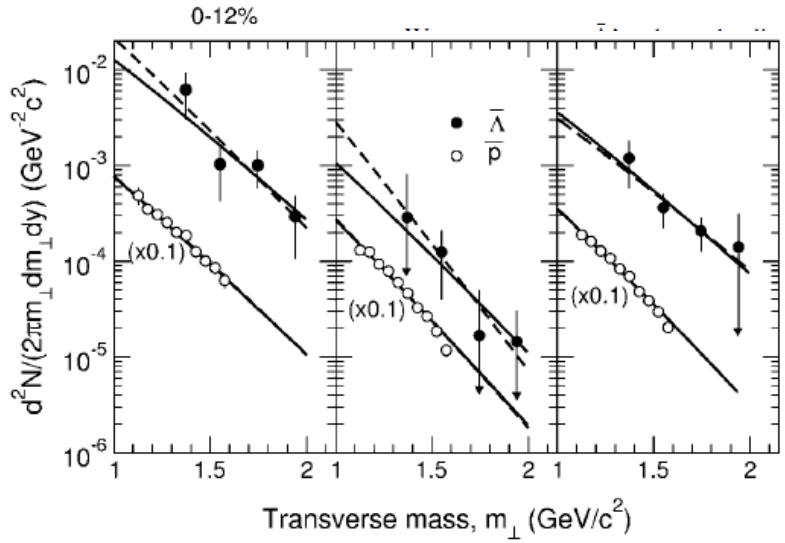


FIG. 1. Invariant yields as a function of transverse mass for $\bar{\Lambda}$ (solid circles) and total $\bar{p}$ (open circles, multiplied by 0.1 for clarity) in the three centrality classes. The error bars include a 2% point-to-point systematic error due to acceptance corrections, and an arrow on the bottom error bar is to indicate it extends below the plot limits. The solid lines are from the simultaneous fit as described in the text and the dashed lines are from independent fits to $\bar{\Lambda}$ and $\bar{p}$ data shown for comparison. Solid and dashed fit lines overlap for the $\bar{p}$ spectra.

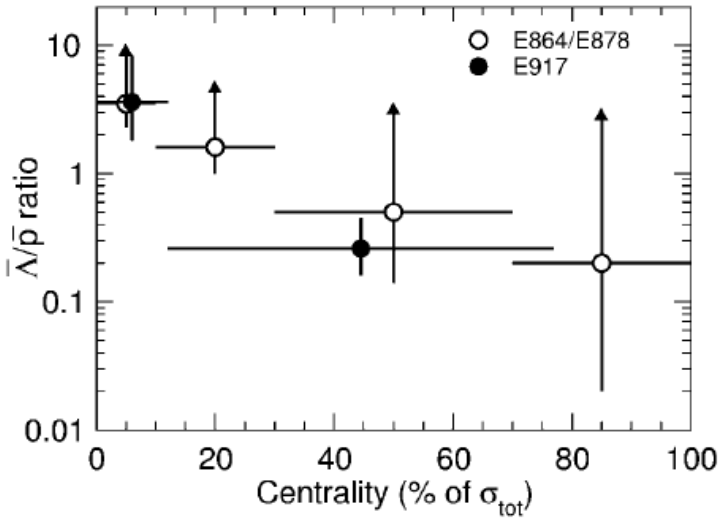


FIG. 3. The $\bar{\Lambda}/\bar{p}$ ratio is shown as a function of the centrality given in terms of the percentage of the total interaction cross section, $\sigma_{\mathrm{tot}}$. The E917 data are integrated over all $p_\perp$ and $1.0 < y < 1.4$ and are shown as solid circles with $1\sigma$ statistical error bars for the $\bar{\Lambda}/\bar{p}$ ratio. The E864/E878 indirect results are at $p_\perp \sim 0$ and $y = 1.6$ and are shown as most probable values with the 98% confidence level of the minimum value indicated by the lower error bar. Upper limits are not given. Horizontal bars indicate bin widths.

# Directed Flow

# Directed Flow -- Protons

E895_PRL84(2000)5488

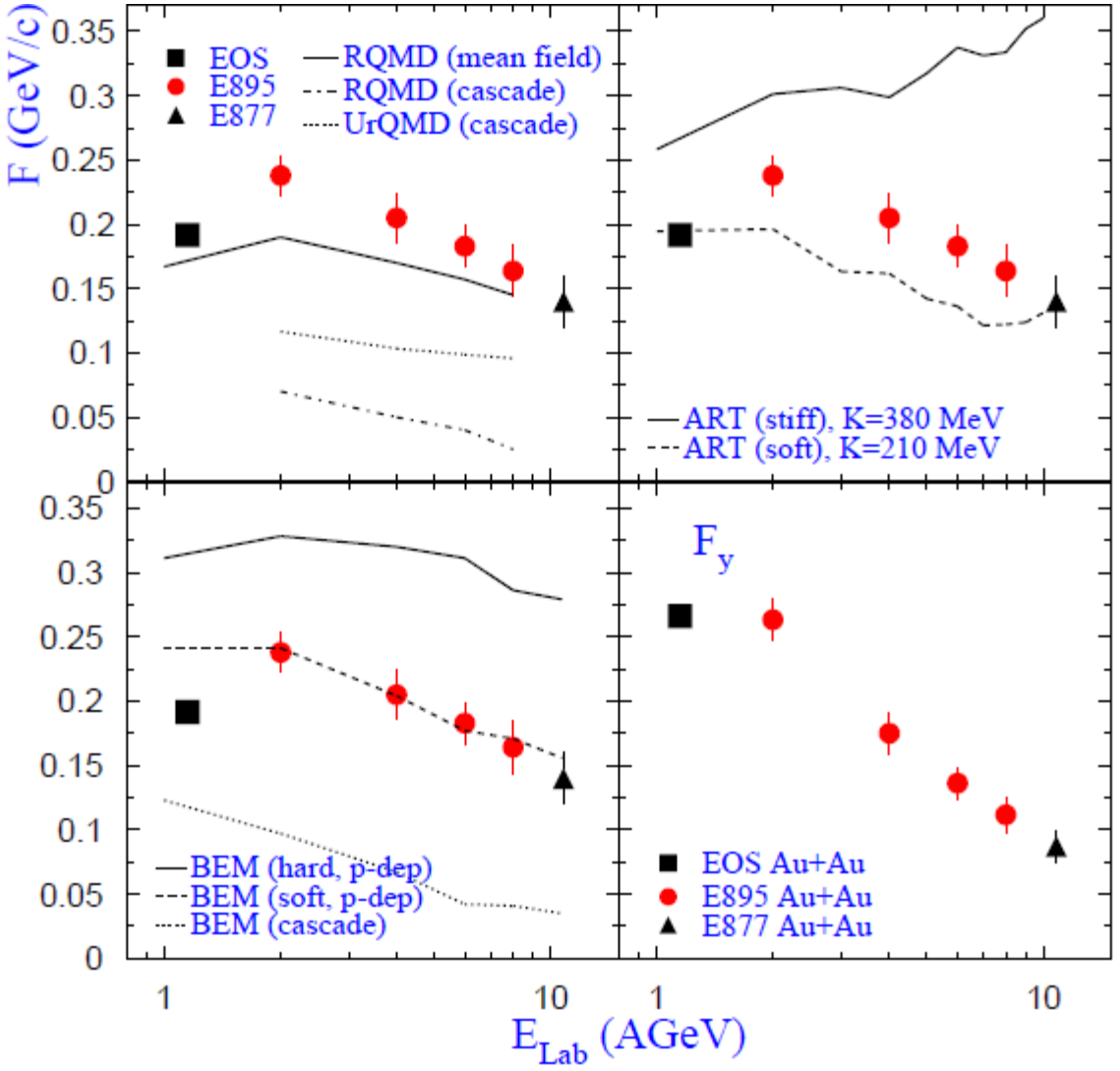


FIG. 2. Proton flow magnitude as a function of beam energy; the lower right panel shows the measured $F_y$, while the other three panels show identical measurements of the parameter $F$ with different transport model calculations superimposed. The error bars include systematic

# Directed Flow -- Lambdas

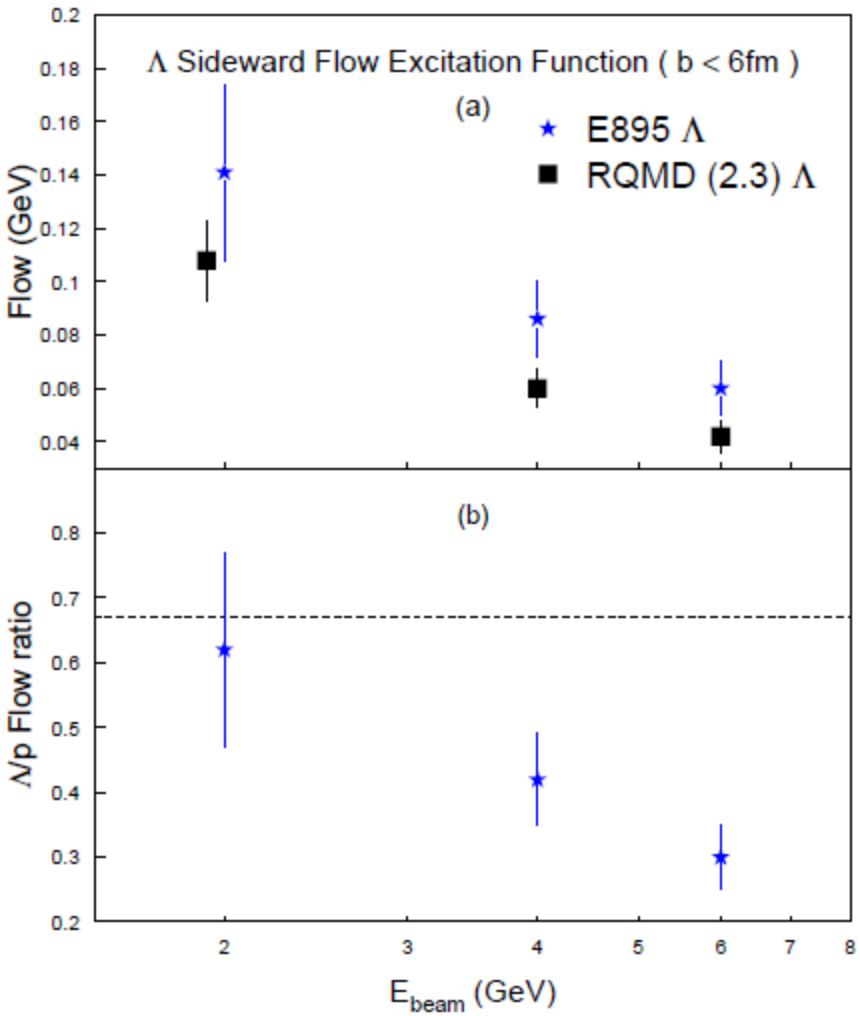


FIG. 4. (a) Λ hyperon flow vs beam energy. Filled stars and squares represent data and RQMD results respectively. (b) Λ/p flow ratio vs beam energy for the same impact-parameter range. The dashed line indicates a value of 2/3.

E895_PRL86(2001)2533

# Directed Flow – pions and nucleons

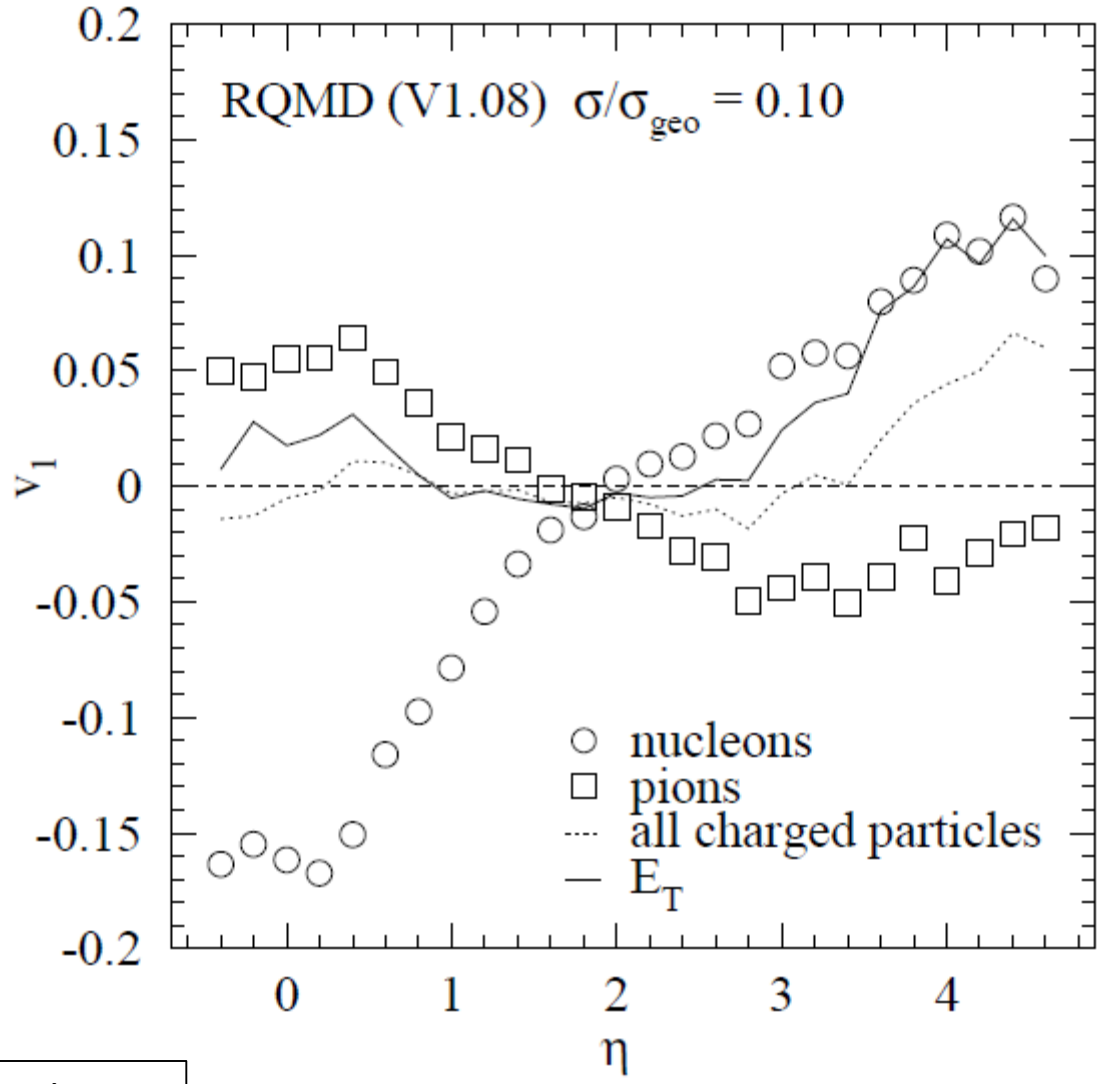


E877_PRC55(1997)1420

FIG. 11.

# Directed Flow – protons and pions

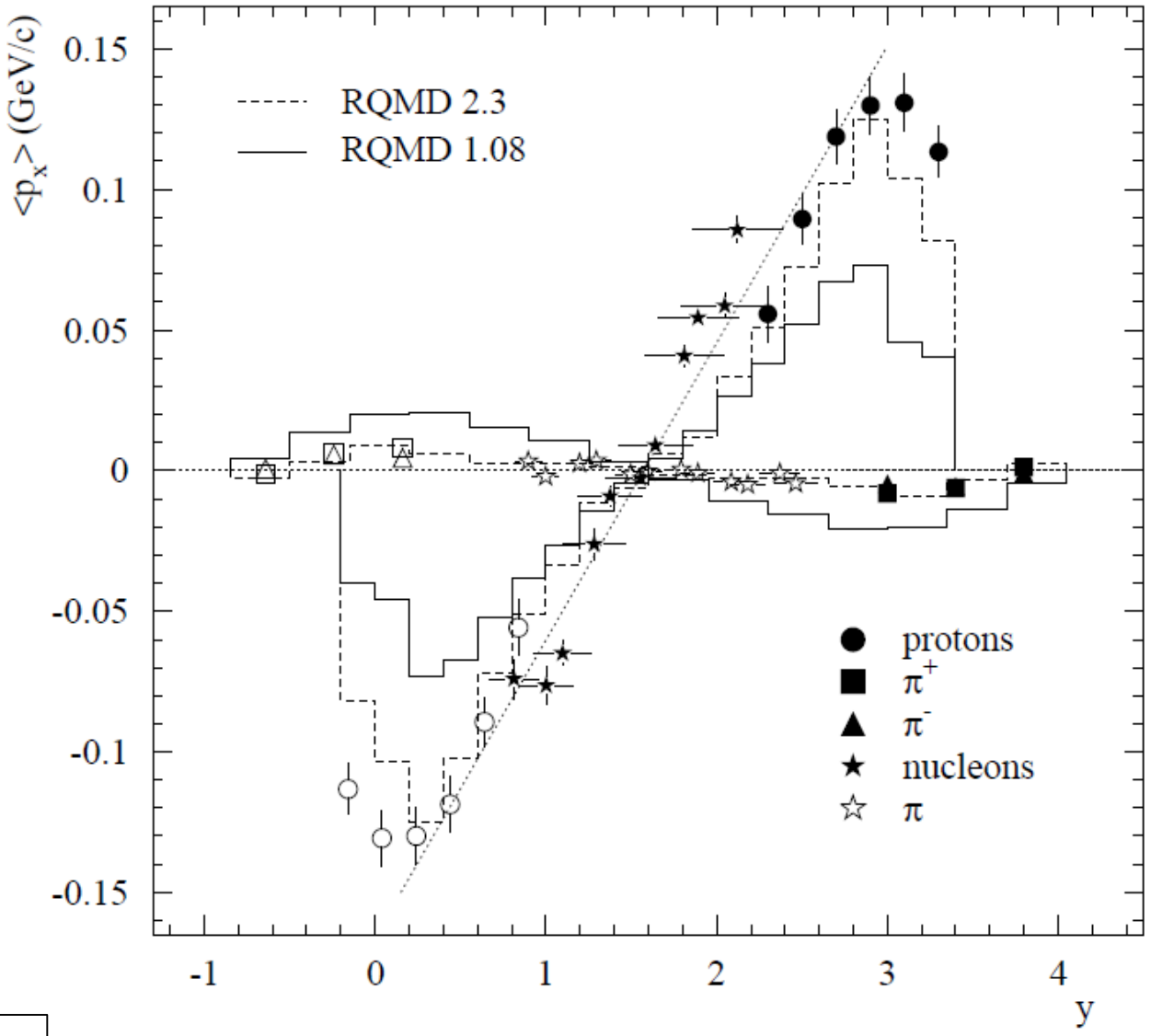


E877_PRC56(1997)3254

. 11. Mean projection $\langle p_x \rangle$ of the proton and pion transverse momentum onto the reaction

# Directed Flow – Protons and anti-protons

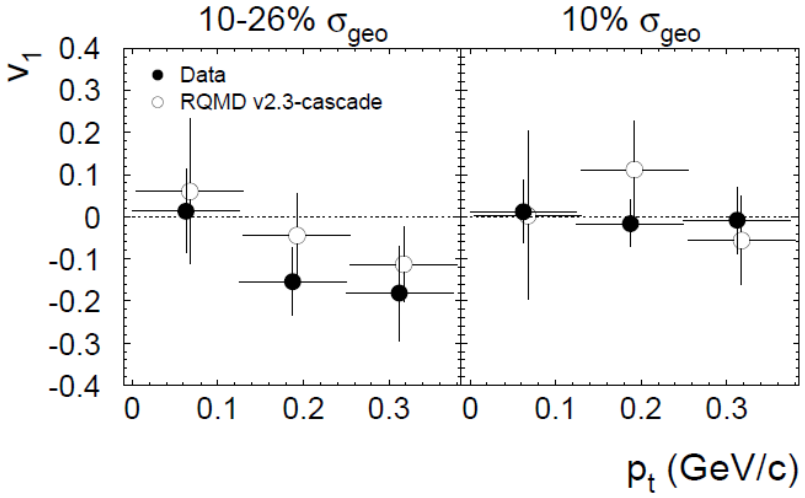


Fig. 5. $v_1(p_t)$ of antiprotons for rapidities $1.8 < y < 2.2$ and two collision centralities. The data (solid circles) are compared with the calculations using the RQMD v2.3 - *cascade mode* (open circles).

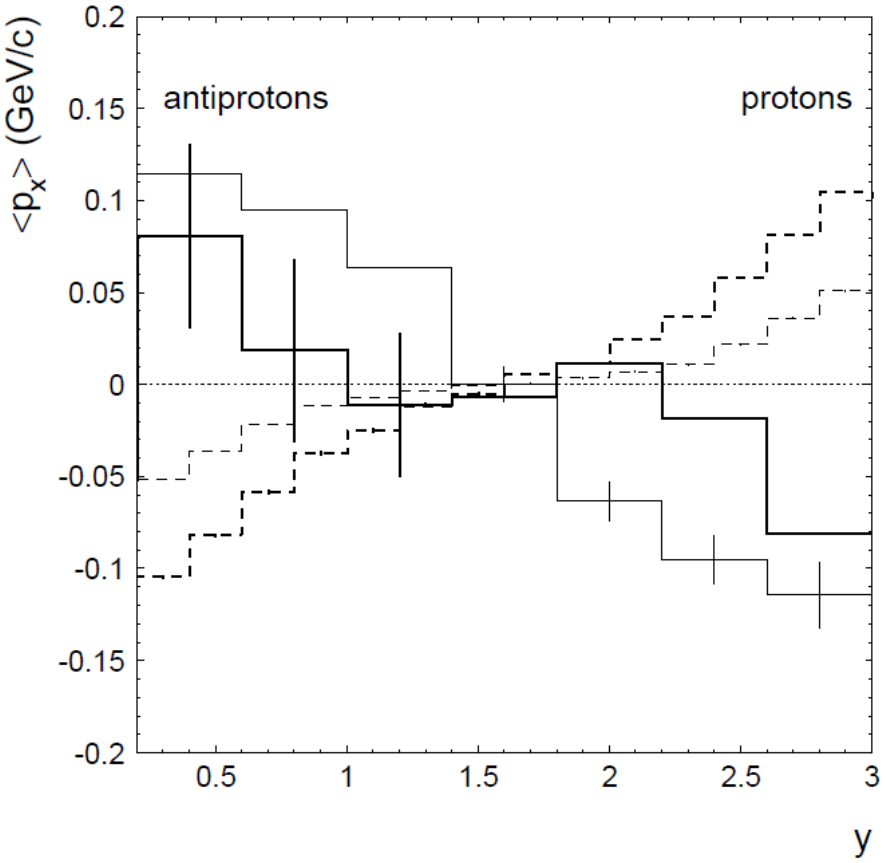


Fig. 6. Mean values of the transverse momentum projected into the reaction plane $\langle p_x \rangle$ of protons (dashed lines) and antiprotons (solid lines) as a function of rapidity for Au+Au collisions at 11.5A GeV/c with impact parameters $b < 10$ fm generated by using the RQMD v2.3 (*cascade mode* - thin lines; *mean field mode* - thick lines).

E877_PLB485(2000)319

# Directed Flow -- Kaons

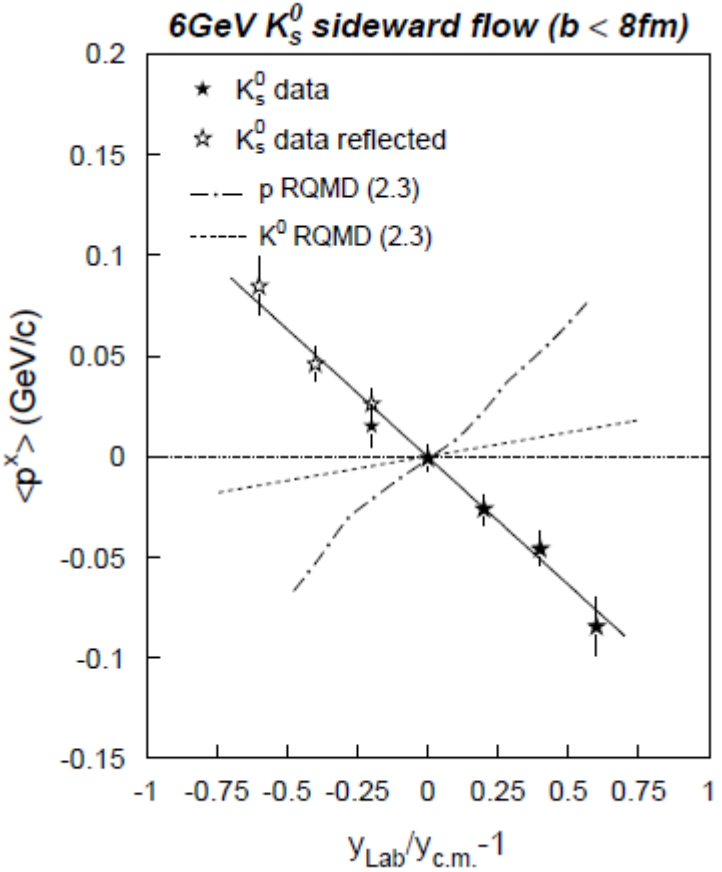


FIG. 3. Experimental $< p^x >$ vs $y_0$ for $K_s^0$ mesons (stars). $< p^x >$ values have been corrected for reaction plane dispersion. The solid curve represents a linear fit to the data. Error bars are statistical. The dashed-dot and dotted curves represent results obtained for protons and $K_s^0$'s from RQMD v (2.3) (with mean-field). The RQMD results have been obtained for the same impact parameter and $p^t$ selection as that for the data.

E895_PRL85(2000)940

# Directed Flow – Lambdas and Protons

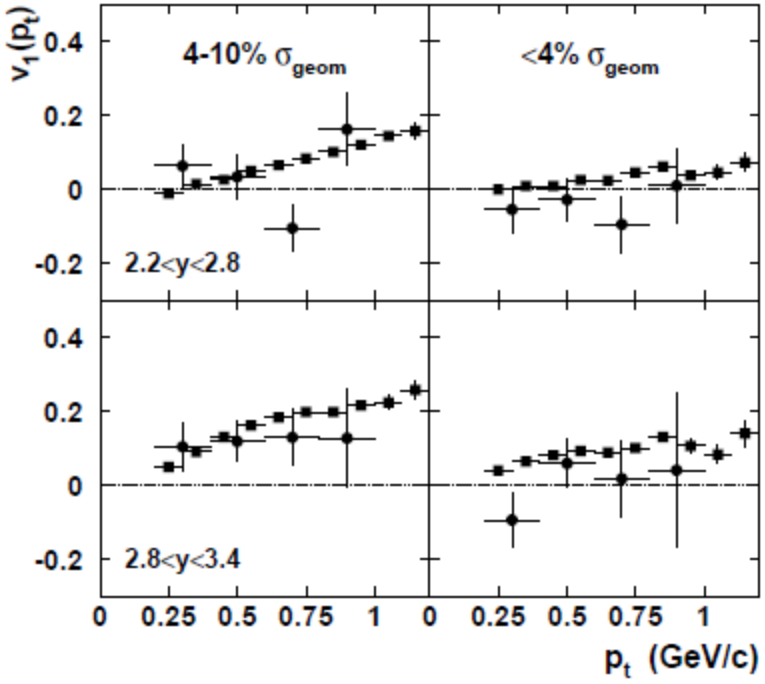


FIG. 9. Comparison of $v_1(p_t)$ data between $\Lambda$'s (solid circles) and protons (solid squares).

E877_PRC63(2001)014902

# Elliptic Flow

# Elliptic Flow -- protons

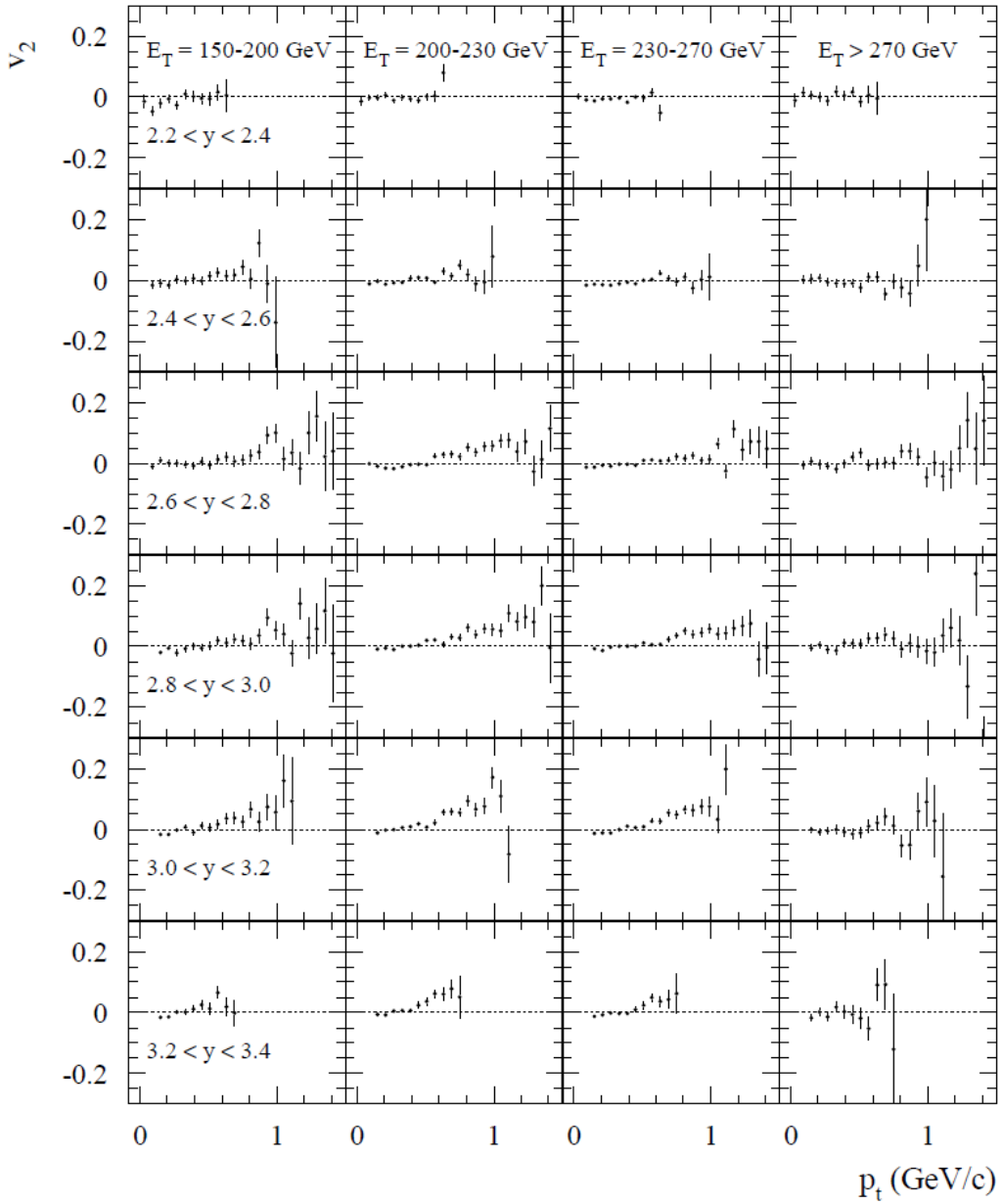


E877_PRC56(1997)3254



Probi

G. 8. The transverse momentum dependence of the second moment ($v_2$) of the proton

uthal distributions for different particle rapidities and centralities of the collision.

# Elliptic Flow -- protons

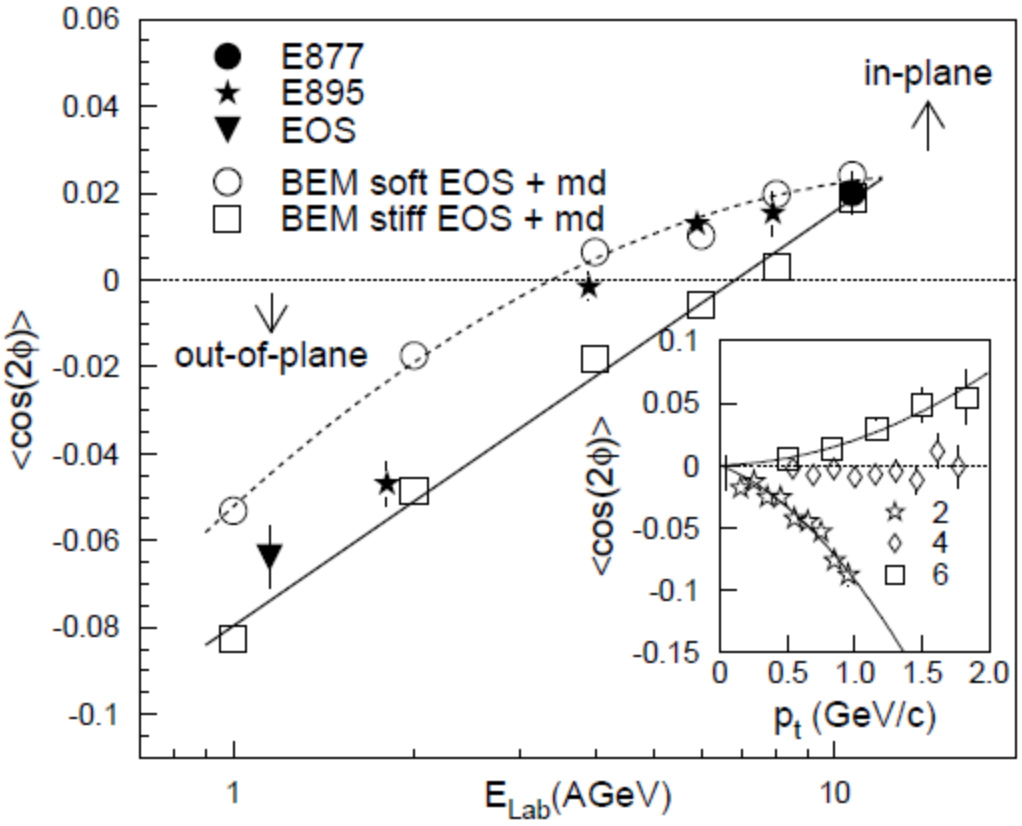


E895_PRL83(1999)1295

# Elliptic Flow --- protons

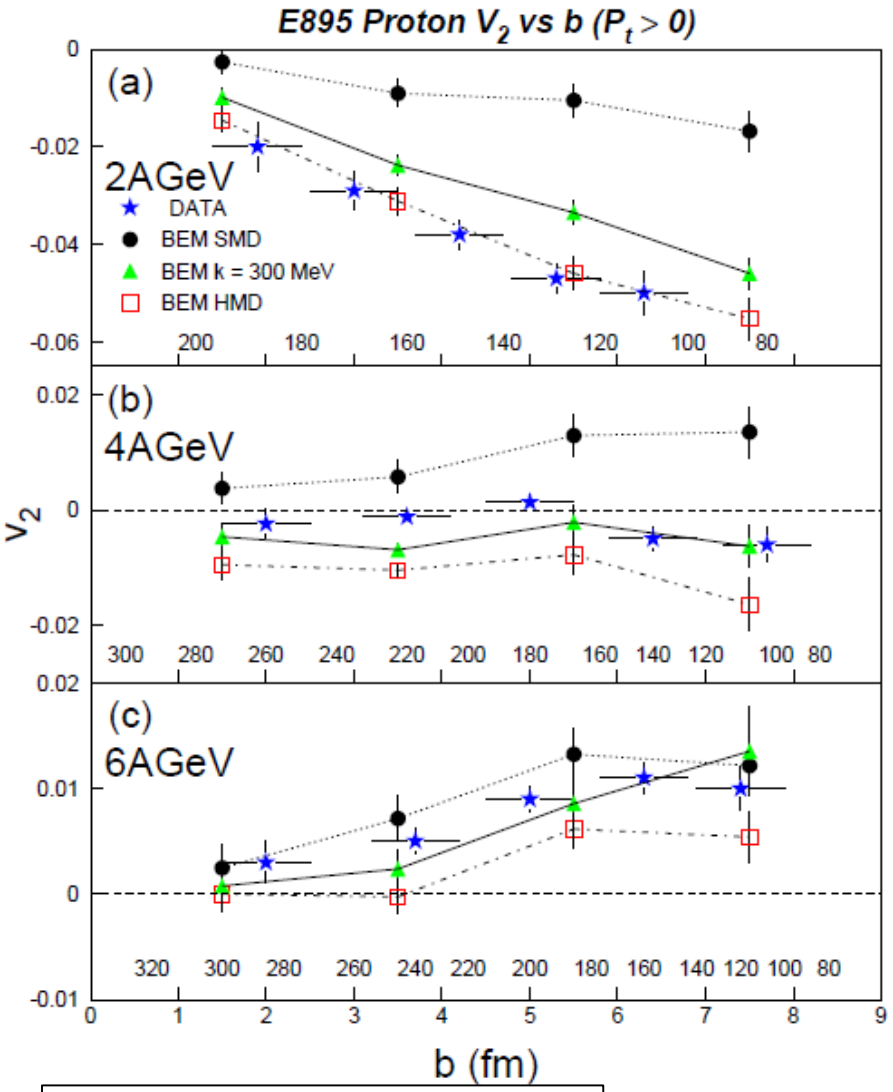


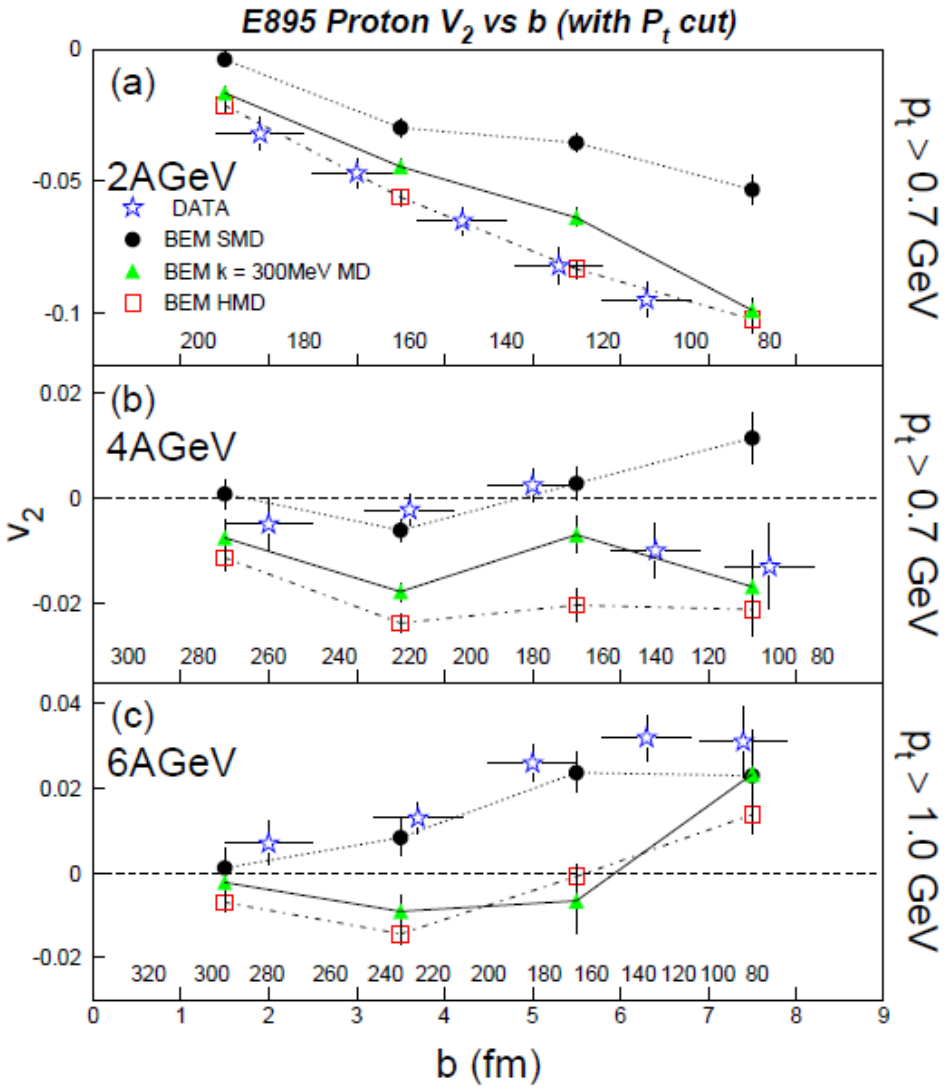


E895_PRC66(2002)021901

# HBT

# HBT -- pions

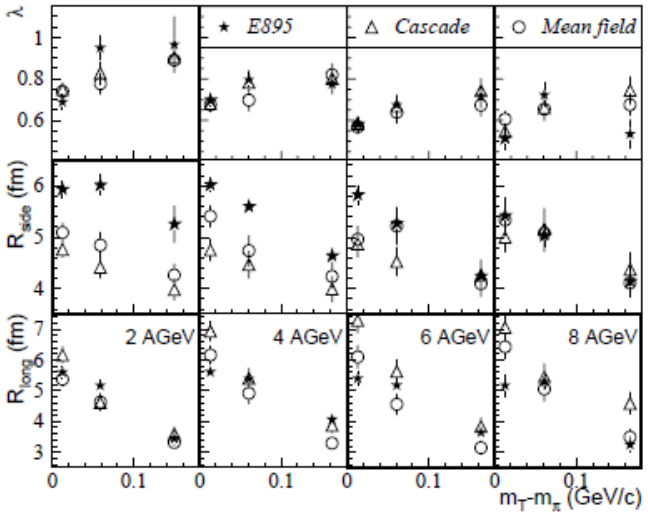


FIG. 2. Filled stars indicate the $m_T$ dependence of the measured BP parameters for midrapidity ($y = y_{c.m.} \pm 0.5$) $\pi^-$ for central (11% $\sigma_T$) collisions at four beam energies. Open symbols show the parameters from fits to correlation functions from RQMD calculations.

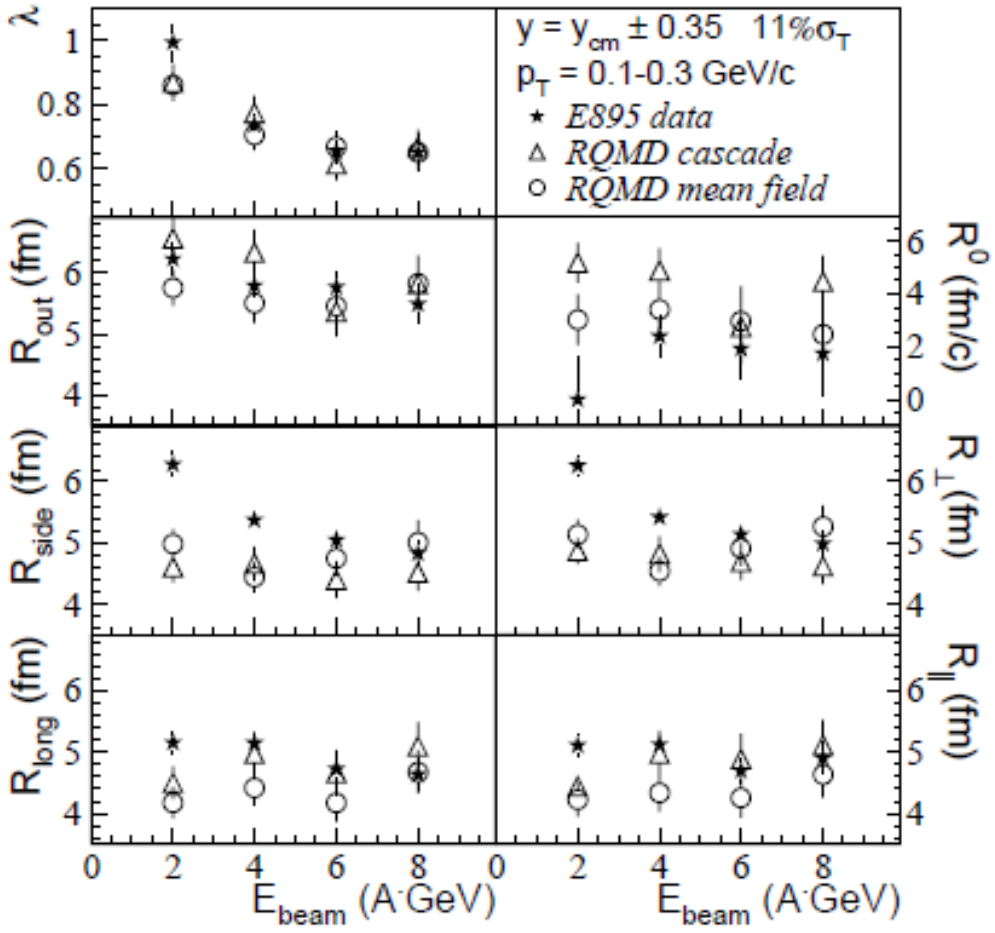


FIG. 1. Fit parameters for the measured correlation functions decomposed with the BP (left panels) and YKP (right panels) decompositions are shown as stars. Triangles and circles represent the results of fits to correlation functions from RQMD in cascade and mean field modes, respectively.

E895_PRL84(2000)2798

## HBT -- pions

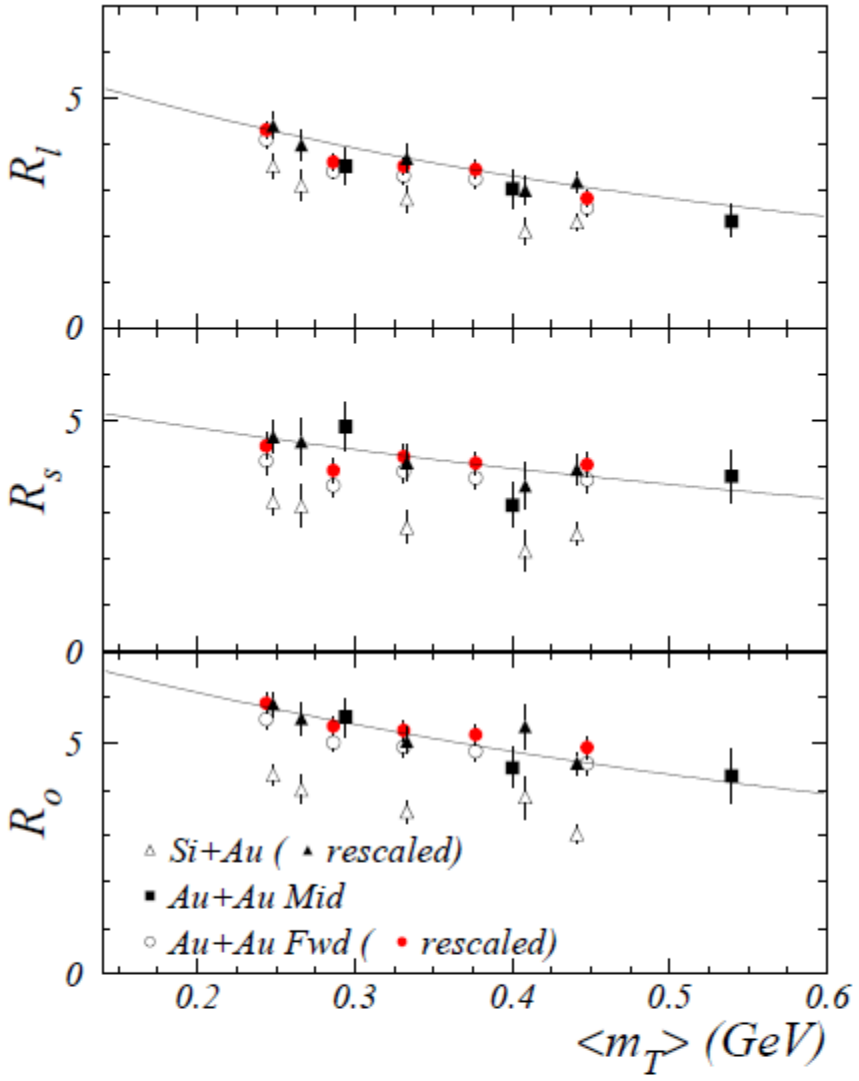


E802_PRC66(2002)054096

FIG. 8: $m_T$ dependence of Bertsch-Pratt radii for Si+Au, Au+Au, Au+Au at forward rapidity [44], and for Si+Au rescaled by $N_{\rm total}^{1/3}$ to match Au+Au. The solid line is a fit of the form $e^{(a+bm_T)}$ to the Si+Au points, rescaled according the $N_{\rm total}^{1/3}$ for Au+Au. The Au+Au forward rapidity data are also shown after being rescaled to match the mid-rapidity

## HBT -- pions

TABLE II. Parameters of the fit to three-dimensional correlation functions $C(q_{\rm out}, q_{\rm side}, q_{\rm long}) = 1 + \lambda \exp(-{R_{\rm out}}^2{q_{\rm out}}^2 - {R_{\rm side}}^2{q_{\rm side}}^2 + -{R_{\rm long}}^2{q_{\rm long}}^2 - 2|R_{\rm ol}|R_{\rm ol}q_{\rm out}q_{\rm long})$. The fit results are corrected for momentum resolution. That is why $\lambda$'s differ from the values in Table I.

| | $\lambda$ | $R_{\rm out}$(fm) | $R_{\rm side}$(fm) | $R_{\rm long}$(fm) | $R_{\rm ol}$(fm) |
|---|---|---|---|---|---|
| $\pi^+\pi^+$ | 0.62±0.06 | 5.8±0.5 | 3.9±0.8 | 5.5±0.4 | 2.4±0.7 |
| $\pi^-\pi^-$ | 0.62±0.05 | 6.5±0.5 | 5.6±0.7 | 5.8±0.4 | 3.7±0.8 |

TABLE III. Pion phase space density at freeze-out as a function of $p_t$ and $y$. The statistical errors from $d^3n/d^3p$ are about 2%. The systematic error from $d^3n/d^3p$, combined with the error from the correlation analysis, is 24% for $\pi^+$ and 18% for $\pi^-$. (This error acts on all numbers in the Table collectively.)

| | $\pi^+$ | | | $\pi^-$ | | |
|---|---|---|---|---|---|---|
| $p_t$ (GeV/c) | y=3.05 | y=3.15 | y=3.25 | y=3.05 | y=3.15 | y=3.25 |
| 0.05 | 0.190 | 0.167 | 0.146 | 0.158 | 0.134 | 0.115 |
| 0.10 | 0.124 | 0.110 | 0.094 | 0.100 | 0.083 | 0.071 |
| 0.20 | 0.039 | 0.033 | 0.027 | 0.028 | 0.022 | 0.018 |

E877_PRL78(1997)2916

# HBT – asHBT -- Pions

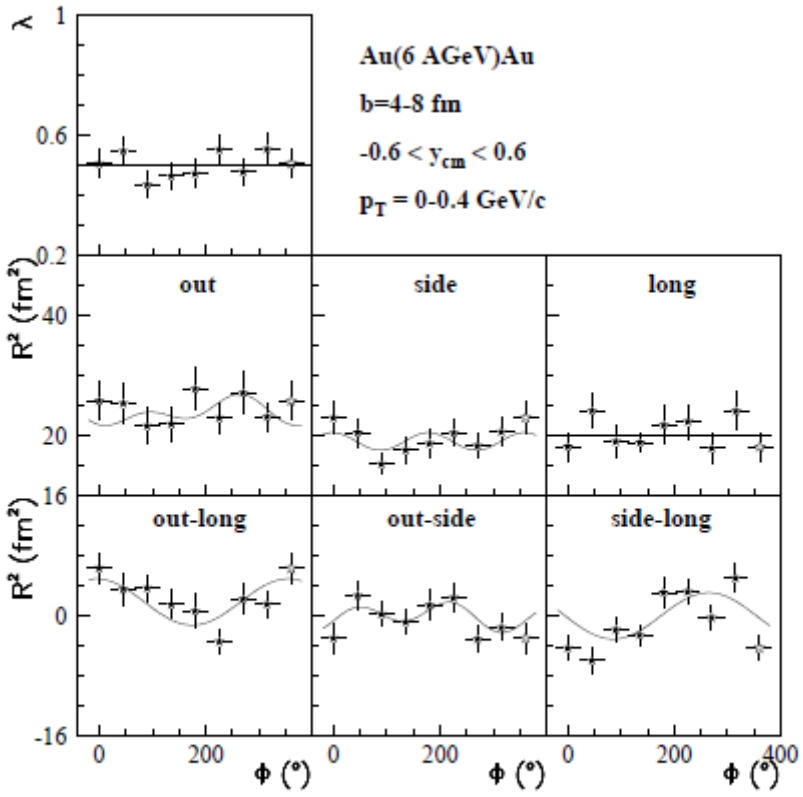


FIG. 5. Same as Figure 3, but for 6 AGeV collisions.

E895_PLB496(2000)1

## HBT -- protons

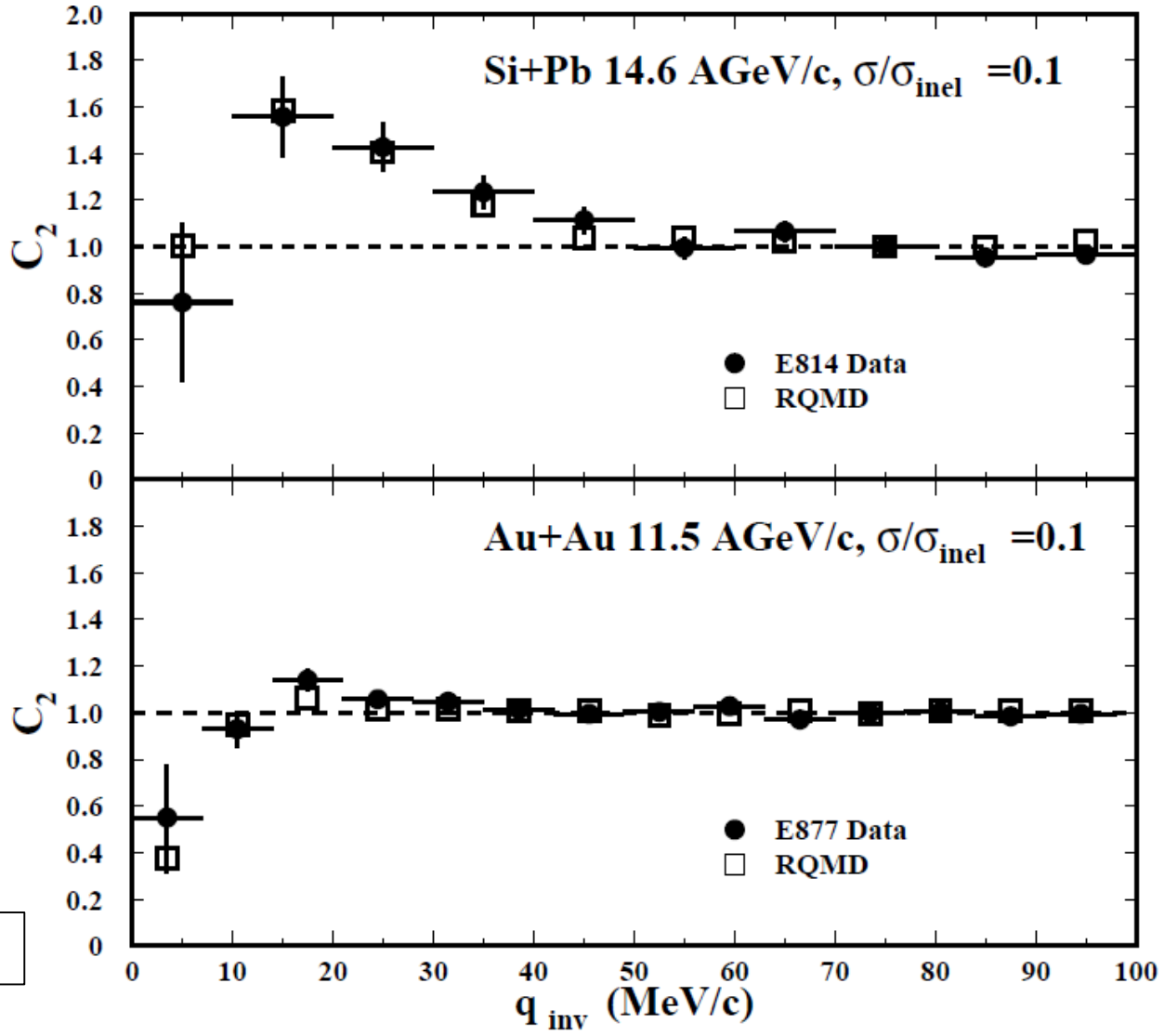


E814_PRC60(1999)054905

3. 3. Two-proton correlation functions for Si+Pb (upper panel) and for Au+Au (lower panel) central collisions. al results are shown as filled circles while the RQMD model predictions are shown as open squares.